Characteristics of Combustion Products: A Review of the Literature

ABSTRACT

To determine the effects of fires in nuclear fuel cycle facilities, Pacific Northwest Laboratory (PNL) has surveyed the literature to gather data on the characteristics of combustion products. This report discusses the theories of the origin of combustion with an emphasis on the behavior of the combustible materials commonly found in nuclear fuel cycle facilities. Data that can be used to calculate particulate generation rate, size, distribution, and concentration are included. Examples are given to illustrate the application of this data to quantitatively predict both the mass and heat generated from fires. As the final result of this review, information gaps are identified that should be filled for fire accident analyses in fuel cycle facilities.

CONTENTS

FIGURES

viii

TABLES

NOMENCLATURE

d	particulate diameter
d_0	initial particulate diameter
D_{vs}	mean particle diameter
F_j	product generation efficiency
F_v	soot volume fraction
$\dot{G}''_j$	mass generation rate of product j
$\dot{G}''_{pj}$	product generation rate of species j for pyrolysis
$\dot{G}''_{bj}$	product generation rate for species of j for combustion
H_a	actual heat of combustion
H_i	heat of combustion
H_t	heat of complete combustion
I	laser intensity
I_0	initial intensity
k	Cunningham correction factor
k_j	yield of product j expected from stoichiometry
K	rate constant which depends on thermal and kinetic properties of fluid
$\overline{L}$	pathlength or mean beam length
L	heat required to generate a unit mass of the fuel vapors
M_{O_2}	mass fraction of oxygen
M_e	soot refractive index
$\dot{M}$	mass loss rate
M_p	total particulate mass
$\dot{M}''_p$	mass loss rate of pyrolysis

$\dot{M}_b''$	mass loss rate of combustion
N_o	total particle concentration
N_p	particle number concentration per cm^3
$(N_p)_o$	initial particle concentration
$N_{(r)}$	particle size distribution
ρ_p	particle density
$\dot{q}_e''$	external heat flow
$\dot{q}_{fc}''$	flame convective heat flux
$\dot{q}_{fr}''$	flame radiative heat flux
$\dot{q}_{fs}''$	total flame heat flux
$\dot{q}_n''$	net heat flux received by the fuel material per unit fuel surface area
$\dot{q}_{rr}''$	surface reradiation heat loss rate
$\dot{Q}_a''$	heat release rate
$\dot{Q}_r''$	radiative heat release rate
$\dot{Q}_c''$	convective heat release rate
Q_{ext}	mean extinction efficiency
r_{max}	most probable particle radius
t	time in seconds
τ	extinction coefficient
V	test chamber volume
T_t	terminal settling velocity
X_a	ratio of actual to complete heat of combustion (combustion efficiency)
X_c	convective fraction of heat of complete combustion
X_r	radiative fraction of heat of complete combustion
Y_j	yield of product j

ϕ equivalence ratio

$\bar{\phi}$ volume fraction

ϕ_{corr} corrected volume fraction

ϕ_{meas} measured volume fraction

EXECUTIVE SUMMARY

The objective of this state-of-the-art literature review on characteristics of combustion products is to identify useful information (mass generation rates of smoke particles, particulate size and distribution, particulate concentration, energy generation rates, etc.) on the combustible materials that are commonly found in fuel cycle facilities (polymethylmethacrylate, polystyrene, polyvinyl chloride, elastomers, cellulosic materials, and organic fluids). This information will be used in analysis of the radiological consequences of fires inside the facilities. At the same time, the complex phenomena of fire, combustion and heat generation are briefly introduced to provide the readers some basic understanding in interpreting and utilizing the collected data.

The characteristics of fire generated products and energy releases are a strong function of three main variables--temperature, oxygen availability in an enclosure, and chemical compositions of fuel materials. The mechanism of soot formation, which is responsible for the particulate size, concentration, and radiation in the fire enclosure, is still a mystery. Many different mechanisms have been proposed. Among them, soot formation, involving processes of dehydrogenation and aggregation via acetylene, polyacetylenes and polycyclic aromatic hydrocarbons (PCAHs), is the most promising route. The study of combustion products found in the flame zones is the basic process in understanding soot formation. Besides the principal combustion product gases (CO, CO_2, H_2, and H_2O), small amounts of acetylene, polyacetylene, carbon particles and several PCAHs were detected in the premixed and diffusion flames of acetylene. Yet, more quantitative data are needed for verification.

The majority of characteristics and energy data of combustion products are found in the fire studies by A. Tewarson et al. of Factory Mutual Research and B. T. Zinn et al. of Georgia Institute of Technology. All these available data were obtained by conducting experiments in a small-scale combustion apparatus. The appendix is a data bank (collection of raw data) with some of the selected characteristics tabulated in Section 3.0. These data are believed to be the best information available in the literature today. Using this selective information in Section 3.0, examples are provided to demonstrate the application of the data.

There is a lack of combustion product data in the literature for cellulosic materials, elastomers, kerosene and for "typical mixtures" (representing fractions) of combustible materials found inside fuel cycle facilities. The effects of radioactive particles on fire-generated particles, and vice versa, are yet unknown. The uncertainty of the utilization of the small-scale data to predict the outcome of a facility fire has been a concern for large-scale accident analysis.

1.0 INTRODUCTION

One of the potentially destructive accidents to a nuclear facility is fire. Radioactive materials which can be released as aerosols during a fire accident impose a potential risk to the public. Both radioactive particulate material and fire-generated particulate material that remain airborne through the ventilation system can cause filter clogging, which can destroy the filter element. A whole new path of the release of radioactive material to the atmosphere results if filter paths are destroyed or plugged. Fire can initiate other possible accidental events inside a nuclear facility, ranging from simple spills of radioactive powder to major accidents like explosions or criticalities. All these accidents would cause airborne releases of radioactive materials within the facility.

Since the generation of particulate material from a fire is inevitable, it is important to understand the characteristics of fire-generated products. By knowing these particulate characteristics and their interaction with airborne radioactive particles, an estimate of radioactive material release can provide the information necessary for safety analysis reports and environmental impact statements.

In this report, state-of-the-art combustion products studies are first reviewed with emphasis on the phenonema of fire and combustion resulting in both mass and energy generation, the behavior of airborne materials, and the various factors that influence the generation of smoke. Next the data available on the characteristics of combustion products and energy releases are discussed and tabulated. With the application of engineering approximations and necessary modifications to the existing data, this information will allow us to analyze fires in fuel cycle facilities. This review will be updated as additional information becomes available.

This report is divided into two parts for discussion:

- Qualitative Assessment (Section 2.0) introduces fire and combustion processes, identifies and discusses the possible mechanisms and the energy involved in combustion product formation and behavior of airborne material; discusses the effect of certain parameters on the characteristics of combustion products; and identifies the methods of experimental fire study.

- Quantitative Assessment (Section 3.0) presents and discusses quantitatively the characteristics of products generated by burning various materials such as those found in the most recent combustion studies. Products in both flames and smoke are discussed. Energy release rate in combustion is also considered.

Background information on fire and combustion (Section 2.0) is given before the more detailed discussion on the characteristics of combustion products (Section 3.0). A reader who has an understanding of the recent fire literature may want to refer directly to Section 3.0.

2.0. THE STUDY OF FIRE AND COMBUSTION PRODUCTS

Fires in buildings generate toxic gases and a complex mixture of solid and liquid particles. These unwanted products are commonly known as smoke. For better understanding of the smoke problems, both physical and chemical properties of these smoke particles are being examined by many researchers. Studies have shown that the particles that make up smoke can be detrimental to safety and health. The purpose of this report is to present available information gathered from a state-of-the-art literature review on characteristics of combustion products, which will implement our further study on fires in fuel cycle facilities which possibly cause the release of radioactive materials to the environment.

The properties of smoke particles are normally studied by simulating fires in both small- and large-scale chambers equipped with measuring devices. Materials used in these experiments are those which are commonly found and used in homes and for building materials; i.e., wood, polyvinyl chloride (PVC), polymethylmethacrylate (PMMA), polystyrene (PS), etc. A few studies have also been conducted by collecting smoke samples during real fires (Burgess, Treitmar and Gold 1979; Long 1972), using prototype sampler systems which were installed in a firefighter's turnout coat. These studies only identified the chemical components of combustion products found in the flame zone and in smoke.

This review will focus on combustion product characterization by burning combustible materials found in nuclear facilities. These combustible materials can be identified as follows:

- PMMA (viewing windows of gloveboxes)
- PS (ion exchange resin)
- PVC (wrapping/covers)
- elastomers (i.e., rubber and other plastics used as seals/gaskets)
- cellulose
- cellulosic materials (i.e., paper and rags for cleaning)
- organic fluids (i.e., kerosene as liquid-liquid extraction solvent and hydraulic fluids as lubricants).

Table 2.1 shows some of the physical properties of the three commercial plastics, and Table 2.2 shows some characteristics and behavior of materials which can be found in fuel cycle facilities. Both physicochemical and combustion/pyrolysis properties of some of the combustible materials listed above are tabulated in Section 3.0.

At this point it is desirable to define the terminology of combustion products common to investigators in the field. When combustible gases or vapors burn in air, smoke as well as heat is released into the air as particles during the processes of pyrolysis and combustion (Saito 1974). Smoke is an aggregation of submicron solid and liquid particles (such as the carbonaceous particles soot, ash, droplet or tar, spotted fragments, and other condensed matter) formed due to poor mixing of fuels with air (Murty 1978). In an actual

TABLE 2.1. Physical Properties of Commercial Plastics[a]

Property	PMMA	PS	PVC
Decomposition temperature range,°C	170-300	300-400	200-300
Ignition temp.,°C			
Flash ignition	280-300	345-360	391
Self ignition	450-462	488-496	454
Limiting O_2 $N_{O_2}/(N_{O_2} + N_{N_2})$	0.173	0.181	0.45-0.49
Surface flammability (burning rate), in./min	0.6-1.6	0.5-2.5	Self-extinguishing
Specific heat, cal/g-°C	0.35	0.32	0.20-0.28
Thermal conductivity $(10^{-4}$ cal/sec-cm^2),°C/cm	4.0-6.0	1.9-3.3	3.0-7.0

_____

(a) Hilado 1969.

fire, the possible constituents of combustion products generated can be categorized as gases, vapors and particulate material. Some components of these products are:

- gases
  - carbon monoxide (CO), carbon dioxide (CO$_2$)
  - oxides of nitrogen (NO$_x$)
  - oxygen (O$_2$)
  - other (e.g., HCl, HCN, H$_2$, C$_6$H$_6$, etc.)

- vapors
  - water (present and generated by combustion)
  - condensible (inorganic and organic)

- particulate material
  - soot
  - mineral ash
  - condensed vapor
  - other (e.g., PCAHs)

2.2

TABLE 2.2. Characteristics and Behavior of Fuel Materials

Material	Characteristics
PMMA[a] $(C_5H_8O)_n$	Easy to ignite and softens as it burns.
PS[a] $(C_8H_8)_n$	Easy to ignite. Softens and bubbles as it burns, and generates some black smoke and airborne carbon. The principal combustion products are CO_2 and CO.
PVC[a] $(C_2H_3Cl)_n$	Difficult to ignite and evolves white smoke. Held horizontally, it is self-extinguishing. The major products of pyrolysis and combustion are CO_2, CO, and HCl. It softens as it burns.
Elastomer[b]	Possesses a high degree of elasticity. Natural rubber illustrates the structural requirements of an elastomer--long, flexible chains, weak intermolecular force, and occasional cross-linking.
Cellulosic material[b]	Easy to ignite. Not noticeably affected by O_2. More volatiles, less char because heating rate is higher. Typical combustion products of volatiles are CO_2, CO, H_2O, N_2.

(a) Hilado 1969.
(b) Morrison and Boyd 1977.

Due to the complex phenomena of combustion, no single study has been able to thoroughly and quantitatively describe the properties of these products initially found in the flames which diffuse away as smoke and gases. The literature we reviewed showed that most investigators quantitatively emphasized the materials generated in the flames or identified and measured the characteristics of airborne materials found in smoke away from the flames. In order to master these transient properties, the mechanisms of product formation and the behavior of airborne particles must be known.

2.1 FIRE AND COMBUSTION PROCESSES

In a classical sense, the processes of pyrolysis (volatilization) and combustion define fire. These two processes do not necessarily coexist in a simple combustion process (e.g., burning of methane gas), but burning requires the presence of oxygen, and combustible volatiles evolve during the pyrolysis of solid and liquid fuels exposed to a high-temperature environment. In order to characterize a burning object, the study of flammability characteristics becomes important.

Fire inside a fuel cycle facility is quite different from other enclosure fires, such as residential and non-nuclear industrial fires, because of differences in 1) the types and amounts of combustible materials and 2) the distribution and the flow pattern of air (or oxygen). (The ventilation system inside a nuclear facility is designed differently than most other industries' systems.)

In a fire, heat and mass (smoke and other toxic gases) are generated. These two variables are dependent on each other. The laws of physics and chemistry predict that, as more heat is formed in a combustion process, more CO_2 and H_2O are formed due to the completeness of combustion; while when less heat is formed, more of other products (i.e., byproducts of incomplete combustion such as soot, CO and organic vapors) are found. Therefore both mass and heat generation in a fire must be considered together when analyzing the accident.

The concepts mentioned above are necessary in understanding fire and combustion processes. More detailed information is discussed in the following sections.

2.1.1 Pyrolysis

In most chemistry texts, pyrolysis is defined as chemical decomposition by the action of heat. The role of oxygen in pyrolysis was subject to controversy in the late 1960s. In the model derived from Fenimore and Jones' (1966) smoke measurement experiments, oxygen from the surrounding atmosphere was assumed to be completely consumed in the flame zone so that polymer degradation occurred by pyrolysis in the absence of O_2. This has been called a thermal degradation model. In another model, referred to as oxidative or thermo-oxidative degradation, Burge and Tipper (1969) postulate that oxygen may play a role in pyrolysis at the polymer surface. They performed a test similar to those by Fenimore and Jones except that they burned the polymeric materials at a subatmospheric pressure of 50 mm Hg in an oxygen-argon mixture with 20 O_2. Cheng, Ryand and Baer (1969) have presented their data from a similar experiment to support the possibility of oxidative degradation under certain conditions. Their conclusion is that it is probable, depending on the material and the combustion condition, that thermal degradation and/or oxidative degradation may be important to polymer combustion.

Condensed fuels found in fires can be viewed as suppliers of gaseous fuels. Thus, from this viewpoint, pyrolysis of the condensed fuel via the chemical breakdown of the fuel constituents under the influence of heat plays a central role in the phenomenon of fire.

Condensed fuels found in a fuel cycle facility are in solid and liquid form. Among the solid fuels, polymeric materials like PMMA, PVC and other plastics are viewing glass for gloveboxes and bagging materials; PS is found in ion exchange resin; natural and synthetic rubber is found in surgeons' gloves and gasketing material on the gloveboxes; and cellulosic materials are found in rags, papers and cardboards. Among the liquid fuels, kerosene, hydraulic fluids and other high-boiling organic fluids are often found in the nuclear facility. On a molecular scale, the mechanisms by which the gaseous fuel is liberated are different for the solid and liquid fuels.

2.1.1.1 Solid Fuels

Some solids are distilled when subjected to heat, while some are melted to a liquid form before the generation of combustible gases. The former is usually called a sublimation process, where the volatile gases emitted in the interior of the solid seep out of the solid before reacting with air. Cellulosic materials usually behave this way when exposed to heat. As suggested by Murty (1978), the study of pyrolyzing this type of solid consequently involves two steps: first, to find the rate of evolution of volatiles in the interior of the solid as a function of the external surface heat flux condition; and second, to find the flame stand-off distance and surface heat flux in the gas phase as a function of quantity and quality of the volatiles transpiring from the surface. When subjected to heat, other solids are melted to a liquid form before the generation of combustible gases. This involves two processes--decomposition of solid to liquid phase and vaporization of liquid to gaseous phase. Generation of volatiles via these processes usually requires more energy than sublimation. Polymeric materials like plastic and elastomers usually behave this way.

The complexity of the breakdown schemes of most solid fuels is so great that appreciable uncertainties always remain in a description of their pyrolysis mechanisms. Nonetheless, information on heat of decomposition (i.e., amount of heat required to decompose a unit mass of material), heat of vaporization (also called gasification or sublimation), and heat of depolymerization for simple chemical compounds is often obtainable in physics and chemistry textbooks (e.g., Hilado 1969; Morrison and Boyd 1977). For most of the combustible materials found in a fuel cycle facility, Tewarson et al. (1980b) have been able to provide information on heat required to generate a unit mass of vapor by measuring the steady-state mass loss rate in pyrolysis in their Factory Mutual combustion test chamber in a nitrogen environment. (See Table 3.10 of Section 3.2.1. For other fuel materials refer to Tables A.1.1 and A.1.3 of Appendix A.1 and Tables A.7.2 and A.7.3 of Appendix A.7.)

2.1.1.2 Liquid Fuels

In a conventional sense, pyrolysis is unimportant in the condensed phase for liquid-fueled fires. Usually temperatures within the liquid phase are too low for a significant amount of chemical breakdown to occur during a typical fire. This may not be true, however, for high-boiling liquids or for the higher-boiling residues that remain toward the end of a fire in liquid-fuel mixtures.

Pyrolysis of liquid fuels involves the transition from liquid to gas (vaporization). Liquid fuels can be classified into two types: those that are easily vaporized and those that are not, depending on their chemical and physical properties. After they have vaporized, as in solid fuel, the volatile vapors can burn with air.

2.1.2 Combustion

Combustion itself is a very complex phenomenon. Generally, it may involve both mass and heat transfer processes (i.e., diffusion of oxygen and combustion products), thermodynamics, aerodynamics, and kinetics of several simultaneous and/or competing chemical reactions (i.e., series of oxidation reactions, thermal decomposition of fuel).

Fundamentally, combustion requires three important elements: 1) fuels, 2) oxygen and 3) external energy. (External energy refers here to ignition sources or a high-temperature environment where combustible vapors can be self-ignited in the presence of oxygen.) Without any one of these elements, combustion would not exist.

Combustion is known as the mechanism by which hydrocarbon volatiles (pyrolyzates) oxidize at the high temperatures encountered in a flame. Three main zones are typically identified in order of occurrence in premixed flames (i.e., flames generated by combustion of a specified ratio of air and gaseous fuel in a mixture): a nonluminous zone, a main reaction zone and a glowing burned gases' zone. In a nonluminous zone, complex fuel molecules are thermally unstable at combustion temperatures. As these fuel molecules enter the reaction zone their internal energy increases rapidly due to collisions with other very energetic, high-temperature molecules. Bond rupture occurs so that chemical potential energy is transformed into thermal and mechanical energy. A fuel containing energy-rich bonds such as carbon-carbon, carbon-hydrogen and hydrogen-hydrogen is a common source of chemical potential energy. Besides formation of energy in the reaction zone, the mechanism of cracking or dissociation of fuel molecules produces simpler monatomic or diatomic species that react to form gaseous combustion products (i.e., CO_2, CO, H_2O, and H_2). In addition to these predominant products of combustion, trace amounts of other species such as NO_x and particulate materials may form in the reaction zone of the flame. The glowing burned gases' zone contains the newly formed particulate materials, which are responsible for the color of the flame.

Beside flaming combustion, there are other types of combustion processes such as char oxidation and oxygen depletion of solid fuel interior cavities known as deep-seated fires (Krause et al. 1980). These processes require less oxygen (ranging from 3 to 9%) and are most often found in burning of charcoal or in the dying period of a solid-fuel fire.

The quantification of combustion (i.e., stoichiometry) is the most useful type of technical analysis of any physical or chemical phenomenon in the study of combustion. A stoichiometric mixture is one in which the proper ratio of fuel to oxygen is theoretically correct, causing complete oxidation in a chemical reaction. For example, to have stoichiometric combustion of one mole of methane, two moles of oxygen are required. The reaction yields one mole of CO_2 and two moles of water:

$$CH_4 + 2O_2 \rightarrow CO_2 + 2H_2O \qquad\qquad (2.1)$$

2.6
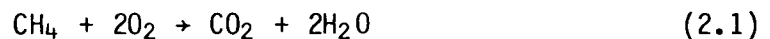
(Assume that the dissociation of CO_2 and H_2O to CO, O_2, OH^- and H_2 is not accounted for by the above reaction.)

In a fire, there are usually situations when combustible mixtures contain excess oxidant ("lean" mixtures) or excess fuels ("rich" mixtures). The relative proportions of CO_2, CO, H_2O, H_2 and particulate materials that are produced depend upon the degree of richness or leanness and the temperature and pressure conditions in a fire. Equivalence ratios ($\emptyset$) (fuel-air or air-fuel) are the most common ways of quantitatively expressing the richness or leanness of a mixture. This topic will be covered in more depth in Section 3.0.

For the most part, the combustion process utilizes stationary flames rather than propagating or explosion flames such as found, e.g., in the operation of internal combustion engines (Boisdron and Brock 1972). There are two types of stationary flames--premixed flames and diffusion flames. As discussed by Long (1972), no flame may be characterized as being either purely premixed or purely diffusional. For example, rich, premixed bunsen-type flames depend on the outer diffusion flame zone for stability, while diffusion flames depend on a premixing region near the burner rim for stability. Murty (1978) has provided definitions for the two kinds of flames:

● Premixed Flame--a result of the rapid exothermic combustion reaction of the combustion mixture formed by premixing a fuel with an oxidant (i.e., O_2) in the proper proportions. Such a well-mixed combustion is said to be kinetically controlled.

● Diffusion Flame--a result of an exothermic combustion reaction due to the diffusion of oxidant into the fuel zone caused by temperature and gaseous concentration gradients established in space. Such a poorly-mixed combustion is said to be diffusion-controlled.

In the case of a fire, diffusion flames predominate as a result of the combustion processes of a fire.

2.1.3 Flammability Characteristics

It is important that fire researchers be able to describe the behavior of a material when it is exposed to fire. Flammability characteristics are the properties used to define such behavior. For example, to determine surface flammability of a test specimen, rate of burning (or mass loss rate) must be considered; to obtain the heat contribution from a particular combustible, the heat of combustion value is needed; and to characterize the fire gases, measurements of concentrations of decomposition and gaseous combustion products are desired. Table 2.3 is a list of flammability characteristics and some factors for measuring them.

Some of the characteristics found in the above table, e.g., heat and mass generation from combustion processes, are discussed in more detail in Section 2.1.6.

TABLE 2.3. Flammability Characteristics

Characteristics	Some Measures of the Characteristic
Ease of ignition	• Decomposition temperature • Flash-ignition temperature • Self-ignition temperature • Limiting oxygen concentration
Surface flammability	• Rate of burning • Flame spread rating • Extent of burning
Heat contribution	• Heat of combustion • Fuel equivalent • Fuel distribution rating
Smoke production	• Maximum smoke density • Total smoke production • Maximum observation rate
Fire gases	• Concentration of decomposition and combustion gaseous products
Fire endurance	• Hour ratings of resistance • Penetration time

2.1.4 Energy in the Combustion Process

In the process of combustion, products are formed and heat is liberated (exothermic reaction). The amount of thermal energy released depends on the completeness of combustion, which in turn depends on burning conditions and the types of fuel material. The amount of energy released in combustion is dependent upon the availability of oxygen. Thus, heat release is an indication of oxygen consumption (Krause et al. 1980).

In general, the quantity of heat evolved can be defined as heat of combustion when one mole of a hydrocarbon is burned completely to form CO_2 and H_2O. The values of heat of combustion for many substances at standard temperature and pressure (STP) can be found in many physics and chemistry textbooks. With the known mechanism of formation of particular species from combustion, the quantity of heat evolved can then be calculated and corrected to actual temperature and pressure of the burning environment. Table 2.4 is a list of heat-of-combustion data (i.e., kJ/g of fuel consumed). Heat of combustion can also be obtained by an approach which enables one to estimate the energy from bond strength (based on bonds broken and formed). This approach gives a good approximation when heat of combustion data for materials are not readily found in handbooks. Table 2.5 is a list of energy data for bonds between various atoms.

TABLE 2.4. Heats of Combustion[a]

Fuel	Formula	Heat of Combustion	
		KJ/g	KJ/g O_2
Organic Liquids and Gases			
Methane	CH_4	-50.01	-12.54
Ethane	C_2H_6	-47.48	-12.75
n-Butane	C_4H_{10}	-45.72	-12.78
n-Octane	C_8H_{18}	-44.42	-12.69
Polyethylene	$(- C_2H_4 -)_n$	-43.28	-12.65
Acetylene	C_2H_2	-48.22	-15.69
Ethylene	C_2H_4	-47.16	-13.78
Benzene	C_6H_6	-40.14	-13.06
1-Butanol	$C_4H_{10}O$	-33.13	-12.79
n-Butyraldehyde	C_4H_8O	-31.92	-13.08
Butryric acid	$C_4H_8O_2$	-22.79	-12.55
n-Butylamine	$C_4H_{11}N$	-37.96	-12.85
1-Butanethoil	$C_4H_{10}S$	-32.77	-12.32
Ethyl chloride	C_2H_5Cl	-19.01	-12.78
Ethyl bromide	C_2H_5Br	-11.93	-12.50
Synthetic Polymers			
Polyethylene	$(- C_2H_4 -)_n$	-43.28	-12.65
Polypropylene	$(- C_3H_6 -)_n$	-43.31	-12.66
Polyisobutylene	$(- C_4H_8 -)_n$	-43.71	-12.77
Polybutadiene	$(- C_4H_6 -)_n$	-42.75	-13.14
Polystyrene	$(- C_8H_8 -)_n$	-39.85	-12.97
Polyvinyl chloride	$(- C_2H_3Cl -)_n$	-16.43	-12.84
Polyvinylidene chloride	$(- C_2H_2Cl_2 -)_n$	-8.99	-13.61
Polyvinylidene fluoride	$(- C_2H_2F_2 -)_n$	-13.32	-13.32
Polymethyl methacrylate	$(- C_5H_8O_2 -)_n$	-24.89	-12.98
Polyacrylonitrile	$(- C_3H_3N -)_n$	-30.80	-13.61
Polyoxymethylene	$(- CH_2O -)_n$	-15.46	-14.50
Polyethylene terephthalate	$(- C_{10}H_8O_4 -)_n$	-22.00	-13.21
Polycarbonate	$(- C_{16}H_{14}O_3 -)_n$	-29.72	-13.12
Cellulose triacetate	$(- C_{12}H_{16}O_8 -)_n$	-17.62	-13.23
Nylon-6,6	$(- C_6H_{11}NO -)_n$	-29.58	-12.67
Isobutene polysulfone	$(- C_4H_8O_2S -)_n$	-20.12	-12.59

(a) Huggett 1978.

TABLE 2.5. Mean Bond Energies, kcal/mole[a]

Bond	Energy	Bond	Energy
C—C	83	O—H	110
C=C	147	O—N	150
C≡C	194	N—H	93
C—H	98	P—P	51
C—O	84	S—S	50
C=O	172	Cl—Cl	58
C—N	70	Br—Br	46
C≡N	213	I—I	36
C—Cl	78	F—F	37
C—Br	66	H—Cl	103
C—I	57	H—Br	88
C—F	116	H—I	72
C—S	62	H—F	135
O—O	33	H—P	76
O=O	119	H—S	81
N—N	38	P—Cl	76
N≡N	225	P—Br	65
H—H	104	S—Cl	60

(a) Abstracted from Pauling (1964) and Weast (1981).

In an actual fire inside a compartment, turbulent diffusion flames are important. Oxygen is supplied to reaction zones by turbulent mixing of flammable gas and air prior to ignition. As time goes on, the quantity of oxygen may not be sufficient to maintain "clean" combustion due to the earlier consumption in a confined compartment. Incomplete combustion then dominates. Total heat release at that point can no longer be estimated from the heat-of-combustion calculation.

Thus, besides the mechanisms of products formation, determining the total heat liberated in an actual fire is an additional complexity to the study of combustion (Sections 2.1.5 and 3.3).

Huggett (1978) has developed a new technique, oxygen consumption calorimetry, which measures the rate of heat release from a fire. He concluded that the heat release from a fire involving conventional organic fuels is 13.1 kJ/g of oxygen consumed, with an accuracy of ±5% or better (see Table 2.4). Using the oxygen consumption calorimetry method, Huggett also showed that incomplete combustion and variation in fuel have only a minor effect on the rate of energy release in a fire. Thus an accurate rate of heat release in a fire can be determined from three simple measurements: 1) the flow of air into the fire system, and the concentration of oxygen in 2) the inlet and 3) the exhaust streams.

Once the products of combustion become airborne, heat can be liberated or consumed by chemical reactions between combustion products and species generated earlier. These reactions may be exothermic or endothermic, depending on the nature of reactants and products in the presence of available energy. New particulate species may be formed while others disappear, but the energy example, the formation of nitrogen oxides (NO_x) via fixation of atmospheric nitrogen, is an endothermic reaction.

2.1.5 Enclosure Fires

Currently, in the field of fire science, strong emphasis is being placed on the study of enclosure fires. Ignition, fire spread, and fully developed fire inside an enclosure are the most important fire characteristics that are being studied. Among these phenomena, the aspects of both mass and energy generation in various stages of a fire are also considered in understanding the fire hazard.

Flame radiation, the size of combustion zones and flame length, air entrainment, mixing and other physicochemical processes governing the behavior of these fires are not well understood (McCaffrey 1979). Today, many basic research programs on modeling of fire flows (Alpert et al. 1981; Zukoski et al. 1981; and Alvares et al. 1980) involve the prediction of flow and heat transfer patterns produced by pool fires, crib fires, wall fires and ceiling fires. Much progress has been made in experimentally verifying their models.

Fire in a fuel cycle fabrication facility (or other nuclear facility) represents a special kind of enclosure fire. The amount and the types of combustible materials (i.e., viewing windows of gloveboxes) found in these enclosures are unique for the handling of radioactive materials. The noncombustible walls and ceiling are made of concrete and steel. The ventilation system is different, too; it draws fresh air into the enclosure or room through the ceiling ventilator, while the room air is drawn out close to the floor. The dynamics of air flow play an important role in characterizing the results of a fire in a nuclear facility. The enclosure itself is kept at slightly lower than atmospheric pressure, but this negative pressure will not significantly affect the chemistry and physics of the combustion process. As the fire grows, however, pressure in the enclosure increases. This becomes important in characterizing the flow of the fire-generated material. The increase of pressure will also suppress or enhance various chemical and physical reactions in the flame zones and their vicinities.

In a typical enclosure fire (e.g., a fire inside a fuel processing room of a nuclear facility with an ignition source on a piece of processing equipment), the amount of combustible materials and the availability of oxygen are the most important parameters which control the severity of the fire. To help illustrate the combustion process, the progress of a fire in an enclosure will be followed. Let us assume the room initially contains various equipment made of metal and plastic materials that are arbitrarily distributed throughout the room. The wall and ceiling are also constructed of combustible materials.

(Although this is not the case for nuclear facilities, this assumption is made to illustrate a "fully-involved" fire.) The room has a ventilation system where air is continuously drawn in and out through the ventilation system.

The fire starts out on some equipment in a small area in the middle of the room. In the early stages of the fire, oxygen in the flaming vicinity is continuously consumed. An oxygen concentration gradient develops and more oxygen is drawn into the fire region by means of molecular and turbulent diffusion. Both heat and smoke are generated as combustion products. At this point, flames may not reach the ceiling, although there is convective heat transfer to the ceiling since heated air and smoke rise. The smoke cloud above the burning equipment represents the buoyant heat plume, and this heat and smoke will "pool" in the upper portion of the room as times goes on.

As the fire grows and the diffusion flame becomes larger, both heat conduction and flame radiation (mainly due to the luminous part of the flame where soot particles are generated and oxided) become significant parts of heat transfer. The neighboring equipment begins to smolder as the temperature of the environment rises by various heat transport processes (convective and radiative heat transfer), generating various kinds of combustible vapors, and the quantity of these vapors depends on material properties and fire conditions. The temperature of an ordinary enclosure fire ranges from 200 to 1000°C, with a heat flux up to ~10 W/cm^2.

Both pyrolysis and combustion of materials are occurring. There may be multiple ignitions in the vicinity of the original ignition source but if a fire is to become serious, the actual number of burning objects in the lower portion of the room is not as important as the conditions in the zone of hot gases filling the upper portion of the room. At this stage of fire growth, the instant the flames impinge against the ceiling constitutes one of the most important events since combustible gases from pyrolysis and incomplete combustion, or the ceiling itself, can ignite and contribute to the burning in the room. These flames add to the heated zone at the ceiling and reinforce the radiation process which is bathing the entire room. One of the most important consequences of this radiation contribution is that other combustible materials in the process of pyrolysis are ignited. For example, cleaning paper and rags on the rack and eventually other equipment in the room start burning.

As more heat and combustible gases generated from pyrolysis build up in the room and there is increased air flow into the room by the pumping action of the fire plume, there is a point in time known as flashover when all the combustible material in the room ignites and begins to contribute to the fire. From that moment on, the fire in such a room is considered "fully involved." A steady-state fire condition may be achieved with consumption of oxygen and generation of combustion products at some fixed state. The duration of steady-state combustion depends mainly on the chemical and physical properties and the amount of combustible materials that remain. Due to the complexity of the combustion process, the steady state may only exist for an extremely short period of time after the fire growth is exceeded. It is very difficult to pinpoint

this moment and attempt mathematically to predict the fire process. Although steady-state combustion can be described mathematically it is not meaningful for an actual fire.

Although the ventilation system inside the nuclear facility is designed differently than most other enclosures (i.e., houses or industrial buildings), no significant differences in burning are expected initially because in the ventilated fire stage, the amount and the nature of the combustible materials control the progression of the fire. Both combustion products and unburnt vapors and hot gases are generated. The average mass density of these gases is much less than that of the surrounding atmosphere. This makes the gases buoyant and they accelerate upward, creating a pressure change which tends to draw fresh air into the fire. The rate of production and the temperature of hot gases from a fire depend strongly on the rate of air entrainment in the fire plume (Zukoski et al. 1981). As the gas layer builds up from the ceiling (i.e., ceiling layer or hot gas layer), the ceiling inlet air carries some of these gases, during mixing, back to a cooler area (i.e., cool layer or lower layer of an enclosure). Thus the air supplied to the flame may contain portions of combustion products and unburnt vapor or gases from the hot layer. The fraction of hot gases entrained depends on their density. These hot gases will not escape the room until they reach the outlet ventilators near the floor. There is a possibility that they may never reach the exit ventilators, not because the fire ceases, but because the increase in pressure inside the enclosure can cause backflow of the ventilated air inlet from the ceiling. As more burnt and unburnt gases are entrained, the fire becomes "oxygen controlled" (i.e., when oxygen concentration is insufficient to maintain combustion).

Thus depending on the availability of oxygen and the size of the enclosure, the fire inside a nuclear facility can be a very smoky ("dirty") fire. One would anticipate that the characteristics of the combustion products and the amount of energy release can be quite different depending on the orientation of the ventilation system. The ventilated air flow rates into and out of the room also play an important role in the characterization of combustion products.

Many enclosure fire studies have been concerned with more sophisticated problems of combustion phenomena that can affect the characteristics of combustion products. Most of these problems have not been resolved, however, and the understanding of the radiative and turbulent aspects of a fire is limited. Thus entrainment models (e.g., by Zukoski et al. 1981) and many other physicochemical processes (e.g., flame radiation, chemical reactions, etc.) governing the behavior of a fire will not be discussed in this review.

2.1.6 Mass and Heat Generation in the Combustion Process

Both mass and energy generation in a fire do not operate independently of each other. The amount of fire-generated products and the heat generation rate depend on the chemical and physical characteristics of the combustible materials and the availability of oxygen under various fire conditions. In the

studies of physicochemical and combustion/pyrolysis properties of polymeric materials and heat release rate in fires, Tewarson et al. (1980a,b) relate the heat generation rate as a function of mass generation rate. The details of this information and the mass-energy relationship are summarized in Section 3.3. The mass generation rate of some chemical species can also be estimated by knowing the fraction of the species found in the exhaust gases. (See also Section 3.2.1 and Tables 3.10, 3.11 and 3.19 for the tabulation of some experimental mass and energy generation data from combustion of the materials of interest.)

Consider a fire of a glovebox in a fuel cycle facility as a typical enclosure fire. Initially, energy is given off as the result of combustion. The amount of energy generated is the function of:

● the mass and chemical composition of fuel vapors (pyrolysates) evolved from the glovebox materials during the pyrolysis reaction

● the amount of oxygen present and the diffusion efficiency of oxygen to the flame front

● the efficiency of the chemical processes to convert fuel vapors to various products of complete and incomplete combustion.

If all the generated vapors react (are burned) to yield combustion products, total heat release can be obtained simply from the heat-of-complete-combustion table (Table 2.4) by summing the heat contributions of individual materials of the glovebox. These values are based on the following assumed products of combustion: CO_2, H_2O (vapor), HF, HCl, Br_2, SO_2, and N_2.

In the case of an actual fire, however, the fuel vapors do not completely burn; thus actual energy released is only a fraction of the total energy resulting from complete combustion. The ratio of actual to complete heat of combustion is normally defined as combustion efficiency X_a of the fuel. (Section 3.3 discusses energy release rates, and a list of X_a for the materials of interest is found in Table 3.21.)

According to Tewarson et al. (1980a), a portion of the actual energy generated heats the gases (convective heat energy), while the remainder is flame-radiative heat energy. Therefore, actual heat of combustion is the sum of convective and radiative heats of combustion. It follows that the combustion efficiency X_a is the sum of the convective and radiative fractions of heat of complete combustion (X_c and X_r, respectively). The values of X_a and X_r for various combustible materials can be found in Tables A.1.2 and A.1.4 of Appendix A.1 and Table A.2.1 of Appendix A.2.

Radiation from soot particles, CO_2, and water vapor (flame radiation) is the primary heat transfer mode in large-scale fires that induce fuel gasification/pyrolysis. The flux of this radiation depends on the above species concentration, flame temperature and geometry. Again, this shows that energy generation, especially the radiative fraction, is strongly dependent on the type and amount of material generated in large fires.

The chemical composition of fuel vapors and products can change significantly in various stages of a fire and thus actual, convective and radiative heat releases will also change. Tewarson et al. (1980a) presented the data of actual and convective heats of combustion of red oak as functions of time for two external heat flux values for piloted and auto-ignition (see Figure 2.1). The heats of combustion vary with time, external heat flux and the mode of ignition.

The unburned fuel vapor from the flaming glovebox is entrained with the burned gases and air to the ceiling layer via the fire plume. According to Pagni and Shih (1976), all the unburned vapors which enter the upper layer are called excess pyrolysate. As this gas flows from the glovebox, it spreads the fire throughout the structure by burning whenever it reaches ambient oxygen at sufficiently high temperature. Additional amounts of excess pyrolysate may be contributed from combustible material which is smoldering or decomposing due to heat given off by burning objects in the vicinity. This phenomena is believed to be responsible for the rapid involvement of the entire structure observed in full-scale fire tests.
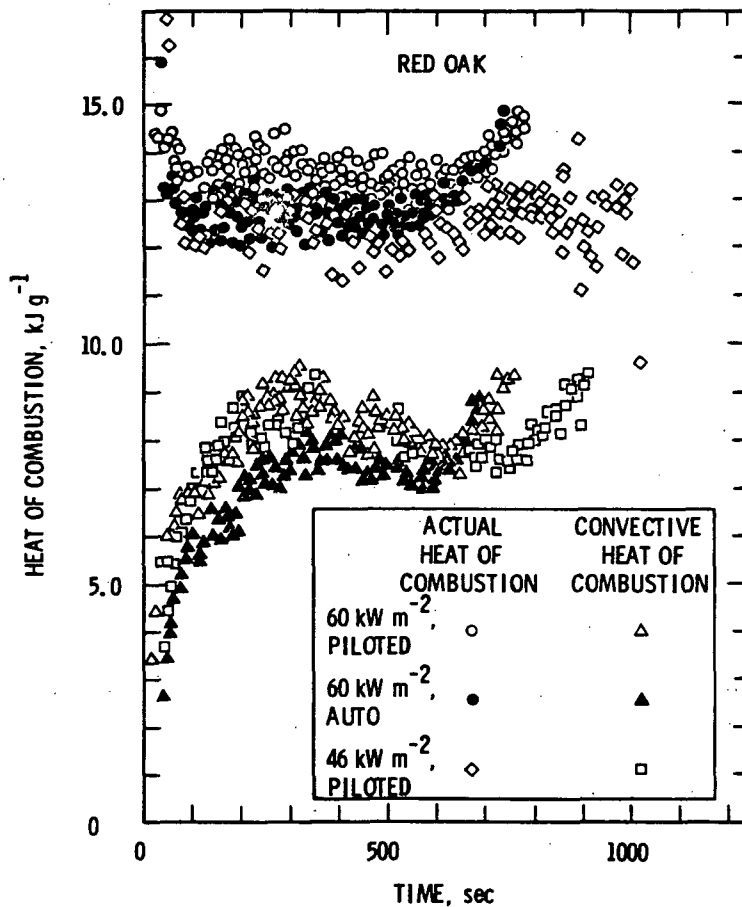
FIGURE 2.1. Actual and Convective Heats of Combustion of Red Oak as Functions of Time

The above example shows that neither mass nor heat generation should be considered independently when analyzing fires in nuclear fuel cycle facilities.

2.2 MECHANISMS OF SOOT FORMATION

The generation of soot particles in flames is not only responsible for the radiant energy in a fire and the amount of these particulate materials airborne, but also their rate of growth, which can affect the rate of filter plugging in nuclear facilities. Particles deposited continuously onto the filter can eventually lead to plugging and breakage of filter elements due to the high pressure that can result from the restrictive flow of burnt gases (from the fire) to the atmosphere. The behavior of airborne particulate materials and how it affects their growth are discussed in Section 2.3. Section 3.2.1 is a collection of experimental data on particulate generation rate for the materials of interest.

This section covers the state-of-the-art studies on soot formation in flames. In the literature, the study of the mechanisms of soot formation is usually divided into two tasks:

- Chemical Task--which deals with the formation of soot precursors from fuel and looks into the possible initiation of the nucleation process. The kinetics of these chemical reactions are of prime concern.

- Physical Task--which deals with the limitation on the growth of freshly formed carbon particles to a certain size. In other words, this part of the study concentrates on the behavior of the airborne materials as discussed in Section 2.3.

Many recent articles were found in which the authors describe their attempts to collect data for elucidation of the mechanisms of combustion product formation. These investigators have studied only the flame zones of both premixed and diffusion flames. No exact mechanisms have been identified that may be combined with some of the well-defined behavior of airborne materials to enable a better understanding of combustion phenomena.

The formation of organic matter (soot and hydrocarbons) in premixed flames has been a mystery for many years, and studies of this area are still continuing. The polycyclic aromatic hydrocarbons (PCAHs) found with soot collected from premixed flames have been considered as end products of side reactions of other reactive cyclic intermediates, and not themselves intermediates in the process of soot formation (D'Alessio et al. 1974). This belief was questioned by those who observed that the PCAH compounds are intermediate in the formation of the large polybenzenoid radials which constitute soot. D'Alessio's study concluded that there are two distinct groups of PCAHs: the "unreactive" PCAHs, which are byproducts of soot formation; and the "reactive" PCAHs, which account for the formation of only a small fraction of the soot observed in both premixed high and low pressure flame.

2.16

For diffusion flames, there is even more uncertainty about the mechanisms of soot formation (Boisdron and Brock 1972). In diffusion flames of organic compounds it is generally believed that soot formation depends on pyrolysis, which at the same time is attended by polymerization rather than degradation. There is some evidence that soot particles are formed by two possible processes within the pyrolytic zones of diffusion flames, one involving nucleation of solid carbonaceous materials from reaction of the intermediate pyrolysis and the other involving free radical polymerization of the products of pyrolysis to yield long chain polymers which may subsequently condense and appear finally as "soot droplets."

The following models, which describe the chemical aspects of soot formation, were briefly discussed by McHale and Skolnik (1979) and Chien and Seader (1975).

2.2.1 Carbon Formation by Charged Bodies (ionic nucleation)

This model, which was proposed by Howard in 1969, is based on the belief that a neutral precursor acquires a charge. Howard believed that the charged precursors do not agglomerate until the particles are large enough to overcome their electrostatic repulsion between crystallites. Howard predicted that the size necessary for agglomeration under normal flame conditions is 20 to 30 Å, which is in agreement with experimental values. Chains will then be formed after particle growth ceases due to the insufficient kinetic energy to overcome electrostatic repulsion. However, this model became unreliable after the study by Wersborg et al. in 1971 to 1973, who claimed that the approach of the model is weak due to its simplicity and the fact that most particles in a flame are not charged.

2.2.2 Polymerization and Dehydrogenation via Acetylene

It was initially proposed by Porter (1953) that carbon or soot particles are formed by two simultaneous chemical reactions--polymerization and dehydrogenation. First of all, fuel material is decomposed by heat; then acetylene and its intermediates (i.e., free radicals, ions, etc.) are found. The process of polymerization, which yields polyacetylenes, is followed by dehydrogenation, which yields soot particles. The polymerization process is thought to involve acetylene with a series of reactions with free radicals to give a distribution of polyacetylenes and then free radicals, according to the following scheme (Boisdron and Brock 1972; Bonne, Homann and Wagner 1965):

$$
\begin{array}{ccc}
PA \longrightarrow & PA \longrightarrow & PA \longrightarrow \\
+ & + & + \\
\end{array}
$$

$$
C_2H + C_2H_2 \longrightarrow \substack{C_4H \ (+H_2) \\ C_4H_2\ (+H)} + C_2H_2 \longrightarrow \substack{C_6H \ (+H_2) \\ C_6H_2\ (+H)} + C_2H_2 \longrightarrow \substack{C_8H \ (+H_2) \\ C_8H_2\ (+H)} \longrightarrow
$$

$$
C_2H_3 + C_2H_2 \longrightarrow C_4H_3 \ (+H_2) + C_2H_2 \longrightarrow C_6H_3 \ (+H_2) + C_2H_2 \longrightarrow C_8H_3 (+H_2) \longrightarrow \quad (2.2)
$$

$$
\begin{array}{ccc}
+ & + & + \\
PA \longrightarrow & PA \longrightarrow & PA \longrightarrow \\
\end{array}
$$
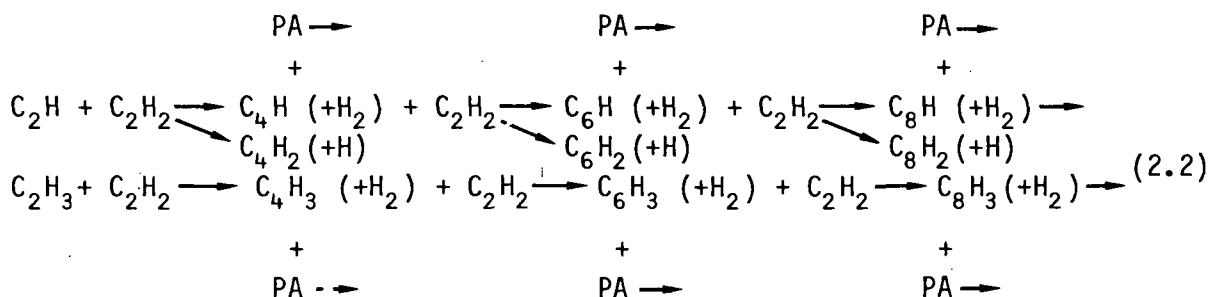
where PA = polyacetylenes. Polyacetylenes up to $C_{12}H_2$ were detected in the study by Bonne, Homann and Wagner (1965). For the overall view of soot formation via acetylene, Williams and Smith (1970) presented a scheme (Figure 2.2) which involved many possible routes.

$$C_2H_2$$

POLYACETYLENES   IONS C_2 RADICALS

(POLYMERIZATION)

NUCLEI

(POLYACETYLENES)

POLYMERIC AROMATICS AND → CARBON PARTICLES AND
POLYMER-LIKE MATERIALS   POLYMERIC SOLIDS   →   SOOT

(AGGLOMERATION,
FURTHER REACTIONS, ETC.)
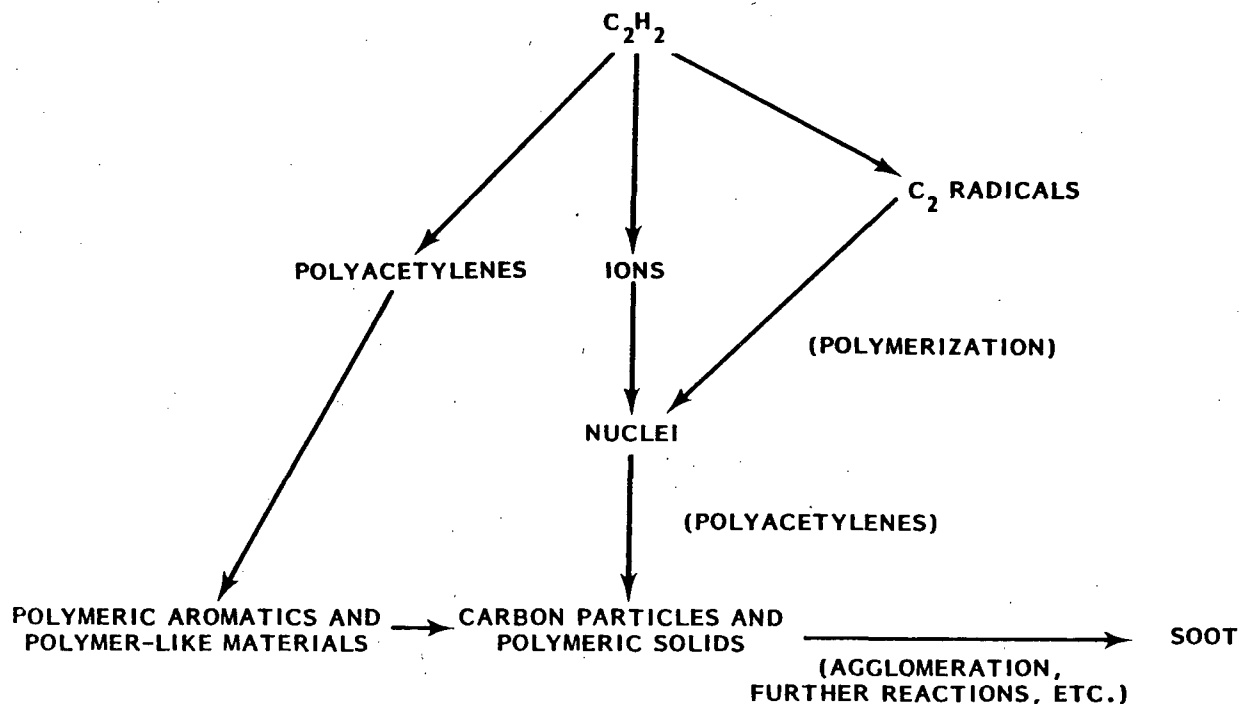
FIGURE 2.2. Summary of Possible Mechanisms of Soot Formation
via Acetylene

2.2.3 Polymerization via Aromatics and Polycyclics

Rummel and Veh (1941) believed that prior to carbon formation, aromatics and polycyclic hydrocarbons are formed in the combustion of hydrocarbon fuels. In a study by Gaydon and Wolfhard (1970), experimental evidence revealed that it is unlikely aromatics and polycyclics are intermediates in soot formation; Palmer and Cullis (1965) proposed that highly unsaturated aliphatics may serve as soot precursors.

2.2.4 Condensation and Graphitization

Condensation occurs when the partial pressure of the vapor pressure becomes higher than the saturated vapor pressure. These condensing vapors form liquid droplets which then graphitize. Parker and Wolfhard (1953) suggest that the formation of soot obeys this mechanism, and it is currently believed to be one of the more promising explanations. They also believed that this mechanism may account, at least partially, for the type of liquid aerosol or smoke that

2.18

results when polymers are pyrolyzed in a nonflaming combustion mode. Chien and Seader (1975) suggested that this mechanism of soot formation is most likely found in diffusion flames, where the residence time is relatively long in the pre-carbon zone. Since graphitization is a process which requires high temperatures and long time periods to occur, the residence time of the particles in a premixed flame is sufficient to form large graphite layers (Bonne, Homann and Wagner 1965). This was also confirmed by x-ray investigation of the soot collected.

2.2.5 Nucleation

There are two principal mechanisms in nucleation (Boisdron and Brock 1972): chemical and physical. Formation of soot particles in combustion processes is an example of chemical nucleation. The second mechanism involves growth from supersaturated vapor and classifies further as either homogeneous or heterogeneous physical nucleation. The study of soot particle formation began in 1959, when Tenser pointed out that nucleation may occur in flaming combustion systems. In 1965, Palmer and Cullins concluded in their study that polyunsaturated hydrocarbon compounds are responsible for the initiation of the nucleation process, which was strongly supported by the work of Bonne, Homann and Wagner in the same year. For example, in an acetylene-oxygen flame at low pressure, Bonne and his associates were able to identify and trace the concentrations of the species C_2H_2, C_4H_2, C_6H_2, C_8H_2, and $C_{10}H_2$ throughout the entire flame zone. Bittner (1978) collected and illustrated a summary of mechanisms proposed over the years in Figure 2.3.

The figure summarizes all the possible mechanisms of soot formation via various identified intermediate species. Since soot particles contain much lower ratios of H/C than fuel molecules do, soot formation must involve processes of dehydrogenation (moving left to right in Figure 2.3) and aggregation (moving top to bottom). Two extreme routes, the C_2 route and the saturated polymer route, are believed to occur at 3000 and 700°K, respectively. In the temperature range of 1200 to 2200°K, the possible mechanisms which are represented by the central portion of Figure 2.3 are most likely to occur in soot formation. The role of PCAHs, which were thought to be stable byproducts, is illustrated in the center of the figure. Polycyclic aromatic hydrocarbons have also been proposed as intermediates of soot formation because they have sufficiently low vapor pressures to physically condense to liquid droplets, which then form soot.

Based on the complexity and the uncertainty of product formation in flames, more quantitative data on this phenomenon are necessary to solve this mystery.

2.3 BEHAVIOR OF AIRBORNE MATERIALS

Now that we have discussed the formation of soot and other possible chemical species in flames, there are questions to be answered concerning the behavior of those airborne particles as they leave the flame zone. For example, the change in particles as a function of time with various forces has been a main
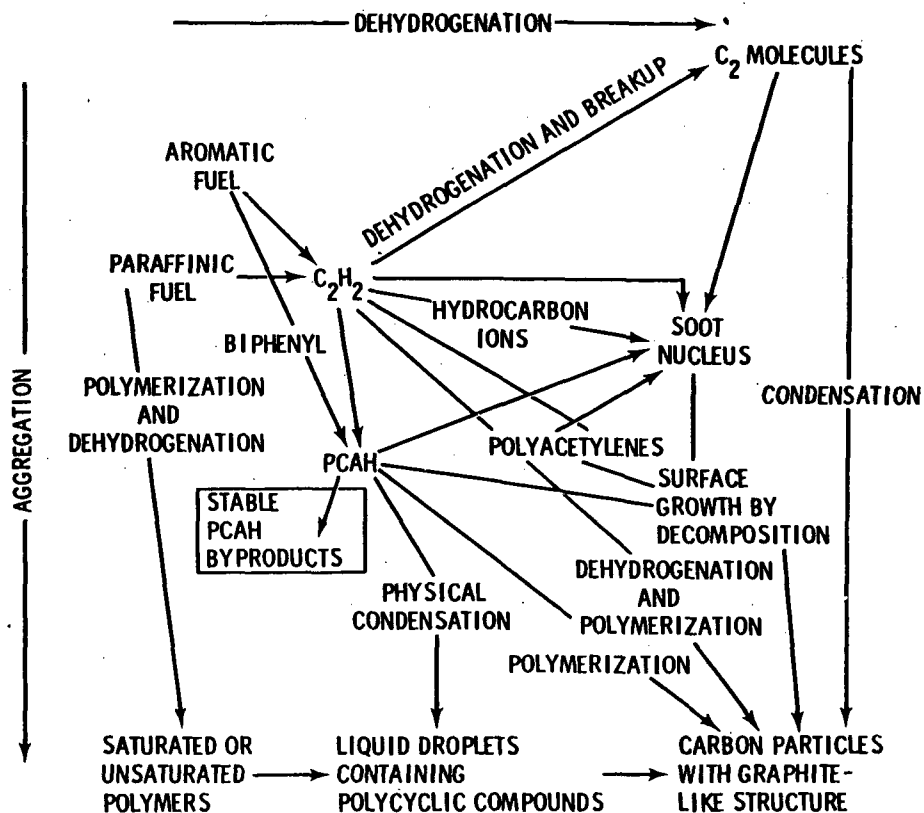
FIGURE 2.3. Summary of Proposed Mechanisms of Soot Formation

concern in fire study. In fact, the study of these particle characteristics is necessary for fire safety and environmental concerns. Changes through time in the conditions of the airborne materials can occur by the following mechanisms (Chien and Seader 1975):

- shear
- evaporation
- condensation
- coalescence (agglomeration)
- settling
- diffusion.

Measurements have been made on the characteristics of airborne materials (i.e., soot and smoke) utilizing laws of optical scattering phenomena (Bouguer's law and Mie theory, etc.), which assume stable smoke suspension. Therefore, the influence of the above mechanism on particle suspension stability can strongly affect the accuracy of the measurements. This is especially significant for the unstable particles of smoke in the vicinity of the flame zone, where the magnitude of external forces (i.e., thermal energy, concentration gradient, etc.) is still great.

Theories describing the particulate behavior for most of these mechanisms are currently available (Chien and Seader 1975). In particular, theories for the phenomena of particle settling and agglomeration have gained the most attention in combustion product study.

2.3.1 Coalescence[a]

Coalescence of airborne particles occurs when they collide with one another and larger particles are formed as a result. The mechanisms and forces causing the collisions are thermal, electrical, magnetic, hydrodynamic, gravitational, etc. Some of these mechanisms may act concurrently, generally in the presence of thermal effect.

For thermal coalescence, particles airborne into the atmosphere above the flame have a tendency to merge together because of Brownian motion or diffusion. The rate of decrease of particulate concentration by these "sticky" collisions is governed by a decay rate equation:

$$\frac{dN_p}{dt} = -KN_p^2 \tag{2.3}$$

where N_p = particulate concentration/cm^3
t = time, sec
K = a rate constant.

The above equation can then be integrated to express particulate concentration as a function of time:

$$\frac{1}{N_p} = \frac{1}{(N_p)_o} + Kt \tag{2.4}$$

where $(N_p)_o$ is the initial particle concentration. Experimental values for K ranged from 5×10^{-9} cm^3/sec for typical particulate clouds to 4×10^{-10} cm^3/sec for very fine material (Corrin 1974). Equation (2.4) can be further reduced to relate the particulate growth in transit. By using Bouguer's law for monochromatic light as applied to smoke of uniform particulate size and concentration (based on single scattering phenomena) with Equation (2.4), Chien and Seader came up with the following equation:

(a) The words "agglomeration and "coagulation," frequently found in combustion literature to describe the behavior of particles, are usually used synonymously (Burgess, Treitmar and Gold 1979). In this report the term "coalescence" will be used in their place.

$$d = \left[d_o{}^3 + \frac{6K\ M_p\ t}{\pi\ \rho_p\ V} \right]^{1/3}$$

<div align="right">(2.5)</div>

where d_o and d are initial and time-dependent particulate diameters, respectively, M_p is the total particulate mass, ρ_p is the particulate density, and V is the test chamber volume.

Assuming a particulate density ρ_p of 1.3 g/cm³, Chien and Seader show a plot of particulate diameter as a function of time for two different initial particulate diameters of 0.05 and 0.5 μm [Equation (2.5)] using the standard volume of a flow-through combustion chamber (Figure 2.4). Notice that total mass concentrations of 0.5 to 2.5 μg/cm³ are used as parameters in the plot. Figure 2.4 also shows that the initial particulate size is a significant factor only during the first few minutes. Very small particles coalesce rapidly at first.

2.3.2 Settling

Gravitational force causes interacting particles to fall as their accumulated mass overcomes the buoyancy and drag forces that originally suspended the particles. For spherical solid particles, settling theory has been well developed and Stoke's law applied. The law relates the terminal settling velocity with other parameters as follows (Chien and Seader 1974):
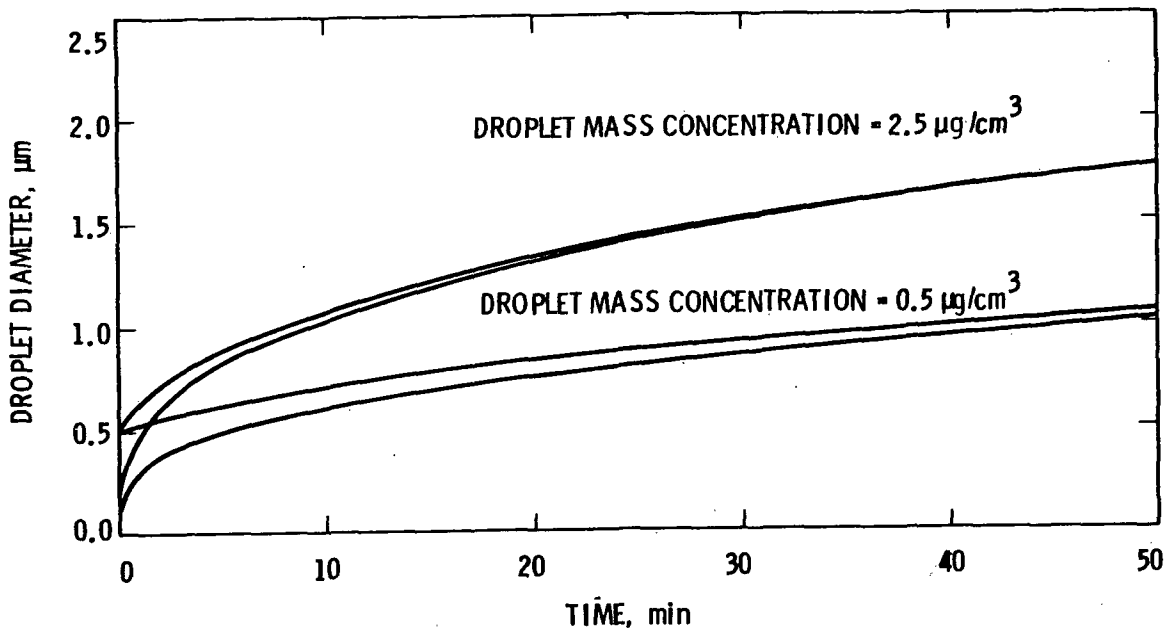
FIGURE 2.4. Effect of Coalescence on Growth of Droplets

$$V_t = \frac{g \, d^2 (\rho_p - \rho)k}{0.18 \, \mu} \qquad (2.6)$$

where
V_t = terminal settling velocity
g = acceleration due to gravity
d = particulate diameter
ρ = density of the gas stream
k = Cunningham correction factor
μ = gas viscosity.

Equation (2.6) contains the Cunningham correction factor k, which is appropriate when the particle size reaches the mean-free path of the fluid molecules. The correction is directly proportional to temperature and inversely proportional to particle size. When droplets form by condensation and then fall through a still gas, one can also utilize Stoke's law to evaluate their terminal settling velocities, provided that the droplets remain essentially spherical and behave like solid particles. Notice that Equation (2.6) applies only to particles smaller than about 10 μm dia.

To predict the particulate and droplet settling in a flow-through combustion chamber under fire-test conditions, Chien and Seader calculated the corrected terminal settling velocity with corresponding k value as a function of particle diameter. Their results are tabulated in Table 2.6 (with air temperature at 70°F and pressure 1.0 atm).

TABLE 2.6. The Minimum Time for Particulates and Droplet Settling in a Flow-Through Combustion Chamber

Droplet Particulate Diameter, μm	Corrected Terminal Settling Velocity, ft/min	Cunningham Correction Factor, k	Minimum Time to Settle at Bottom of Chamber, min
0.1	0.000221	2.88	6500
0.25	0.000806	1.682	1800
0.5	0.00254	1.325	600
1.0	0.00890	1.160	150
2.5	0.0512	1.064	30

The last column in Table 2.6 represents the time required for the corresponding particle sizes to settle 1.5 ft, the height of the chamber. These calculated values indicate that the extent of droplet and particle settling during the first 10 min of a combustion test would be almost negligible.

2.23

2.3.3 Summary

The behavior of airborne materials from a combustion process may affect the stability of suspended smoke particles, which in turn determines the accuracy of measurements of smoke properties. Two important conclusions can be drawn from the literature for two possible mechanisms of particulate behavior:

1. Coalescence. Particle size increases rapidly during the first few minutes after a particle is formed, as shown in Figure 2.4. After 20 min the size becomes fairly constant, especially for low particulate mass density. This implies that by knowing how fast the particles travel, more accurate measurements can be made at a known distance (where particles become stable) from the initial particle source. Although this known distance might be quite far in comparison to the size of the test chamber, unless the particles are moving extremely slowly, which is not the case in a fire, one can use Equation (2.5) to predict the particle diameters as a function of time, provided that the other factors in the equation are known.

2. Settling. Based on the values in Table 2.6, the settling of the combustion-generated particulates (usually <1 μm dia) would be negligible during the first 10 min of the test.

2.4 FACTORS THAT INFLUENCE THE GENERATION OF SMOKE

Extensive studies have considered the effects of various chemical and physical factors on the generation of combustion products. Chien and Seader (1974) have presented a list of factors (Table 2.7) such as light transmission; airborne mass loss; and particulate mass and size, shape, and phase state which affect smoke characteristics.

Both experimental and theoretical studies contribute valuable information on how certain factors affect the generation of combustion products. Tsuchiya and Lier (1975) made a theoretical study of the chemical composition of the surrounding environment of building fires. By assuming complete mixing of all components in the system, the reaching of equilibrium both chemically and thermally by all reactions, and uniform gas temperatures and composition, they relate the following parameters: 1) nature of fuel, 2) adequacy of oxygen supply, 3) temperature, 4) quantity of each combustion product, and 5) quantity of combustion heat. Of these five groups of variables, if any three are fixed, the remaining two may be determined by solving the simultaneous equations of material conservation, heat conservation, and chemical equilibrium. Some of the general conclusions made by Tsuchiya and Leir have been proven experimentally. For example, the quantity of CO produced from carbon-containing materials increases with increasing temperature.

King (1975) stated that factors which can govern a material's tendency to smoke and produce CO include material composition, density, weight, thickness, external surface characteristics, geometry heat flux, air flow, oxygen availability and pressure. He concluded that combustion can change from a flaming

TABLE 2.7. Factors That Affect the Characteristics of Combustion Products

Chemical Factors	Physical Factors
Fuel types	Exposed surface area
Fire retardants	Sample thickness, weight and density
Surface coatings	Orientation
Functional groups	Enclosure volume
	Heat flux
	Oxygen availability
	Ventilation
	Space temperature
	Char formation
	Coagulation, settling
	Diffusion
	Polydispersion

to a smoldering mode as the oxygen concentration is depleted. Many other investigators provided similar information, and they claimed that the quantity and nature of combustion products generated from flaming and nonflaming combustion processes are determined mainly by the chemical and physical nature of materials, the temperature, and the oxygen supply.

2.4.1 Chemical Factors

Types of materials and the fire retardants and surface coatings found on them are some of the more important chemical factors considered in many combustion or fire studies. These factors can drastically change the characteristics of combustion products. The chemistry of these changes can easily be determined by differential thermal analysis, thermogravimetry and time-of-flight mass spectrometry (Hilado 1969).

Gross, Loftus and Robertson (1969) have studied how surface coatings can alter the smoke production of an exterior-grade plywood 1/4-in. thick under nonflaming conditions. The results are plotted in terms of specific optical density and transmittance versus time (shown in Figure 2.5).

Gross' study also presented the smoke accumulation curves for both smoldering and flaming specimens of various materials (shown in Figures 2.6 and 2.7). They summarized that the maximum smoke accumulation values for the flaming tests were always less than those for the smoldering tests, except for PS and PVC (noncellulosic materials), which have rapid rates of smoke production under flaming conditions.

Seader and Einhorn's studies (1976) generally agreed with the above study by Gross, Loftus and Robertson. They showed that some materials, particularly rubber, exhibit large values of smoke accumulation, while glass fiber insulation, chlorinated PVC, asbestos fiber insulation, polytetrafluorethylene, and polyvinylbutynol have low values of smoke accumulation for both nonflaming and flaming conditions.
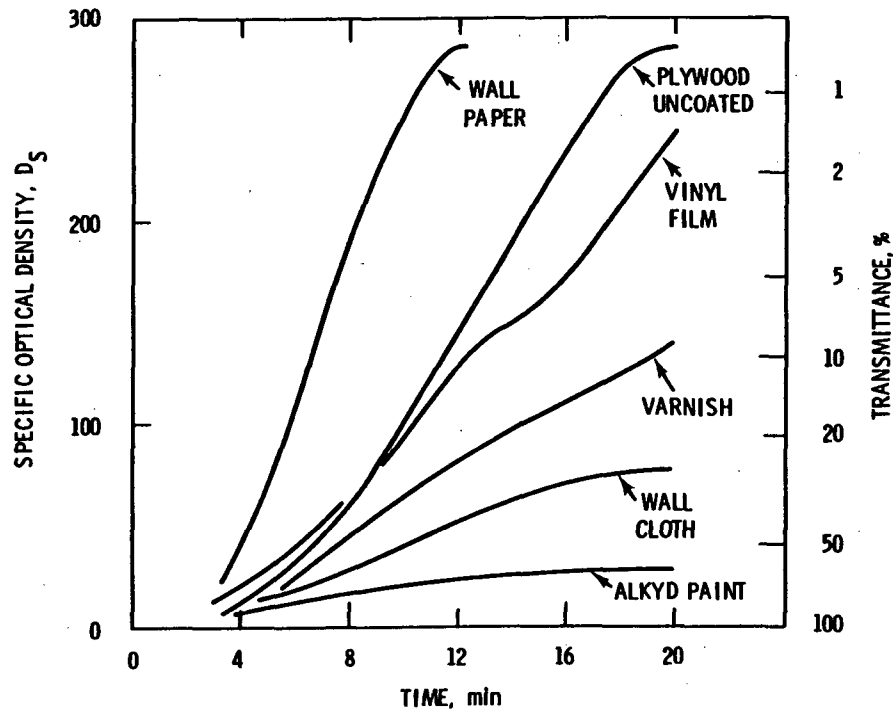
FIGURE 2.5. Effect of Surface Coatings on Smoke Buildup for Plywood in Nonflaming Exposure

In general, fire retardants are thought to increase smoke density or opacity (Seader and Einhorn 1976). However, if materials tend to melt and drip as they burn, this may alter the effect of fire retardants. The complexity of additive interactions for various materials of building construction, interior design, etc., will continue to be the main concern for fire-retardant treatments.

2.4.2 Physical Factors

In general, some of the well-known physical factors which influence the generation of smoke during small-scale fire experiments are sample weight (density) and thickness, its orientation and exposed surface area, heat flux, oxygen availability and ventilation, space (ambient) temperature, pressure, and particulate coalescence. Parameters that specifically affect particle size and/or particle statistics include relative humidity and rate of smoke generation (Welker and Wagner 1977; Gross, Loftus and Robertson 1969). Some of the important physical factors are examined below.

2.4.2.1 The Material Itself

Three physical factors influencing smoke generation which are commonly found in combustion product studies are material thickness, material density and horizontal or vertical orientation. Seader and Einhorn have collected the

2.26
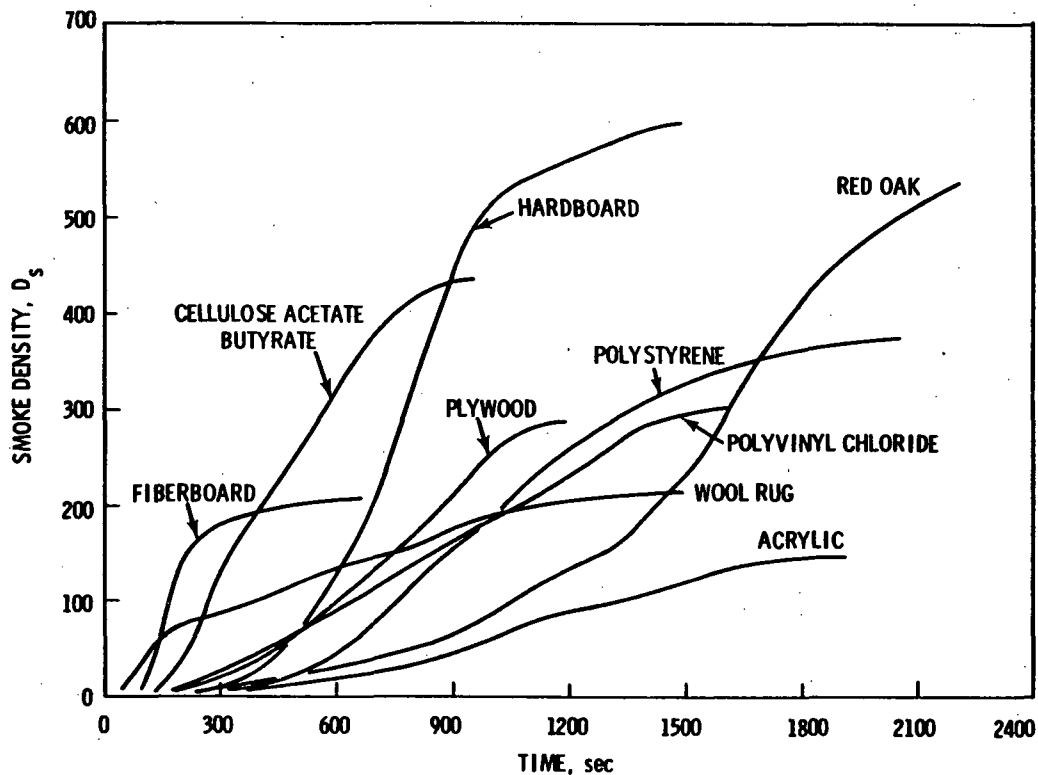
FIGURE 2.6. Smoke Accumulation Curves for Smoldering Samples of Various Materials

results from several combustion studies that show how these physical factors have affected smoke production (Figures 2.8, 2.9, and 2.10). As shown in Figure 2.8, for thin materials or layers of the same material, the specific optical (smoke) density is almost directly proportional to the thickness. According to Seader and Einhorn, when a certain critical thickness is exceeded, the specific optical density remains essentially constant with increasing thickness. This critical thickness varies and may depend on several other factors including sample density, thermal conductivity, and tendency to form a char layer; for nonfoamed plastics, the critical thickness may be as small as 0.25 in. In Figure 2.9, adapted from Zinn and Cassanova's work (1976), smoke forms faster for horizontal materials than for vertical materials. They stated that this is true for both thermoplastic and nonthermoplastic materials. In Figure 2.10, the relationship between the maximum specific optical density of rigid-urethane foam and foam density is fairly linear. Figure 2.10 also illustrates that a thinner rigid-urethane foam produces less smoke under the non-flaming mode of the fire test, while for the same thickness, the foam produces more smoke in a nonflaming mode than in a flaming mode of combustion.
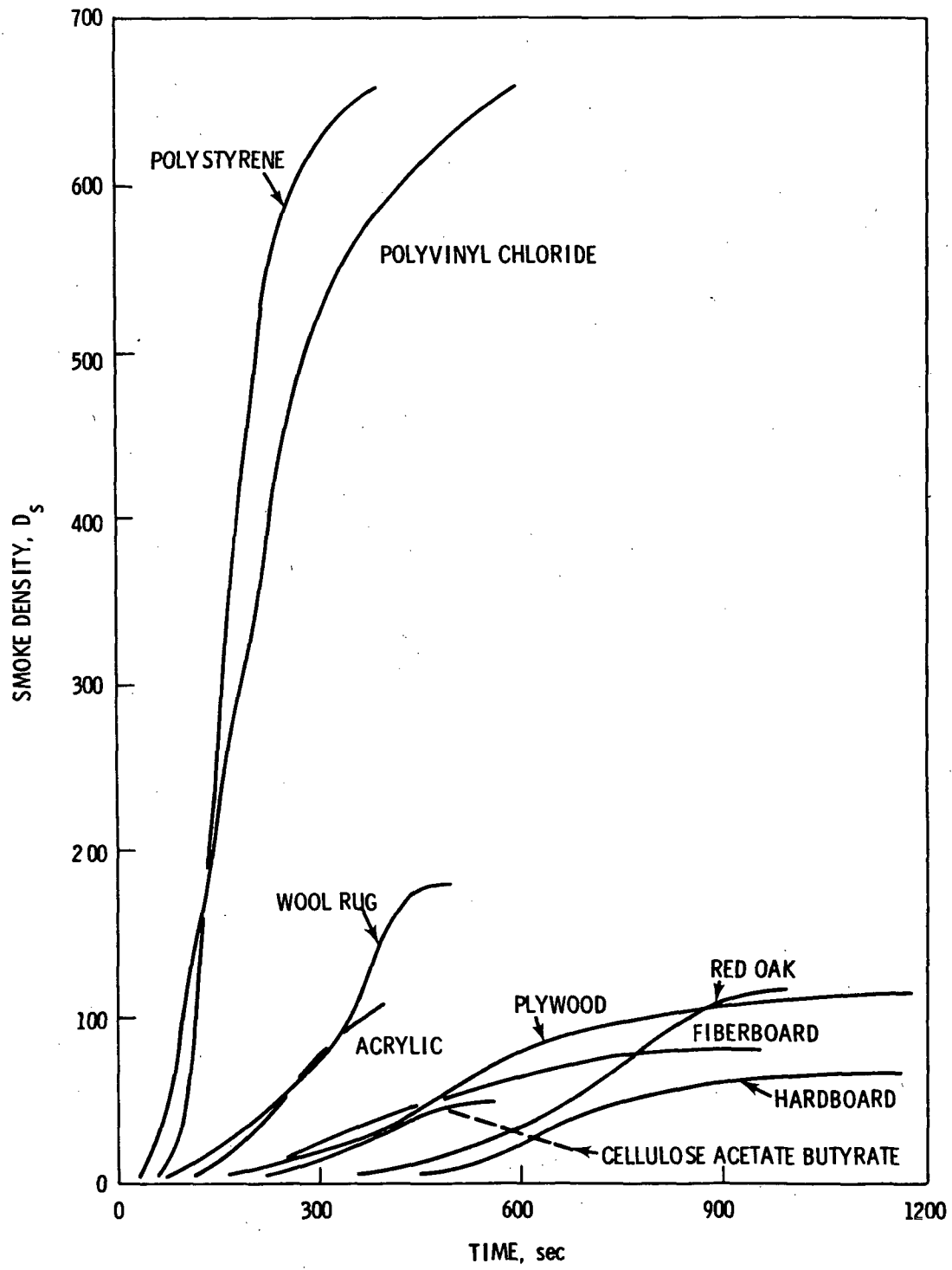
FIGURE 2.7. Smoke Accumulation Curves for Active Flaming
Combustion of Samples of Various Materials

2.28
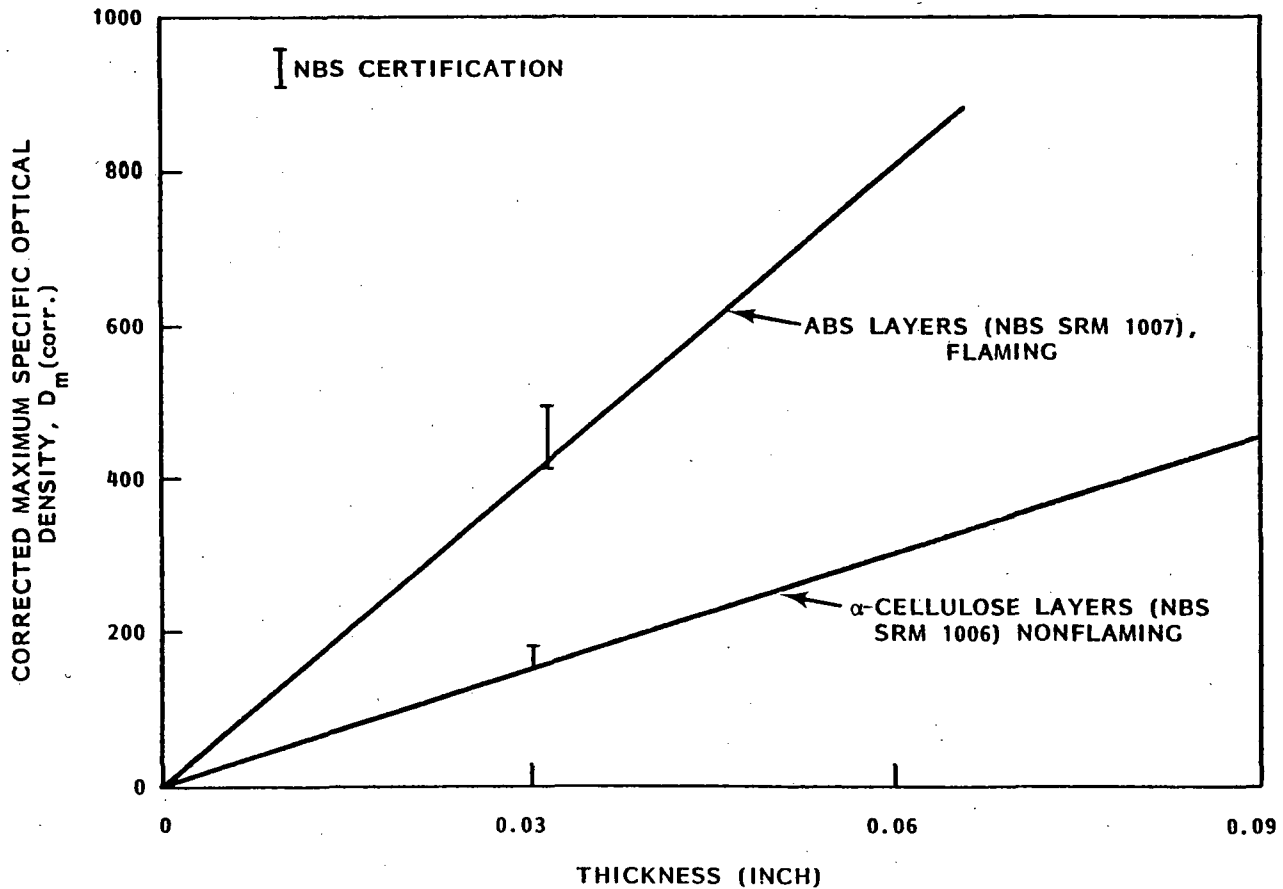
FIGURE 2.8. Effect of Layer Thickness on Maximum Specific
Optical Density

2.4.2.2 Temperature

Temperature is a major factor that will predetermine the existence of combustion. According to Hilado (1970), the temperature of burned gas is much higher than the ignition temperature, and the difference between these two provides the driving force for maintaining combustion. The fire is extinguished when the difference is too small to support combustion. In an actual fire, a material is subjected to a broad range of irradiance levels, from pre-ignition to flashover.

From the burning of hardboard (batch operation) in a small-scale smoke chamber (where smoke is confined to the chamber during testing), Gross, Loftus and Robertson (1969) observed that smoke accumulation from pyrolytic decomposition was low at temperatures below 300°C, and peak smoking occurred when the temperature was approximately 380°C (see Figure 2.11). At higher temperatures, self-ignition with flaming combustion occurred, reducing smoke accumulation drastically. At very high temperatures the smoke accumulation again increased.

2.29
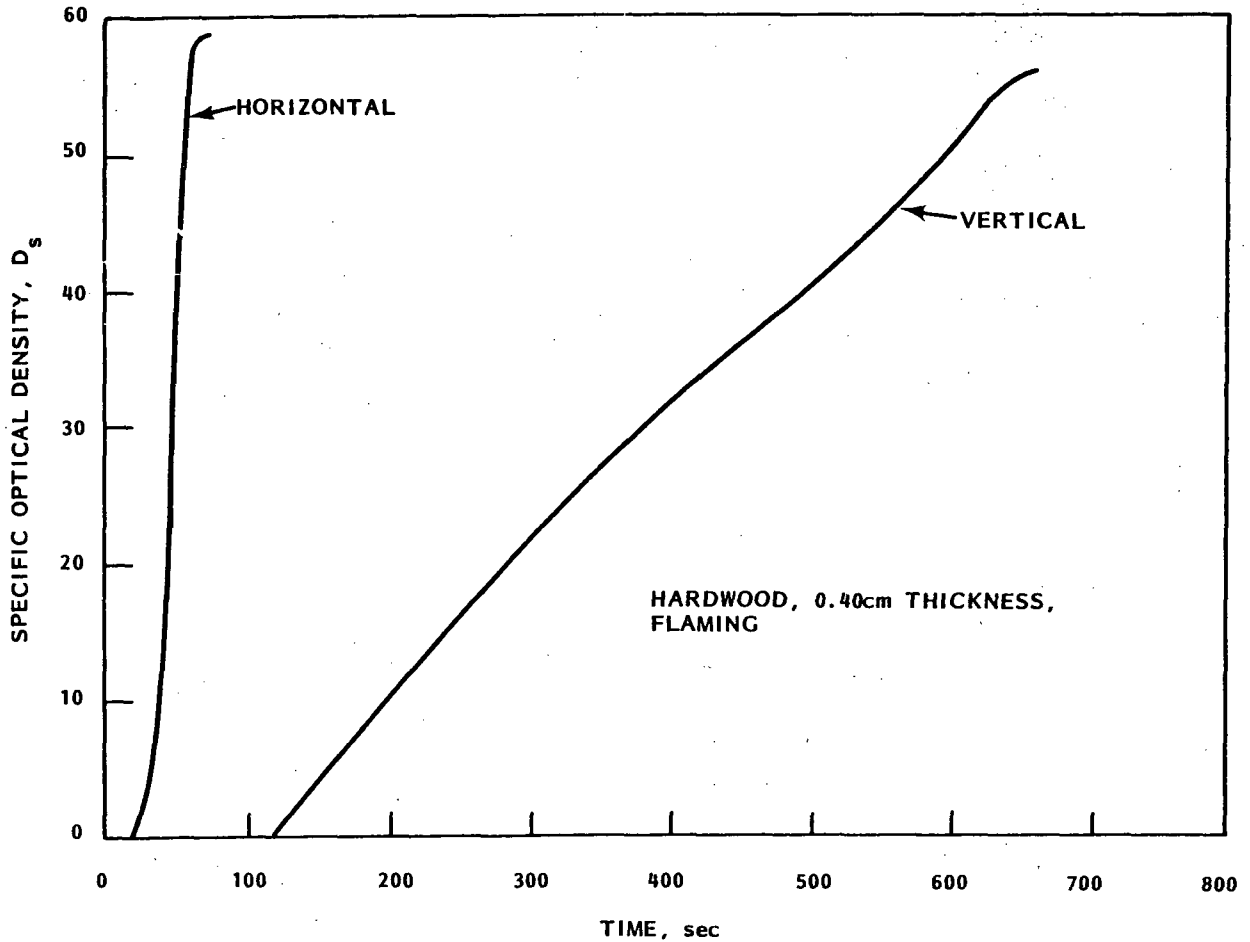
FIGURE 2.9. Effect of Sample Orientation on Specific Optical Density

This could be caused by flaming combustion, which enhances smoke generation due to depleted oxygen and high temperatures inside the closed chamber. A similar relationship would be expected as a function of irradiance level on a single exposed surface of cellulosic materials.

Seader and Einhorn found that temperature affects smoke accumulation in the same way (Figure 2.12), except that the effect is in terms of increasing energy flux with Douglas fir as test specimens.

Figure 2.12 illustrates that a heat flux of 2.5 W/cm², used in the standard nonflaming test, is insufficient to ignite most materials. Therefore, in many standard flaming experiments, the radiant heat flux is supplemented with propane-air pilot flames. Heat fluxes in actual fires can attain levels of at least 10 W/cm², and the temperatures found in ordinary building fires range from 500 to 1300°K (Tsuchiya and Leir 1973).
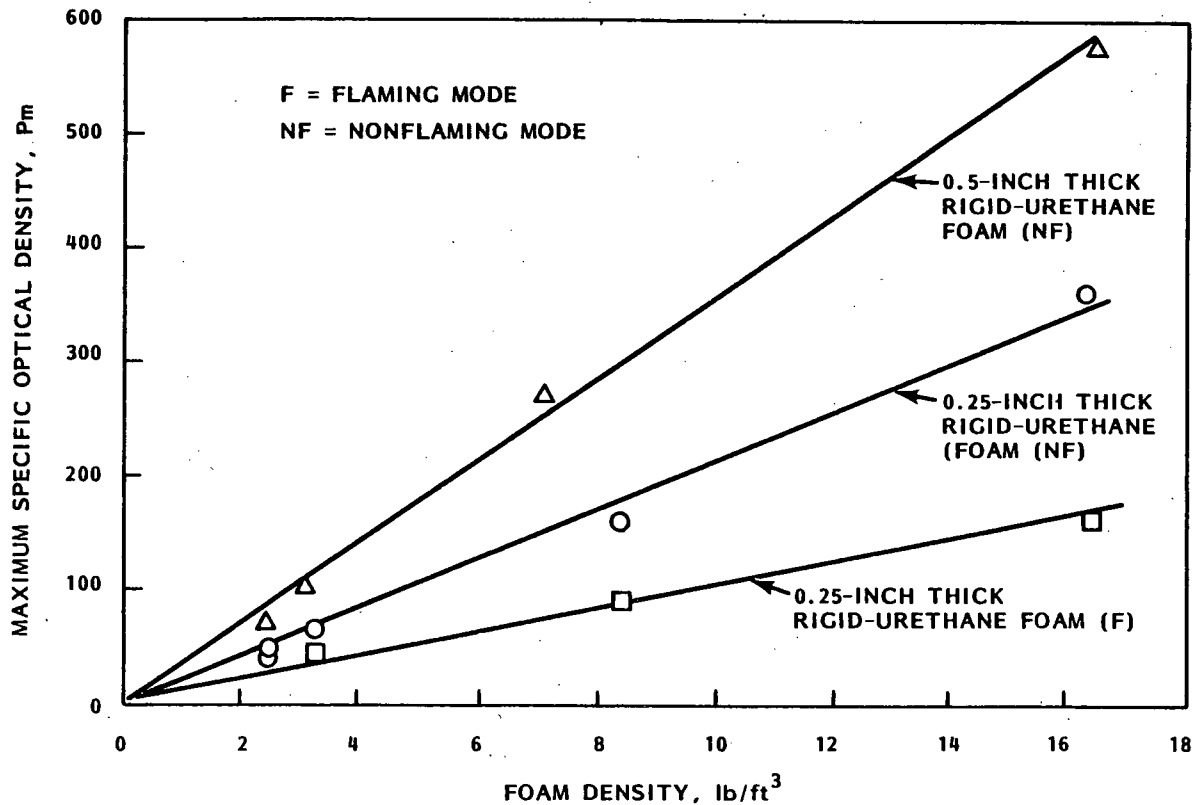
FIGURE 2.10. Effect of Material Density on Maximum Specific Optical Density

In an actual fire the combustion of a given material will usually occur in the temperature environment produced by the combustion of neighboring materials. This is especially true in a room in which flashover has occurred (Powell et al. 1979). This aspect of elevated temperature environment has been thoroughly examined (Bankston et al. 1978) for both flaming and nonflaming combustion by burning many plastic and cellulosic materials in small-scale flow-through chambers (smoke flows out of chamber during test). The collected data indicate that in flaming tests of both PVC and wood, higher environmental temperatures generally result in greater optical densities and larger smoke particles, while in nonflaming tests of wood higher temperatures result in lower smoke densities and smaller smoke particles. Bankston's results do not agree with Figure 2.11 for nonflaming tests, probably because different types of chambers and experimental conditions were used in the two studies.

Powell et al. (1979) also studied the effect of elevated temperatures upon the rates of sample weight loss for Douglas fir and rigid PVC under both nonflaming and flaming conditions (Figures 2.13 and 2.14). Under nonflaming conditions, the rates change drastically for both materials as temperature is raised, while the rates are only slightly affected in flaming tests.

2.31
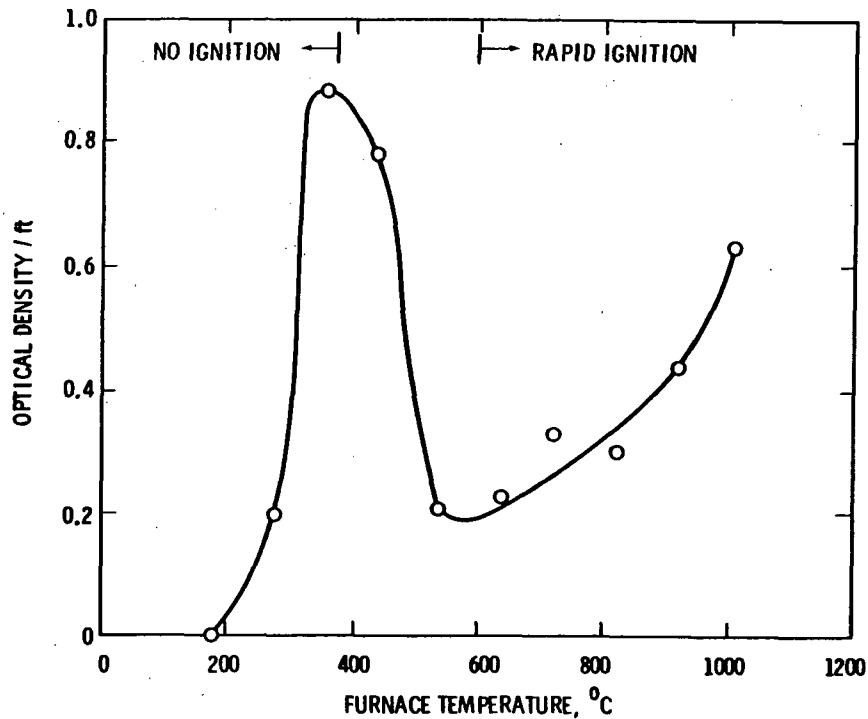
FIGURE 2.11. Smoke Production of Hardboard Within a Heated Furnace

2.4.2.3 Quantity of Available Oxygen

The presence of oxygen is necessary for burning. The partial oxygen pressure at the time of the fire in a compartment can strongly affect the smoking and burning rate. Saito (1974) and Gross, Loftus and Robertson (1969) showed that changes in the oxygen concentration of the ambient atmosphere surrounding the specimen significantly influence smoke production (Figure 2.15).

The rate of smoke produced in nonflaming combustion increases with oxygen concentration for cellulosic materials. Gross, Loftus and Robertson also discovered that the rate of smoke production depends upon the spacing between the sample and the front face of the furnace in a combustion chamber. They believe that with adequate space between sample and furnace face, free convection of air passes over the sample during pyrolysis and causes continuous smoke generation.

For flaming conditions King (1975) studied the effects of normal (initial 21% O_2 concentration) and oxygen-lean (initial 15% O_2 concentration) atmospheres on the rates of smoke and CO production from burning PVC, red oak, ABS and PS. They found that small changes in O_2 concentration had very little effect on the rate of smoke production. They also indicated that the rates of CO production increase with decreasing atmospheric oxygen concentrations. Figure A.1.2 of Appendix A.1 also illustrates this effect.

2.32
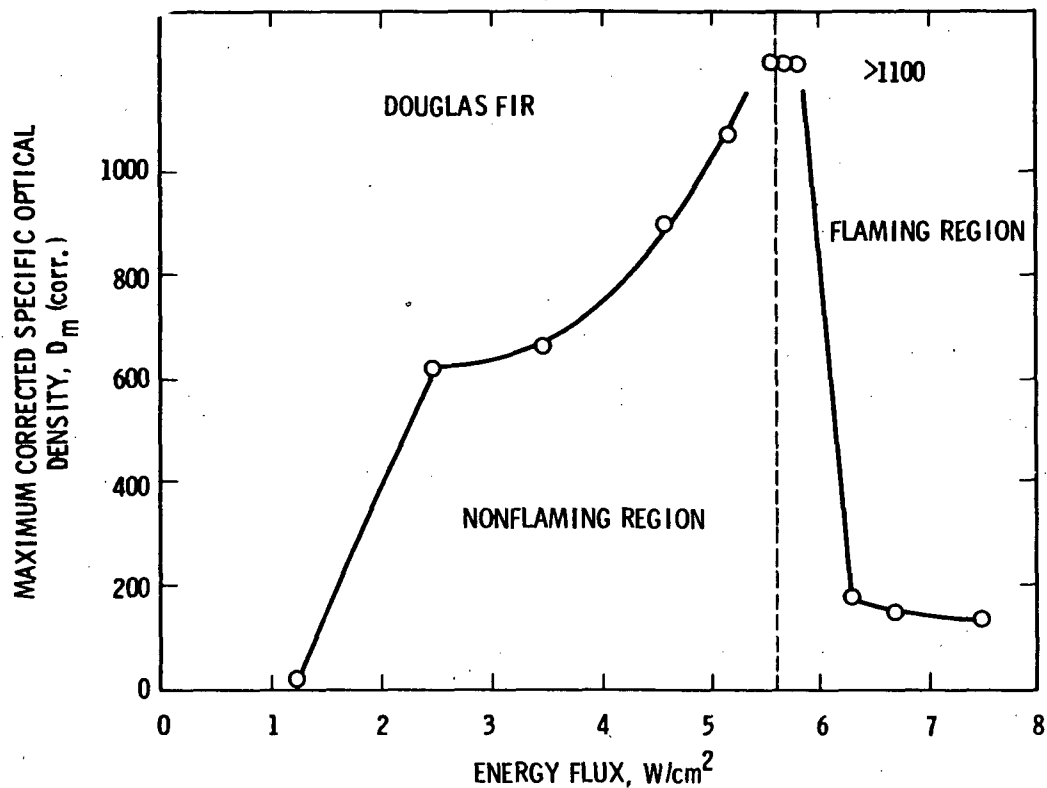
FIGURE 2.12. Effect of Energy Flux on D_m of Douglas Fir

To study changes in burning smoke production rates for different types and sizes of openings, Saito (1974) used the empirical formula

$$R_B = 5.5 \ AH^{1/2} \qquad\qquad (2.7)$$

where

R_B = burning rate
A = area of the opening
H = height of the opening
$AH^{1/2}$ = ventilation parameter.

His results did not correlate well with the above equation so Saito concluded that smoke generation rate is inversely related to burning rate.

2.5   METHODS OF EXPERIMENTAL FIRE STUDY

Experimental studies of combustion products have been broken down into two categories: products in flames and smoke. The studies concentrated in the flame zone help identify possible chemical species as a function of flame height and width in time. From this, possible mechanistic formulations of carbon particles (soot) are proposed. There is also interest in the chemical and
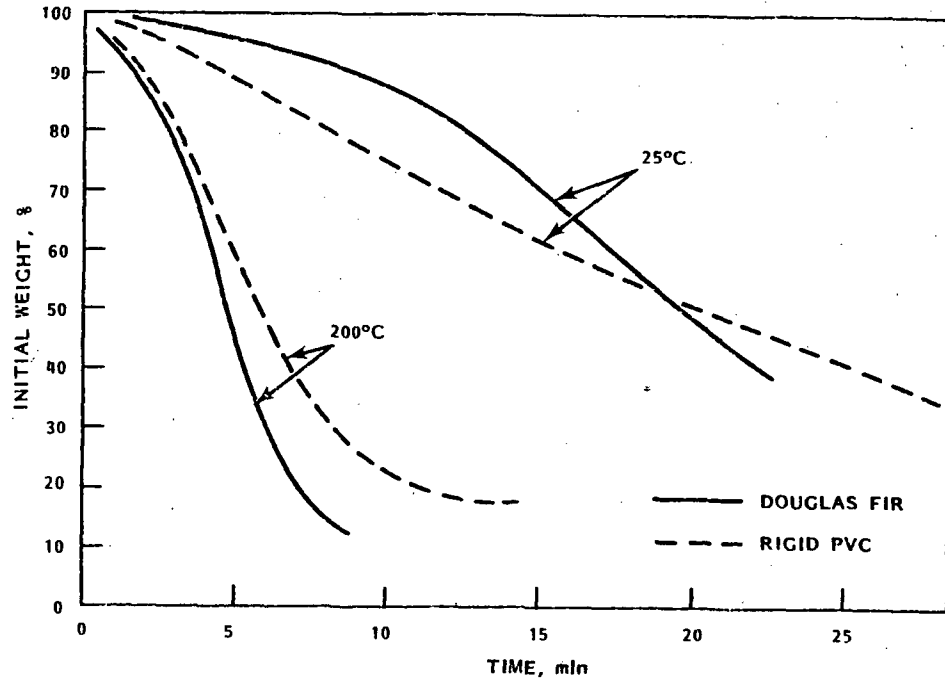
FIGURE 2.13. Weight Loss for Wood and PVC Samples Burned Under Non-flaming Conditions at Different Environmental Temperatures
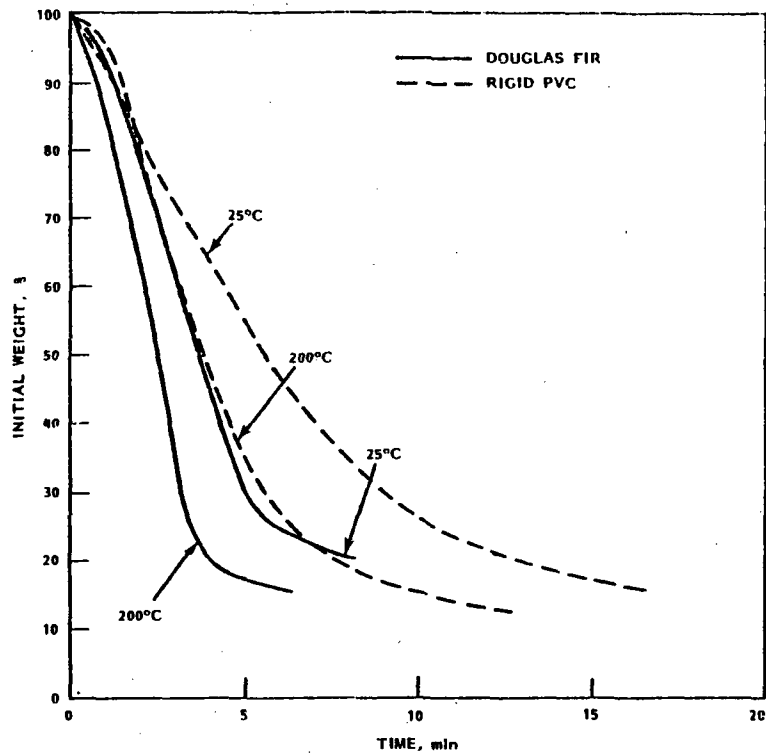
FIGURE 2.14. Weight Loss for Wood and PVC Samples Burned Under Flaming Conditions at Different Environmental Temperatures

2.34
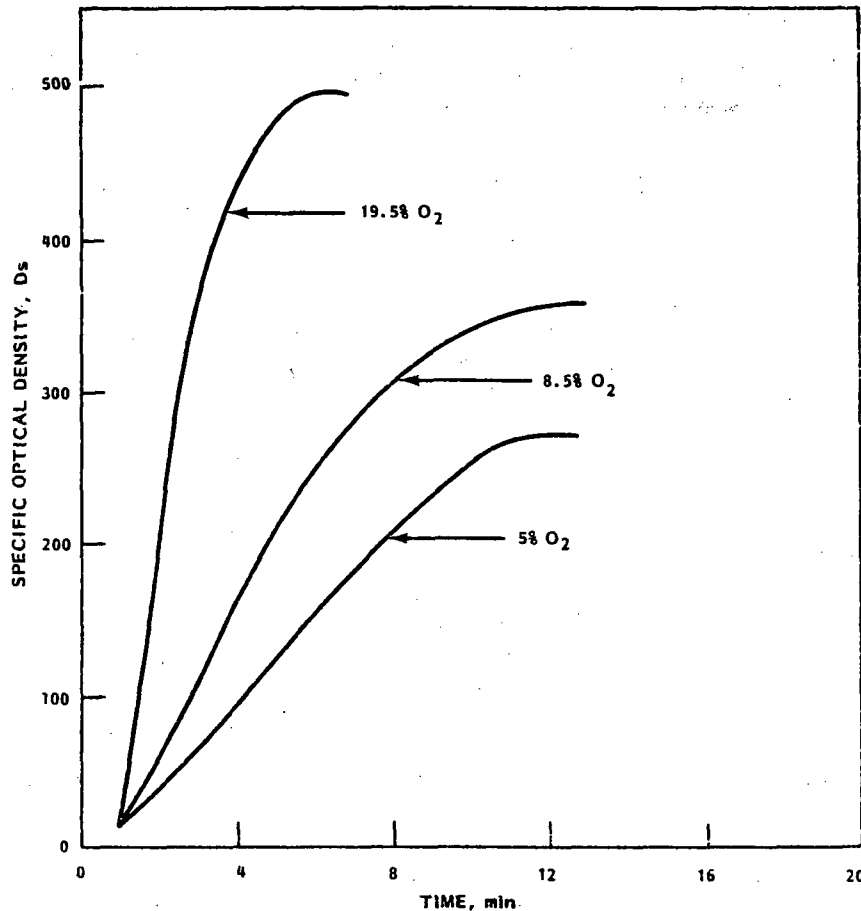
FIGURE 2.15. Smoke Buildup for Fiberboard Burned Under Nonflaming Combustion in Reduced Oxygen Atmospheres

physical properties as well as the opacity of smoke evolved from the fire. This knowledge of smoke characteristics provides information for assessing safety during a fire.

2.5.1 The Study of Combustion Products in Flames

The methods of generating a flame are different with respect to the fuel materials being used. For gaseous fuel, a bunsen burner may be used to produce a premixed flame; a diffusion flame can be obtained by using a special burner constructed with two concentric tubes with fuel flowing from the inner tube and air (or O_2) from the outer tube. For liquid fuel, the fuel material may be vaporized and mixed with air (or O_2) to give a premixed flame, while a diffusion flame is normally obtained by igniting a small pool of liquid fuel in a pan of a specific size with the presence of air (or O_2). For solid fuel, diffusion flames of various materials are usually studied by burning a small

2.35

sample with another flame source or by wetting a sample with liquid fuel and burning it until the solid sample can sustain its own flame.

In general, samples are drawn directly from the flame with probes for analysis. After the samples are drawn from the flame, chemical composition can be identified with a gas chromatograph and/or a gas chromatograph/mass spectrometer. Optical methods (scattering and extinction) are often used to measure particle numbers and mass concentrations. Particle size measurements can be made by diffusion-broadening spectroscopy or electron micrography.

In the 1970s more advanced equipment such as electrical aerosol analyzers (EAAs) and condensation nuclei counters (CNCs) were developed to measure the particulate sizes and distributions. These devices are commonly used to study smoke characteristics by in-situ measurements.

2.5.2 The Study of Combustion Products in Smokes

Many researchers have studied thermal degradation and characteristics of combustion products found in smoke produced by burning of both natural and synthetic materials used in building structures and interior furnishings. It has been a concern that simulating fire in small-scale enclosures may not produce results similar to those one would get in a real structural fire. With the assistance of two Boston fire companies, Burgese, Treitman and Gold (1979) studied toxic gases produced in an actual fire. They used a prototype sampling system which was designed into a firefighter's turnout coat. No comparison of the results has yet been made with data obtained from other fire studies in small chambers.

Most of the published studies of smoke characteristics have been performed by simulating flaming and/or nonflaming tests in small-scale combustion chambers. (For example, a National Bureau of Standards chamber, sometimes modified for specific types of smoke studies, is a well-known standard apparatus.) The fire conditions simulated in the small-scale tests may not be severe enough to adequately gauge the behavior of the test materials in real fires. Today many scientists are designing and generating their fire experiments under conditions which closely resemble the actual fire scenario in a room or entire structure.

In recent years, the study of smoke evolved during combustion in fire has gained attention from scientists and engineers, who have developed a number of smoke test methods to measure certain physical characteristics. Seader and Einhorn (1976) have tabulated a list of the more widely known devices (Table 2.8).

Opacity of the smoke is determined by continuous measurement of the amount of light transmitted through smoke particles generated from a combustion source. A photocell is commonly used, parallel to the light source, to collect the transmitting light. Portions of the nontransmissible light source are either scattered or absorbed by smoke particles present. According to Gross, Loftus and Robertson (1969), optical density is the single measurement most

characteristic of a "quantity of smoke" with regard to opacity. Therefore, a fundamental law by Bouguer, based on percent light transmittance, is an appropriate measure of opacity:

$$\text{Optical density} = \log_{10} (F/F_0) \qquad\qquad (2.8)$$

where   F = transmitted light or flux
        F_0 = incident light or flux.

Another way of quantifying the particle density in smoke is by continuously filtering the smoke through a known area of filter paper (Gross, Loftus and Robertson 1969); the resultant spot is classified according to its degree of blackness, commonly referred to as "smoke shade."

In the United States the most widely accepted flow-through and batch devices for determining smoke opacity are the Steiner Tunnel (ASTM E-84 test) and the NBS-AMINCO Smoke Density Chamber, respectively (Seader and Einhorn 1976). By filtering the smoke particles, accumulated particulate mass is also determined. In some tests, however, the sample weight is monitored continuously; thus the rate of material airborne can be determined.

A strategy has been developed at the Flammability Research Center, University of Utah for the chemical analysis of combustion products from natural and synthetic materials (Seader and Einhorn 1976). A schematic illustration of the scheme is presented in Figure 2.16.

2.37

TABLE 2.8. Test Devices for Studying Smoke

Designation	Type of Operation	Optical Opacity	Particulate Mass or Concentration (gravimetric)	Particulate Properties
ASTM E-84 Steiner tunnel test	FT	X		
ASTM E-286 8-ft tunnel test	FT	X		
ASTM D-2843 smoke test (Rohm and Haas XP-2 Smoke-Density Chamber)	B	X		
ASTM E-162 radiant panel test	FT	X	X	
NBS-AMINCO smoke-density chamber	B	X		
Monsanto chamber (based on ASTM D-757 Test)	FT		X	
NBS-LRL smoke-density chamber	B, FT	X		
FRS fire propagation furnace	B	X		
Michigan chemical oxygen index/smoke densitometer (Modified ASTM D-2863 Test)	FT	X		
Wayne State chamber	FT		X	
Modified TGA apparatus	FT	X		
Ohio State combustibility apparatus	FT	X		
Japanese Building Research Institute and NRC of Canada apparatus	FT	X		
Japanese Industrial Standard A-1321 smoke chamber	B	X		
Arapahoe smoke chamber	FT		X	
SRI mass burning rate apparatus	FT		X	
Georgia Tech Combustion Products test chamber	FT	X	X	X

(a) B = Batch operation (smoke confined to chamber during test)
FT = Flow-through operation (smoke flows out of chamber during test).
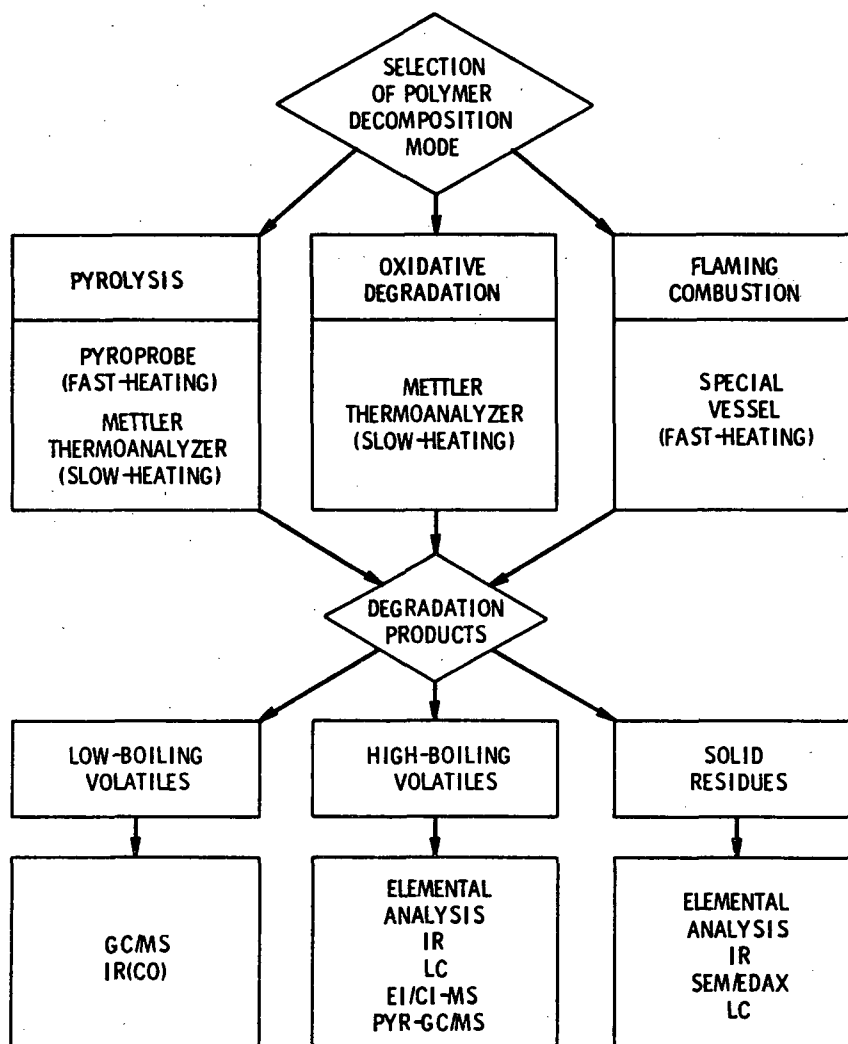
FIGURE 2.16. General Analytical Scheme for Chemical Analysis of Smokes

2.39

3.0 CHARACTERIZATION OF FIRE-GENERATED PRODUCTS

Our objective is to be able to characterize the energy output, the combustion products and the airborne radioactive materials generated as a function of time and conditions in the event of a fire accident inside a fuel cycle facility. In particular, the characteristics that we are most interested in are as follows:

- percentage of initial combustibles that becomes airborne
- particle size distribution and particulate concentration
- chemical composition of airborne materials
- energy input to the combustion gases.

The airborne combustion products (gases, vapors, and particulates) entrained with extraneous particulate materials (i.e., radionuclides, ambient dust, etc.) present a potential hazard to the environment if they escape the building. The materials which are most available as combustible fuels in a facility fire are:

- polymethylmethacrylate (PMMA)

- polyvinyl chloride (PVC)

- elastomers (i.e., rubber and other commercial samples or plastics such as polyethylene and polypropylene)

- cellulose

- cellulosic materials (i.e., papers and rags)

- organic fluids (i.e., kerosene, acetone, alcohol, hydraulic fluids and other high-boiling organic liquids).

Data from the literature on these combustibles were collected to be used as input to gas dynamics and material transport codes which predict the combustion product histories of the facility atmosphere under various fire conditions. Some of the airborne particulate characteristics will be used to evaluate the engineering safety system (i.e., filters) of the facility. Finally, a method will be developed to calculate and predict the fire energy and combustion product generation.

Because the combustion process is very complex it is rather difficult to describe for an enclosure fire. Nonetheless, it is important to predict and evaluate the hazards presented by a fire. Currently, several fire modeling techniques are in the process of development and refinement. These techniques function at different technical levels and fire scales (Tewarson 1980b). Data inputs to these fire models include enclosure geometry, availability of oxygen, heat of combustion, smoke generation, etc. Therefore, various physical/ chemical and combustion/pyrolysis properties of materials (i.e., plastics,

celluosic materials and organic fluids) are being determined in many fire research organizations. For example, Tewarson and other researchers at Factory Mutual Research Corporation (1976, 1980, 1980a and 1980b) are heavily involved in studying materials properties in their small-scale test apparatus. Some of the information they can provide are mass loss rate in pyrolysis and combustion of various materials, heat release rate based on the concepts of convective and radiative heat transfer, and product generation rate of various chemical species (i.e., CO, CO_2, gaseous hydrocarbons and soot).

B. T. Zinn et al. of Georgia Institute of Technology (1978, 1980) have been characterizing airborne materials in their Combustion Products test chamber over the past few years. Their objective is to define the percentage of the original material becoming airborne, particle size and distribution, chemical composition, and quantity of airborne material in terms of volume concentration.

Table 3.1 shows the data available from the literature reviewed, and the characteristics of combustion products of various materials of interest are tabulated in Sections 3.1 and 3.2. These data were obtained from small combustion-test apparatuses under a limited set of approximate fire conditions.

TABLE 3.1. Information Available in the Literature for the Fuel Materials of Interest Found in Fuel Cycle Facilities

Fuel Materials	Percentage of Original Material Airborne or Mass Generation Rate	Particle Size and Distribution	Chemical Composition	Airborne Material Concentration	Energy Release from Combustion
PMMA	X(P)(F,NF)	X(P)(F,NF)	NX	X(P)	X(F)
PS	X(P)(F,NF)	X(P)(F,NF)	NX	X(P)	X(F)
PVC	X(P)(F,NF)	X(P)(F,NF)	X(P)(F,NF)	X(P)	X(F)
Elastomers (i.e., rubber and plastics)	X*(P)(F,NF)	X*(P)(F,NF)	NX	X*(P)	X*(F)
Cellulosic materials (i.e., paper and rags)	NX	NX	NX	NX	NX
Cellulose	X(P)	X(P)	NX	NX	X(F)
Organic liquids –					
Kerosene	NX	X(PS)	X(P)	X(P)	NX
Hydraulic fluids	X(P,V)	X(P)	X(P,V)	X(P)	NX

X = information available in literature
NX = information not available in literature
F = flaming combustion
NF = nonflaming combustion (pyrolysis)

V = vapor (in pyrolysis) only
P = particulate only
PS = particle size only
X* = information available for some plastics only

3.2

Two areas of combustion products study are found in the literature--
characterization of combustion products in flame and in smoke. Figures 3.1 and
3.2 show the general trends of how combustion products in flame and smoke
(respectively) have been studied. In general, materials are divided into three
classes--gaseous, liquid and solid combustibles--and analysis is made of size,
chemistry, mass quantity and energy of the airborne materials generated from
combustion. Both flaming and nonflaming combustion (pyrolysis) are usually
examined for each material being tested. In flaming combustion, two types of
flames, premixed and diffusion, are usually considered. Diffusion flames are
dominant in enclosure fires because this type of flame is diffusion controlled,
which is characteristic of uncontrolled fires. The reason that many
researchers study the combustion products of flames is to better understand the
formation process of soot particles and to be able to elucidate the mechanisms
of soot formation.
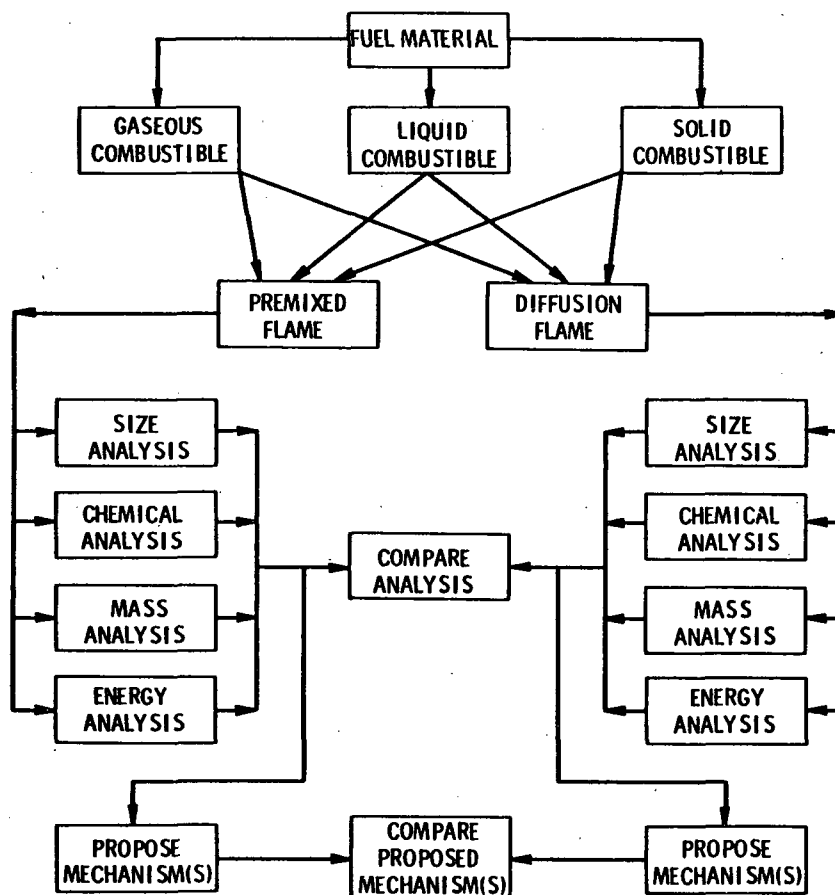
FIGURE 3.1. Schematic Representation of Combustion Products
Study in Flame
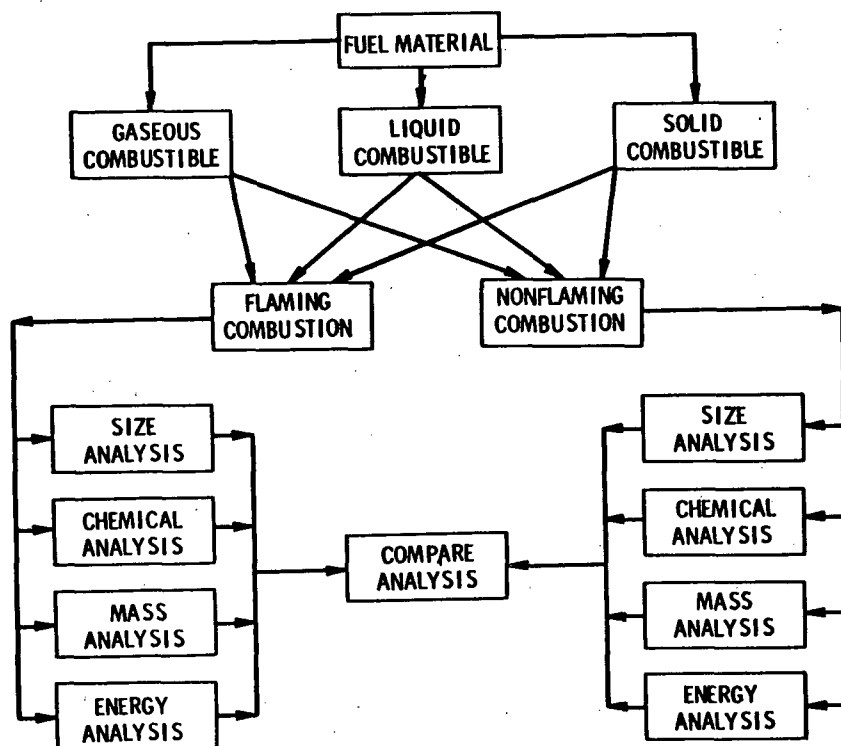
FIGURE 3.2.   Schematic Representation of Combustion Products
              Study in Smoke

3.1 PRODUCTS IN FLAMES

The characteristics of combustion products found in the flame zones are not necessarily the same as those found in their vicinity, even for the simple combustion process of burning a candle. This is due to the complex behavior of particles, which are impacted by various forces as they leave the flame zone. Determining the degree of change of these characteristics is more uncertain in an accidental fire. It is important to identify data on the principal species found in both premixed and diffusion flames because these species may serve as nuclei which promote particle growth or possible further chemical reaction after they escape from the flame zone. Unfortunately, the literature has very limited data on characteristics of combustion products in flames. Most of the data were obtained from both premixed and diffusion flames by burning combustible gases and liquids. Very few solid fuels were tested. In all hydrocarbon flames studied, carbon (soot) formation was observed.

Since data on the fuel materials that we are interested in are not available in the literature of premixed flames studies, data on other fuel materials will be presented to compare with data from materials of interest found in diffusion flame studies. The ideal combustible used for the premixed flame studies is acetylene (C_2H_2) because its flame is very stable (Bonne, Homann and Wagner 1965; Bittner 1978; Chippet and Gray 1978; Driscoll et al. 1978).

Flames with various $C_2H_2:O_2$ ratios and gas velocities were studied at both low- and high-pressure environments (ranging from 20 mm Hg to 760 mm Hg). Low-pressure premixed flames were used to study the kinetic relationships between soot, PCAHs and other hydrocarbon species that may be important in soot nucleation or surface growth.

In all flames three different zones (Bonne, Homann and Wagner 1965; D'Alessio et al. 1974; Bittner 1978) can be distinguished based on their appearance: 1) a nonluminous (dark) zone directly above the burner (found in all premixed flame studies); 2) the blue-green main reaction zone, where the volatiles generated from the fuel are oxidized; and 3) the reaction zone, which is followed by the upwards-extended region of the yellow- to orange-flowing burned gases, a criterion for the onset of carbon formation. Two zones, the reaction zone and the burned gases' region, were the main areas for sampling. In 1965, Bonne, Homann and Wagner used both aromatic and aliphatic hydrocarbon mixtures with oxygen for fuel materials in their premixed flame study at low (20 mm Hg) pressure.

A similar study was conducted in 1978 at the same pressure by Bittner, using acetylene-oxygen mixtures only. The experimental conditions are the same in both studies: a $C_2H_2:O_2$ ratio of 0.95 (or the equivalence ratio,[a] $\emptyset$ = 2.4) with an unburned gas velocity of 50 cm/sec. (Note: 5 mole % argon was added to the unburned gas for measurement purposes in Bittner's study.) The concentration profile measurements of major stable species in the burned gas region agree well with Bonne et al.'s study. Figure 3.3 illustrates their similar results in a $C_2H_2-O_2$ flame.

As can be seen in Figures 3.3 and 3.4, oxygen is completely consumed by about 13 mm (end of reaction zone) above the burner. At this point CO and H_2 have nearly reached their final values. Carbon dioxide and H_2 mole-fractions peak near 10 mm, and decrease slightly into the burned gas region. All values become constant >30 mm. Thus, based on these studies, the mole fractions of the major stable species found in the burned gas region of the premixed $C_2H_2-O_2$ flames are tabulated in Table 3.2.

Besides the major oxidation products, species that can be detected in the burned gas region are polyacetylenes and soot particles. Each represents a very small fraction of the total burned gas, about 10^{-3} mole. According to investigators (Bonne, Homann and Wagner 1965; Bittner 1978), the concentrations of the polyacetylenes are greatest early in the reaction zone and reach a constant final value in the burned gas. Before the end of the reaction zone, polyacetylene hydrocarbons up to a mass of 146 (unsaturated hydrocarbons

---

(a) Equivalence ratio, $\emptyset$, is defined as the actual fuel-air ratio divided by the stoichiometric fuel-air ratio (F/A):

$$\emptyset = \frac{(F/A)_{actual}}{(F/A)_{stoichiometric}}$$

If $\emptyset$ > 1, mixture is rich.
If $\emptyset$ = 1, mixture is stoichiometric.
If o < $\emptyset$ < 1, mixture is lean.
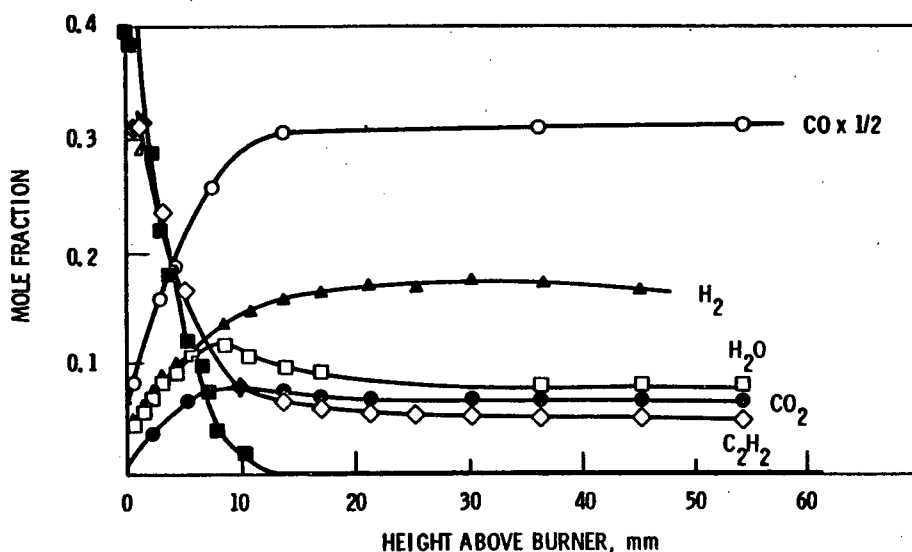
FIGURE 3.3. Concentration Profiles in a Flat Acetylene-Oxygen Flame ($C_2H_2:O_2$ = 0.95, or $\emptyset$ = 2.4) at a Pressure of 20 mm Hg and a Flow Velocity of the Unburned Gas of 50 cm/sec (reprinted with permission from Bonne, Homann and Wagner, Copyright 1965, The Combustion Institute, all rights reserved)

containing more C-atoms than the fuel molecules) are identified but the concentrations of these intermediate products become immeasurably small at the end of the reaction zone, where oxygen is also completely consumed.

Bittner (1978) has also considered the variation of gas produced from rich $C_2H_2-O_2$ mixtures at different equivalence ratios. At $\emptyset$ = 2.0, the features of the flame core are essentially the same but with lower CO, H_2, acetylene and polyacetylene concentrations, which might be expected. At $\emptyset$ = 1.5, no acetylenes or polyacetylenes were detectable in the burned gas, while at $\emptyset$ > 2.4 the concentrations of both acetylenes and polyacetylenes were increased. In addition to the species observed in the flame at $\emptyset$ = 2.4, several high-molecular-weight aromatic hydrocarbons were observed. Their masses, molecular formulas, and possible structures are listed in Table 3.3. The quantities of these particles were not measurable. They are believed to serve as surface growth precursors because they were airborne with the burned gas.

In 1974, D'Alessio et al. measured the concentrations of major stable gases of a methane-O_2 flame at 1 atm with an unburned gas velocity of 7.4 cm/sec. Figures 3.5a and 3.5b show the major stable chemical species found as a function of distance from the tip of the burner.

As can be seen from Figure 3.5, the concentrations of both H_2 and CO are similar in a CH_4-O_2 flame. This is quite different from the $C_2H_2-O_2$ flame, where at a similar $\emptyset$ the concentration of CO is almost three times as much as the concentration of H_2 (see Figures 3.3 and 3.4). This might be explained by

3.6
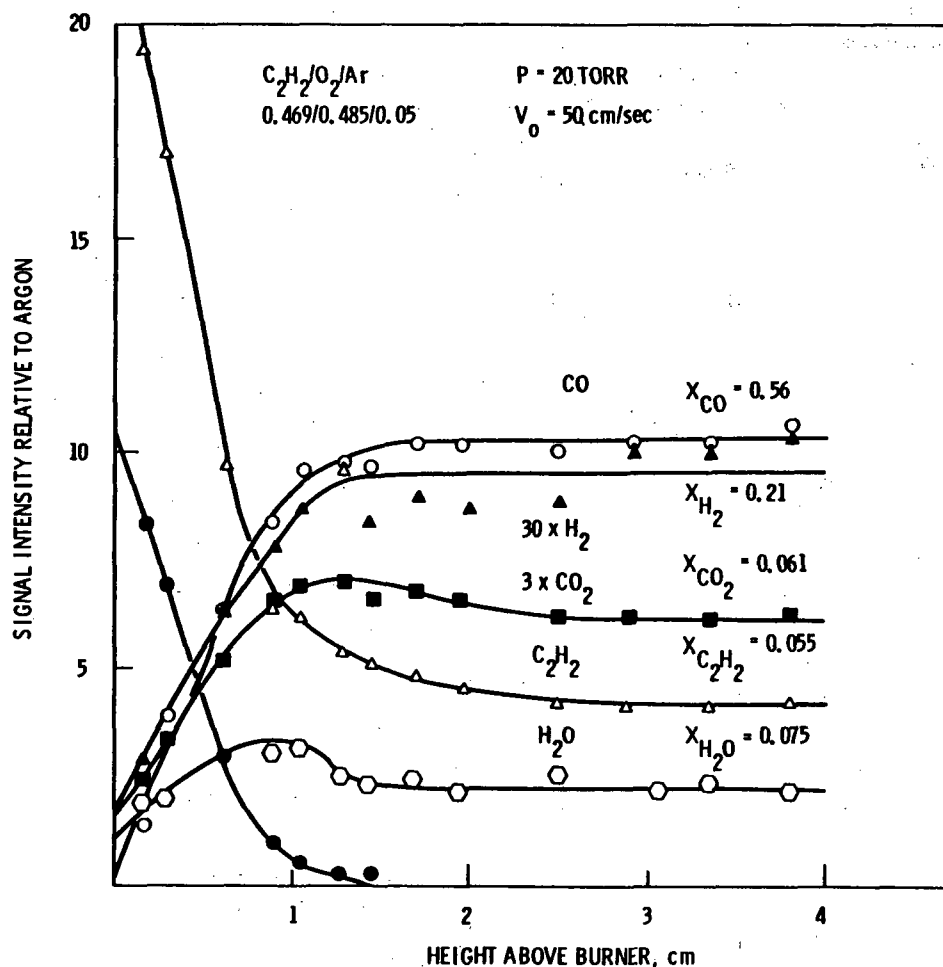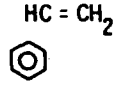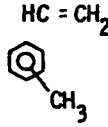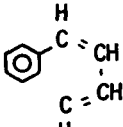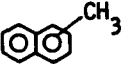
FIGURE 3.4. Profiles of Signal Intensities Relative to Argon for Major Stable Species in an Acetylene-Oxygen Flame Near the Sooting Limit ($\emptyset$ = 2.4, P = 20 torr, V_0 = 50 cm/sec, 5 mole % argon, X = mole fraction) (Bittner 1978)

TABLE 3.2. Mole Fraction of Major Stable Species Expected in the Burned Gas of a C_2H_2-O_2 Premixed Flame ($\emptyset$ = 2.4, P = 20 mm Hg, gas velocity = 50 cm/sec)

Species	Mole Fraction, X		Average Mole Fraction, X_{Ave}
	Bonne et al.	Bittner	
CO	0.62	0.56	0.59
H_2	0.16	0.21	0.19
H_2O	0.075	0.075	0.075
CO_2	0.06	0.061	0.06
C_2H_2	0.05	0.055	0.05

3.7

TABLE 3.3. Additional Species Near the End of the Reaction
Zone in a $C_2H_2-O_2$ Flame ($\emptyset$ = 3.0, P = 20 torr,
V_0 = 50 cm/sec)

MASS	MOLECULAR FORMULA	POSSIBLE SPECIES	STRUCTURE
92	C_7H_8	TOLUENE	
102	C_8H_6	PHENYLACETYLENE	
104	C_8H_8	STYRENE	
118	C_9H_{10}	METHYL STYRENE	
128	$C_{10}H_8$	NAPHTHALENE	
130	$C_{10}H_{10}$	PHENYL BUTADIENE	
		DIHYDRONAPHTHALENE	
142	$C_{11}H_{10}$	METHYL NAPHTHALENE	
146	$C_{12}H_2$	HEXACETYLENE	

$$HC \equiv C(-C \equiv C-)_4 C \equiv CH$$

the fact that acetylene contains more carbon and less hydrogen than methane.
The concentration of CO_2 found in a CH_4-O_2 flame is quite comparable with that
found in a $C_2H_2-O_2$ flame. Oxygen was used up in the oxidation reaction at
~7 mm above the burner, fairly low in comparison to the 13 mm found with C_2H_2.
Figure 3.5b shows other possible hydrocarbon intermediates which have substan-
tially higher concentrations than those found in the $C_2H_2-O_2$ flame.

Thus, based on the available data, one can predict and identify the pos-
sible major components of the burned gas found in premixed flames of hydrocar-
bon fuel, but often the quantities of these major species are impossible to
estimate by generalizing from the available information (i.e., $C_2H_2-O_2$ and
CH_4-O_2 flames). Therefore, in order to determine the amount of each major
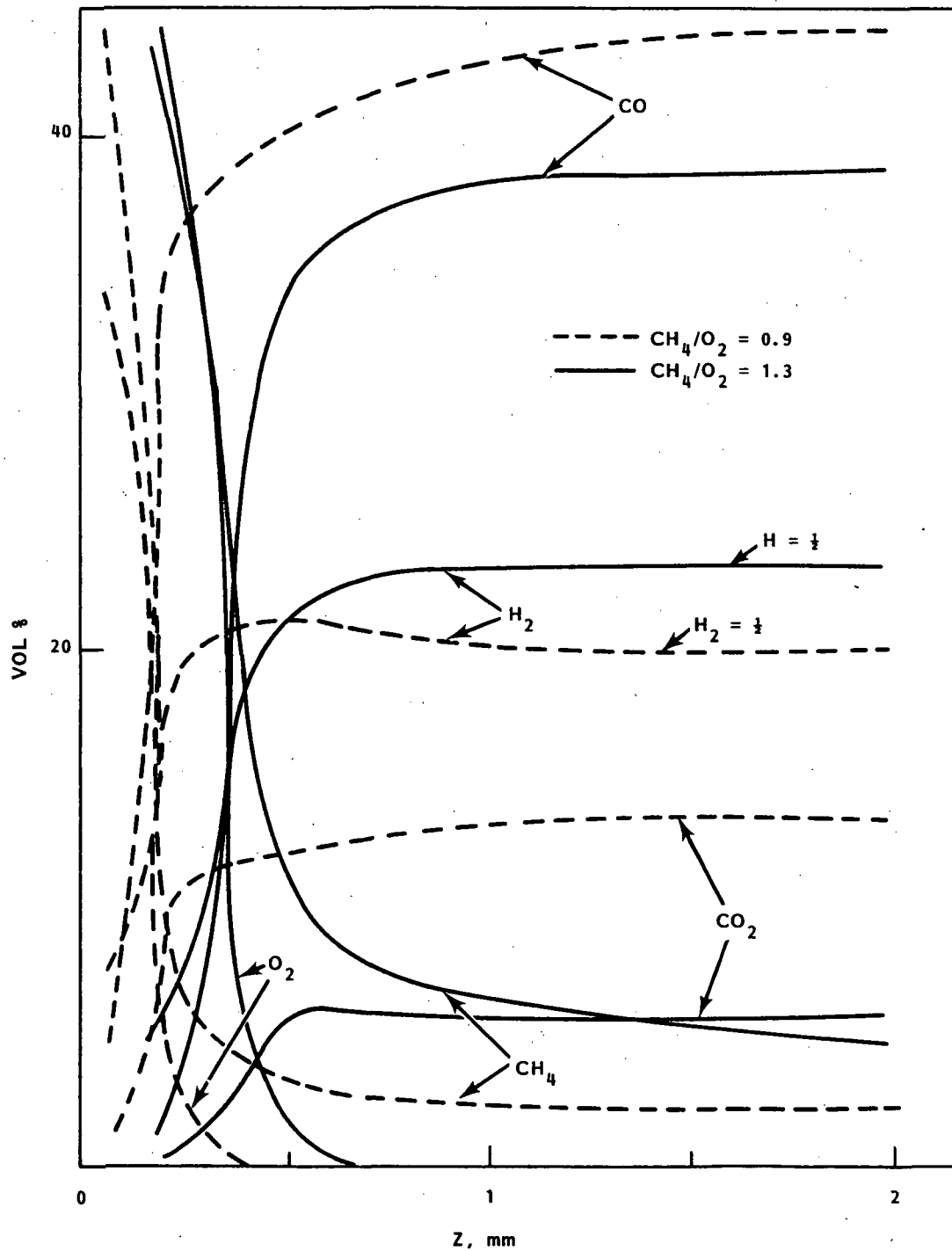
FIGURE 3.5a. Concentration Profiles of the Gaseous Compounds O_2, H_2, CO, CO_2 and CH_4 Along the Flame for Different $CH_4:O_2$ Feed Ratios

$$CH_4:O_2 = 0.9, \quad \emptyset = 1.8$$
$$CH_4:O_2 = 1.0, \quad \emptyset = 2.0$$
$$CH_4:O_2 = 1.3, \quad \emptyset = 2.5$$

3.9
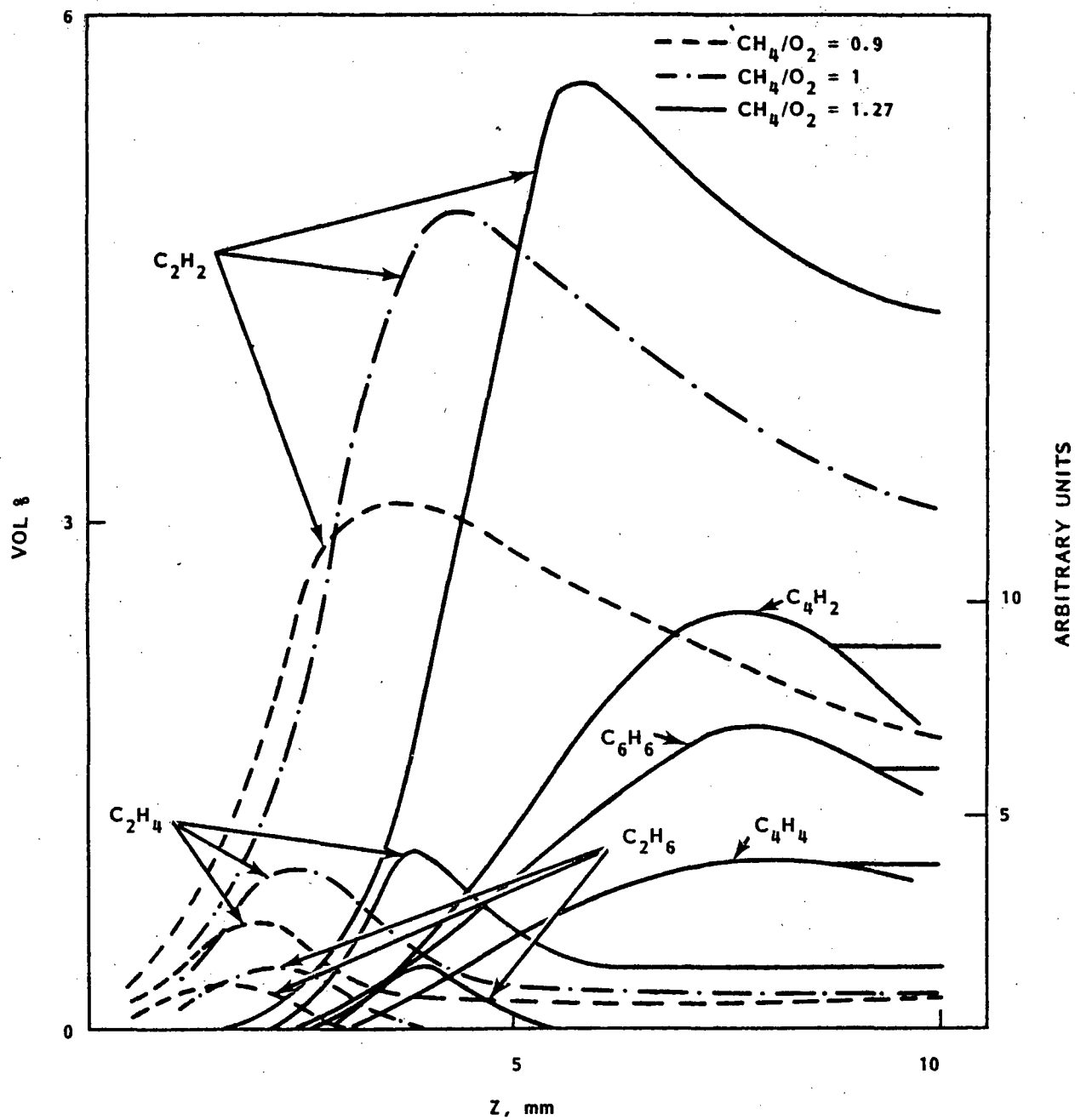
FIGURE 3.5b. Concentration Profiles of the Gaseous Compounds C_2H_2, C_2H_4, C_2H_6, C_4H_2, C_4H_4 and C_6H_6 Along the Flame for Different $CH_4:O_2$ Feed Ratios

$CH_4:O_2 = 0.9$, $\emptyset = 1.8$
$CH_4:O_2 = 1.0$, $\emptyset = 2.0$
$CH_4:O_2 = 1.3$, $\emptyset = 2.5$

component in the burned gas of a certain fuel at various conditions, one must conduct the experiment of interest.

Particle diameters of carbon were also measured in studies of $C_2H_2-O_2$ premixed flames. Table 3.4 shows the particle diameters measured by various investigations with methods indicated. These studies show that at low pressure, mean particle diameter slightly increases as equivalence ratio increases, with the mean diameter ranging from 0.016 to 0.018 μm. At a higher pressure (1 atm), the particle diameter is considerably larger (0.2 μm) and varies little as a result of equivalence ratio changes from 2.5 to 5.0. Diffusion broadening spectroscopy and electron micrography were used to measure particle diameters and their results show reasonable agreement.

3.1.1 Products in Diffusion Flames

It is quite interesting to compare the carbon particle diameters from a sample withdrawn from a diffusion C_2H_2 flame with those from a premixed flame. Magnussen et al. (1978) have studied the effects of turbulent structure on soot formation and combustion in C_2H_2 diffusion flames. Utilizing the eddy-dissipation model modified with the influence of structural changes in the flow due to variation of the Reynolds number (Re), the particle diameter is calculated (Table 3.5).

In this study the fuel C_2H_2 was introduced upward into stagnant air through a convergent nozzle with an exit diameter of 3 mm. The combustion air was entrained from the surrounding air into the flame by turbulent diffusion. Surrounding air temperature and pressure were approximately 20°C and 1 atm. Magnussen et al. observed that the computational particle diameters were of about the same magnitude as those observed experimentally in flames.

By comparing these results with those in Table 3.4, one can see that the carbon particles found in turbulent diffusion flames are an order of magnitude smaller than the particles found in premixed flames at the same pressure. Again, these data are for illustration only. In an actual fire inside a fuel

TABLE 3.4. Carbon Particle Diameters of $C_2H_2-O_2$ in a Premixed Flame Under Various Experimental Conditions

Reference	Experimental Conditions P, mm Hg	V_o, cm/sec	ϕ	Height Above Burner Where Samples Were Withdrawn, mm	Particle Diameter, μm	Method of Measurement
Bonne et al. (1965)	20	50	3	--	dm = 0.016	Electron Micrography
	20	50	4	--	dm = 0.018	
Driscoll et al. (1978)	760	20	2.5-5.0	30	0.25	Diffusion Broadening Spectroscopy
	760	20	2.5-5.0	30	0.20	Electron Micrography

TABLE 3.5. Carbon Particle Diameters in Turbulent
Diffusion Flames Calculated by Utilizing
the Modified Eddy-Dissipation Model

Re	Gas Velocity, m/sec	Particle Diameter, μm
40000	121.0	0.00204
50000	151.3	0.01785
52500	216.6	0.01324
55000	166.4	0.01686
55000	165.2	0.01424
55000	164.0	0.01180
56500	233.7	0.01195

cycle facility, C_2H_2 is not likely to be present. Even though it may be present, its unburned gas velocity is not likely to be $\geq$100 m/sec.

3.1.1.1 Kerosene

Information on particulate diameter, mass loading of soot particles and identified PCAHs from turbulent diffusion flames of kerosene is available in the study by Prado et al. (1978). Three atomizing air pressures were studied: 184 kPa (12 psig), 205 kPa (15 psig) and 239 kPa (20 psig). For determining mass loading of soot particles, two cold gas velocities were used: 0.96 m/sec and 2.67 m/sec, with an equivalence ratio of 1 and total air flow at a constant value of 56.7 kg/hr (15.75 g/sec). Figures 3.6a and 3.6b (Prado et al. 1978) show the mass loading of soot under these conditions. .

Both figures show that there can be two distinct chemical processes in the flame: soot can form to maximum loading, and then can disappear through combustion. Figure 3.6a shows one exception: the profile at 184 kPa exhibits a plateau rather than a peak. Other experiments (Bittner 1978) also showed that as equivalence ratios increased, so did the amount of soot formed. Therefore, based on this information, considerable amounts of soot particles will survive and become part of the product gases at low atomizing-air pressure, high equivalence ratios, and low O_2 concentrations in surrounding air. The O_2 in air can oxidize the available carbon particles and reduce the amount of soot escaping through the flame zone.

Particle size was analyzed by electron microscopy at a magnification of 81,000X, which was increased to 200,000X. Two types of carbonaceous material were observed. Close to the nozzle, in the zone of soot formation, the particles looked like agglomerates of partially coalesced spherical units. The individual spherical units in this material were very poorly defined and it was not possible to measure their size. Farther from the nozzle, the material had

3.12
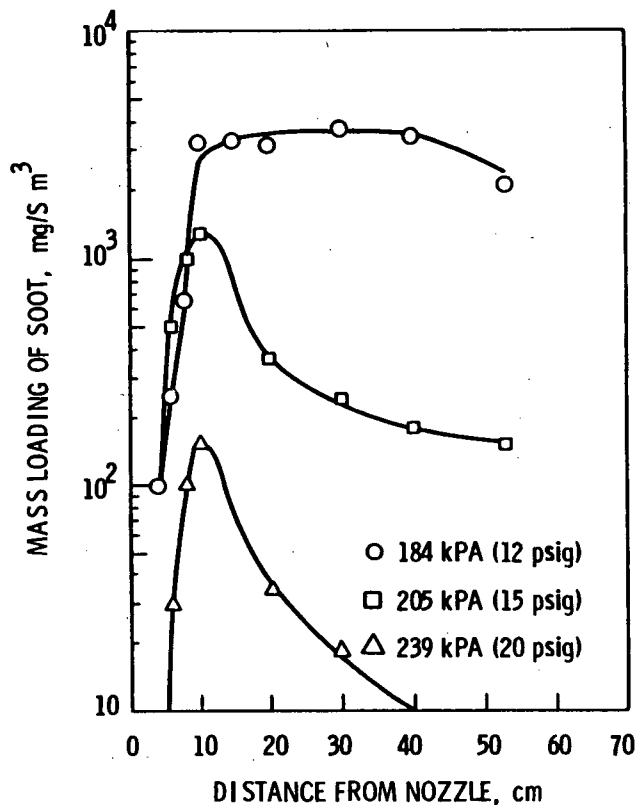
FIGURE 3.6a.   Influence of Atomizing
                Air Pressure on Axial
                Profile of Soot Mass
                Loading at Cold Gas
                Velocity of 0.96 m/sec
                [Kerosene:air fuel
                equivalence ratio =
                1.0; atomizing air
                pressure = (o) 184 kPa
                (12 psig), (□) 205 kPa
                (15 psig), and (Δ)
                239 kPa (20 psig)]
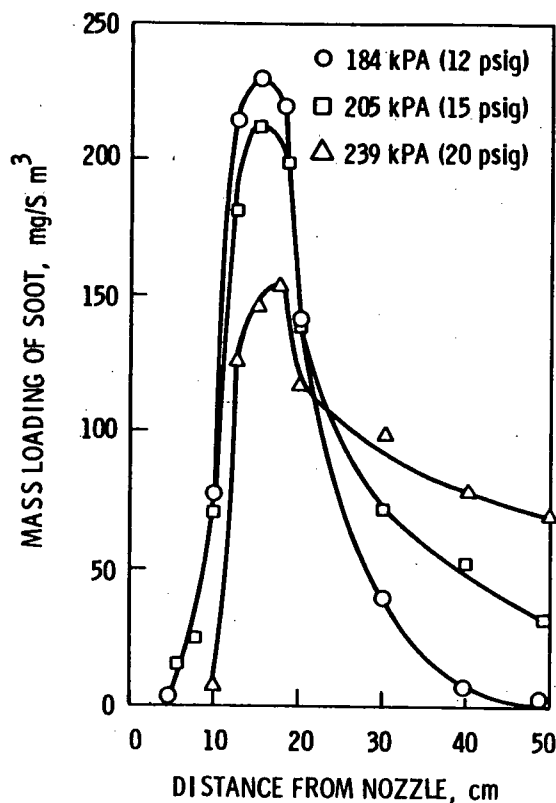
FIGURE 3.6b.   Influence of Atomizing
                Air Pressure on Axial
                Profile of Soot Mass
                Loading at Cold Gas
                Velocity of 2.67 m/sec
                [Kerosene:air fuel
                equivalence ratio =
                1.0; atomizing air
                pressure = (o) 184 kPa
                (12 psig), (□) 205 kPa
                (15 psig), and (Δ)
                239 kPa (20 psig)]

the classical appearance of necklace-like units of spherical particles. The
sizes of these well-defined units are reported in Tables 3.6a and 3.6b (Bittner
1978).

From Tables 3.6a and 3.6b, Bittner drew these conclusions:

● Changes in the atomizing air pressure, even when drastically
  changing the total amount of soot emitted, do not affect the
  particle size (Table 3.6a).

3.13

TABLE 3.6a. Arithmetic Mean Particle Diameter (Å) of Spherical Kerosene Particles at Cold Gas Velocity of 0.96 m/sec (mean fuel equivalence ratio = 1.0)

Distance from Nozzle, cm	Arithmetic Mean Particle Diameter, Å		
	Atomizer Air Pressure, 184 kPa	Atomizer Air Pressure, 205 kPa	Atomizer Air Pressure, 239 kPa
6	191	(a)	(a)
10	211	220	254
53 (exhaust)	249	298	(a)

(a) Poorly defined carbonaceous material.

TABLE 3.6b. Arithmetic Mean Particle Diameter (Å) of Spherical Kerosene Particles at Cold Gas Velocity of 2.67 m/sec [atomizer air pressure = 184 kPa (12 psig), distance from nozzle = 20 cm]

Mean Fuel Equivalence Ratio	Arithmetic Mean Particle Diameter, Å
0.8	(a)
0.9	146
1.0	145
1.2	139

(a) Poorly defined carbonaceous material.

● Increasing the equivalence ratio by increasing cold gas velocity results in a higher temperature through the reduction of heat loss per unit energy input. An increase in temperature results in a decrease in the size of particles through an increase in the number of particles formed per unit volume, all other parameters being constant.

From gas chromatographic-mass spectrometric (GC-MS) analysis of the methylene chloride extracts of the soot samples, and subsequent peak area integration of the chromatographic peaks, Magnussen et al. (1978) have determined the detailed quantitative and qualitative composition of the PCAHs formed within the flame. Quantitative values for the identified PCAHs ranging from

two- to seven-ring structures at two points along the burner axis (atomizing air pressure of 184 kPa) are reported for kerosene in Table 3.7. Some additional conclusions can be drawn:

- There is an enrichment of heavier PCAHs as the samples are collected at greater distances from the burner nozzle.

- There is a reduction of PCAHs containing methyl and phenyl groups, which are expected to disappear as they move further downstream in the burned gas.

TABLE 3.7. Polycyclic Aromatic Hydrocarbons in the Combustion Products of Kerosene

Major PCAHs Identified (particulate in burned gas)	Mass Loading, mg/S m^3	
	20 cm from Nozzle	40 cm from Nozzle
Naphtalene	0.8	1.9
Acenaphthylene	18.0	19.0
Acenapthene	0.8	0.6
Fluorene	0.3	0.2
Phenanthrene/anthracene	2.1	1.3
4H-Cyclopentha(def)phenanthrene	1.2	0.6
Fluoranthene	4.5	3.2
Benzacenaphthylene	2.1	1.2
Pyrene	1.6	9.2
Methylfluoranthrene/methylpyrene	0.5	0.3
Benzo(ghi)fluoranthene	3.7	2.2
Cyclopenta(cd)pyrene	17.0	16.0
Benzofluoranthene	1.3	1.1
Benzo(e)pyrene/benzo(a)pyrene	1.2	0.8
Perylene	0.8	1.2
Indeno(1,2,3-cd)pyrene	0.8	0.7
Benzo(ghi)perylene/anthanthrene	5.4	5.4
Coronene	2.6	3.9
TOTALS	78.0	67.0

3.1.1.2 Plastics and Flammable Liquids

In a diffusion flame study by Pagni and Bard (1978), soot volume fractions in flames have been measured in situ for solid (i.e., PS and PMMA were included), cellular (foam) and liquid hydrocarbon fuels. Approximate detailed size distributions of carbon particles in flames were also determined using a multiwavelength laser transmission technique. The most probable particle size was obtained based on the extinction coefficient ratio derived from the Mie scattering theory. This information is shown in Table 3.8.

TABLE 3.8. Soot Volume Fractions and Size Distributions in Experimental Flames

	r_{max}, μm	$N_0 \times 10^{-9}$, cm^{-3}	$f_v \times 10^6$
Solids			
PS, $(C_8H_8)_n$	0.021	27	4.6
Polypropylene, $(C_3H_8)_n$	0.005	155	0.36
PMMA, $(C_5H_8O_2)_n$	0.018	2.9	0.31
Polyoxymethylene, $(CH_2O)_n$	---	---	0.22
Foams			
PS (GM-48), $(C_8H_8)_n$	0.061	1.1	4.7
Polyurethane (mattress), $(C_{3.2}H_{5.3}ON_{0.23})_n$	0.014	16	0.80
Polyurenthane (GM-21), $(C_{3.4}H_{6.1}ON_{0.16})_n$	---	---	~0.80
Liquids			
Iso Octane, C_8H_{18}	0.023	2.7	0.62
Acetone, C_3H_6O	---	---	0.18
Alcohol, C_2H_6O	---	---	0.11

Figure 3.7 shows an apparatus schematic for the multiwavelength transmission experiments. It consists of two lasers, a calculator which serves as a timer, a narrow band pass filter, and a movie camera. The initial dimensions of the fuel material were as follows:

Solid -- Thin disk 1-cm high and 7.5-cm dia (flame height ~8 cm).
Foam -- Rectangular parallelepiped 15 cm x 7 cm x 10 cm (flame height ~8 cm).
Liquid -- Dish 1-cm high and 10-cm dia (flame height ~18 cm).

The equation for the calculation of soot volume fraction in flames (f_v) was based on the Mie scattering theory, and its final form is:

$$f_v = 18.62 \, N_o \, r_{max}^3 \qquad (3.1)$$

where

r_{max} = most probable particle radius
N_o = total particle concentration
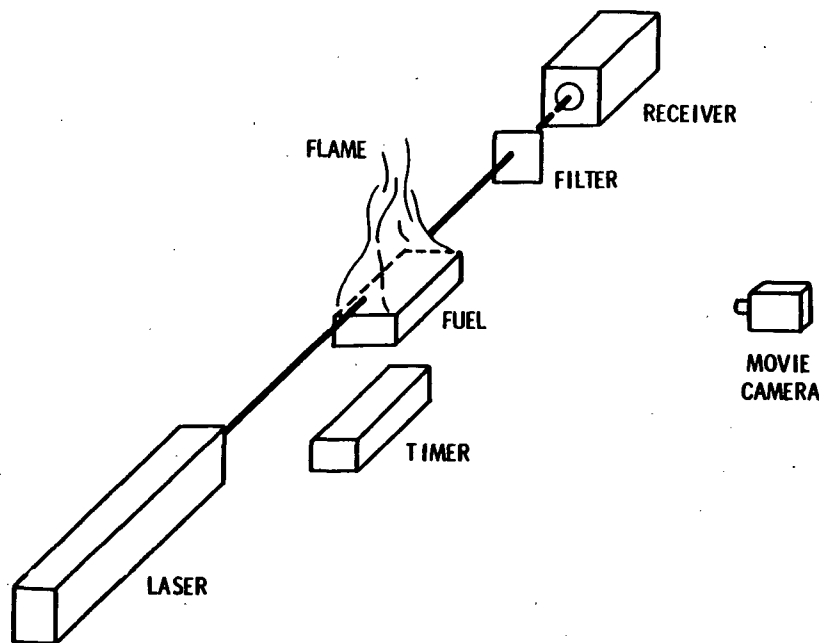
FIGURE 3.7. Schematic of Apparatus for Monochromatic Transmission Measurements

3.17

and

$$N_0 = \frac{\ln (I/I_0)}{L \, r_{max}^2 \, \tau'}$$ (3.2)

where

I = laser intensity

I_0 = initial intensity

τ' = extinction coefficient

L = pathlength or mean beam length.

Table 3.8 shows that PS flames are an order of magnitude "sootier" ($f_v \simeq$ 5 x 10^{-6}) than all the other fuels. Although both solid and foam PS have the same f_v, the latter has particles much larger (~0.06 μm) than any other fuel (~0.02 μm) considered. Pagni and Bard (1978) agreed that the ranking of the f_v results is consistent with observed flame luminosity and smokiness, and with data in the literature. Good agreement exists between experimental mass pyrolyzing rates and rates calculated from a radiation model for f_v of solid PS and PMMA, derived independently from infrared flame transmittance and radiance data. Using the parameters in Table 3.8 in the following equation (Pagni and Bard 1978),

$$N_{(r)} = N_0 (27 \, r^3/2 \, r_{max}^4) \, \exp(-3r/r_{max}),$$ (3.3)

most probable particle size distribution $N_{(r)}$ versus particle radius is plotted in Figure 3.8 for the fuel materials considered.

3.1.2 Summary

The study of combustion products in flames has been reviewed and the characteristics of these products as detailed in the literature are recorded. Since information on the fuels of interest is currently unavailable, to gain perspective we presented the characteristics of burning an acetylene and oxygen mixture. The acetylene flame was chosen because it was found to be very sooty and stable and so served as an ideal combustible for soot formation study.

Besides the principal burned gases (CO, CO_2, H_2, H_2O, C_2H_2), small amounts of acetylene, polyacetylene, carbon particles and several PCAHs were detected in the burned gas region of the flame at higher equivalence ratios. At a low equivalence ratio ($\emptyset < 1.5$) no acetylene or polyacetylenes were detectable, but the concentration of species increases with increasing equivalence ratio. The soot mole fraction has a fairly constant value of ~2.5 x 10^{-3} in the burned gas region under the following conditions: $C_2H_2-O_2$ = 1.4; P = 20 mm Hg; flow velocity = 50 cm/sec. The particle diameter is ~0.02 μm at low pressure and an
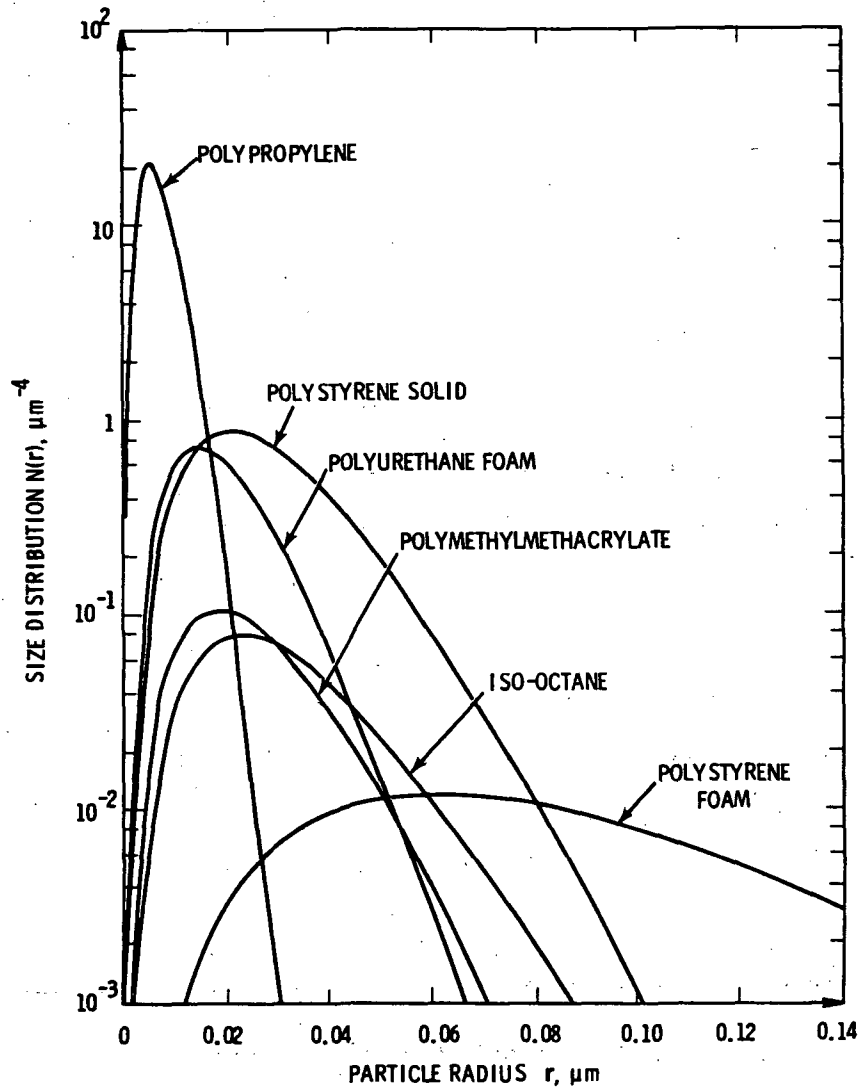
FIGURE 3.8. Approximate Size Distributions $N_{(r)}$ Versus Particle Radius r as Determined from Multi-wavelength Monochromatic Transmission Experiments

order of magnitude larger at higher pressure. In a C_2H_2 diffusion flame, the particle diameters are between 0.01 and 0.02 μm.

Some characteristics of combustion products in diffusion flames are available for fuel materials such as kerosene, PS, PMMA, acetone and alcohol. In a pressurized kerosene diffusion flame, the amount of soot formed depends strongly on atomizing air pressure, high equivalence ratio and cold gas velocity. At an atomizing air pressure of 184 kPa (12 psig), an equivalence ratio

of 1.0 and a cold gas velocity of 0.96 m/sec, the mass loading of soot is about 10^3 mg/S m^3 in the burned gas zone of the flame. As the cold gas velocity increases to 2.67 m/sec, the soot mass loading is as low as zero (see Figure 3.6a). The particle diameter found in kerosene flame ranges from 0.015 μm to 0.03 μm under conditions listed in Tables 3.6a and b. The mass loading of total PCAHs found within the flame was 70 mg/S m^3 at a distance of 40 cm from the burner nozzle. Qualitative compositional information on these hydrocarbons is listed in Table 3.7. There is a possibility that these small species will serve as surface growth precursors as they travel with the burned gases.

Various solids and liquids in buoyant diffusion flames were studied. The characteristics of particle diameter, particle concentration and volume fraction are available for PMMA, PS, acetone and alcohol. For the solid fuels the initial fuel geometry was a thin disk 1 cm high and 7.5 cm dia. Table 3.8 contains information on fuel characteristics, and the parameters in the table were used to determine most probable particle size distribution (Figure 3.8).

3.2 PRODUCTS IN SMOKE

Numerous studies of the properties of the combustion products generated by fires in buildings have been made at the Georgia Institute of Technology (GIT). In their studies, samples of polymers and hydraulic fluid were burned under controlled conditions to obtain measurements on smoke particle size distribution, total smoke particulate mass generated, particulate size and the chemical properties of smoke particulate products. The ventilated Combustion Products test chamber (CPTC) being used at GIT can simulate a wide variety of environmental conditions that may be encountered in actual fire situations. Information on smoke particulate generation is also presented in the study by Seader and Einhorn (1975).

From steady state heat balance at the surface, Tewarson et al. (1978, 1980) derive equations for mass loss rate in combustion and pyrolysis. Product generation rates for some chemical species are also considered. These data are available for limited combustible materials at present.

The information on smoke products introduced above is tabulated and presented in the Sections 3.2.1 through 3.2.4.

3.2.1 Percentage of Smoke Particulates Airborne, Mass Loss Rates, and Product Generation Rates

The percentages of particulate materials found in smoke were measured for the following combustible fuels (Chien and Seader 1975; Bashston et al. 1978; Zinn et al. 1978, 1980):

- wood--red oak, white oak, Douglas fir, and redwood
- polymers--PMMA, PVC, PS, polypropylene, and polyethylene
- hydraulic liquids.

The information obtained is tabulated as follows:

- percent of initial material converted to smoke particulates
- percent of sample weight loss that became smoke particulates
- percent of initial material that became char residue.

These data are summarized in Table 3.9a, and the corresponding experimental methods and conditions and their influences are given in Table 3.9b. Notice that for the nonflaming mode with a heat flux of 5 W/cm and air temperature of 25°C, the time required for total sample weight loss ranges from 10 to 25 min. (For other combustible materials, see also Table A.3.1 of Appendix A.3, Tables A.4.1, to A.4.4 and A.4.6 to A.4.11 of Appendix A.4, Tables A.5.1 to A.5.3 of Appendix A.5, and Tables A.6.2 and A.6.4 of Appendix A.6). None of these materials left any appreciable amount of char residue, with the PVC taking the longest time to lose 99% of its original weight (24 min in the nonflaming mode). (The weight losses of these materials as a function of time can be found in Figures A.5.1, A.5.5 and A.5.7 of Appendix A.5 and Figure A.6.1 of Appendix A.6). To obtain the particulate mass, filters were used to collect the smoke.

Based on surface heat balance, Tewarson et al. derived two equations for mass loss rate--one for pyrolysis and another for smoke generation. The mass loss rate of a fuel depends on the magnitude of net heat flux the fuel receives in a fire and the heat required to generate a unit mass of the fuel vapors (Tewarson 1980b). The equations are expressed as follows:

Mass loss rate in pyrolysis: $(\dot{M}_p'')$

$$\dot{M}_p'' = (\dot{q}_e'' - \dot{q}_{rr}'')/L \tag{3.4}$$

Mass loss rate in combustion: $(\dot{M}_b'')$

$$\dot{M}_b'' = (\dot{q}_e'' + \dot{q}_{fs}'' - \dot{q}_{rr}'')/L \tag{3.5}$$

where $\dot{q}_{fs}''$ is the total flame heat flux to the fuel surface and equal to the summation of flame convective heat flux $\dot{q}_{fc}''$ and flame radiative heat flux $\dot{q}_{fr}''$. Value $\dot{q}_{rr}''$ is the surface reradiation energy and L is the heat required to generate a unit mass of vapors. Both L and $\dot{q}_{rr}''$ are functions of material properties only and are independent of fire conditions (Tewarson 1980b).

The mass loss rates for various combustible materials are tabulated in Table 3.10. Those in the flaming combustion mode are higher than the mass loss rates in pyrolysis because of the additional energy from heat convection and radiation due to the flame at the combustible's surface. It is also true that both external heat flux and availability of O_2 increase the mass loss rate in combustion for all materials except PS and oak, which are char-forming materials whose combustion efficiency X_a is smaller than for the nonaromatic polymers.

TABLE 3.9a. Percentage of Smoke Particles Generated from Various Fuel Materials

Fuel Material	Flaming or Non-flaming Combustion	Initial Material Converted to Smoke Particulates,%	Sample Weight Loss to Become Smoke Particulates,%	Initial Material To Become Char Residue,%	Remarks
Woods[a]	F	0.2-0.4	--	0.2-1	The range of % refers to the range of wood samples (i.e., red oak, white oak, Douglas fir, redwood). All the smoke particulates evolved from a known weight of material were collected by a filter and weighed at normal atmospheric composition.
Douglas fir[b]	NF	--	3-17	20-30	Heat flux of 3.2-6.2 W/cm^2. Air flow rate of 142-425 ℓ/min, and normal atmospheric composition.
	F	--	2.6-1	20-30	Heat flux of 2.5-5 W/cm^2. Air flow rate of 280-425 ℓ/min, and normal atmospheric composition.
	NF	--	22-33	20-30	Heat flux of 6.2 W/cm^2, and atmospheric compositions of 80% N_2, 10% O_2, 10% CO_2; and 80% N_2, 5% O_2, 10% CO_2, 5% CO.
PMMA[c]	F	0.6	-	0	See Table 3.9b, (a).
	F, NF	--	<1	~0	Heat flux of 5 W/cm^2, air flow rate 425 ℓ/min, at room temperature and normal atmospheric composition.
PVC	F	10.2	--	7.9	See Table 3.9b, (a).
	F	--	2.5	~0	See Table 3.9b, (c).
	NF	--	9.3	~0	See Table 3.9b, (c).
PS	F	21.0	--	0.2	See Table 3.9b, (a).
	F	--	3.2	~0	See Table 3.9b, (c).
	NF	--	8.4	~0	
Polyethylene	F	8.3	--	0.05	See Table 3.9b, (a).
	F	--	1.2	~0	See Table 3.9b, (c).
Polypropylene	F	--	1.8	~0	See Table 3.9b, (c).
	NF	--	12.1	~0	
Polypropylene	F	--	1.8	~0	See Table 3.9b, (c).
	NF	--	12.1	~0	
Hydraulic fluid	F	--	2.8	0 (10 min)	Type (2190 TEP, MIL-2-17331A) The given value is inaccurate because the lower stages of Cascade impactor became clogged by large soot particles.

Radiant thermal fluxes of 3.5, 5, 7.5 W/cm^2 correspond to surface temperatures (nonflaming) of 240, 340 and 470°C, respectively. (a),(b),(c),(d) are explained further in Table 3.9b.

TABLE 3.9b. Experimental Methods and References (from Table 3.9a)

Fuel Material	Apparatus, Initial and Environmental Conditions		Reference
(a) Wood	Apparatus:	Modified ASTM D-757 globar flammability testing chamber (flow-through chamber)	Chien and Seader (1975)
	Conditions:	Initial sample wt. = 0.5 g Air flow rate = 8.1 cm/sec Heat flux = 3.8 W/cm^2 Environmental conditions = normal	
(b) Douglas fir	Apparatus:	Ventilated Combustion Products chamber (CPTC)	Bankston et al. (1978)
	Conditions:	Initial sample wt. = not given Initial sample volume = 75 mm x 75 mm x 6.4 mm Exposed surface area = 56.25 cm^2 Air flow rate = 142 to 425 ℓ/min Heat flux ranges from 2.5 to 6.2 W/cm^2	
	Environmental Conditions:	Normal or atmospheric compositions of --80% N_2, 5% O_2, 10% CO_2, 5% CO --80% N_2, 10% O_2, 10% CO_2	
(c) PMMA (and other polymers)	Same apparatus and range of conditions in (b) above except the initial sample volume = 75 mm x 75 mm x 3.2 mm, and sample wt. ≃ 15-20g. The exposed surface area ≃ 56.25 cm^2.		Zinn et al. (1978)
(d) Hydraulic fluid	Apparatus:	CPTC	
	Conditions:	Initial sample wt. = 20 g (in shallow circular aluminum dish 7.6 cm dia and 1 cm deep) Exposed surface area = 45 cm^2 Air flow rate = 425 ℓ/m at 25°C Heat flux = 5 W/cm^2	Zinn et al. (1980)

TABLE 3.10. Mass Loss Rates for Combustible Materials

Combustible	$\dot{q}''$ (kW/m²)	$\dot{V}$ (m³/sec)/10³	M_{O_2}	$\dot{q}''_{fs}$ (kW/m²)	L (kJ/g)	$\dot{q}''_{rr}$ (kW/m²)	$\dot{M}''_p$ (g/m²sec)	$\dot{M}''_b$ (g/m²sec)
PMMA	0	1.4	0.183-0.531	21-56	1.63	11	0	6-28
	31[a]-60[b]	N[b]	0.233	29-45	1.63	11	25-30	30-60
PVC	0	2.0	0.671-0.874	63-65	2.47	21	0	17-18
Granular PS	0	1.4	0.233-0.524	39-35	1.70	14	0	15-12.5
Polypropylene	0	1.4	0.196-0.507	23-66	2.03	18	0	3-24
	52[a]	0.86	0.233	58	2.03	18	17	45
Oak[a]	31[a]-71	1.4	0.233	16.7	1.7[c] 5.5[d]	16	9-10	18-11

(a) Data taken from Tewarson's previous studies.
(b) Natural air flow.
(c) For $\dot{q}''_e \leq 46$ kW/m².
(d) For $\dot{q}''_e \leq 46$ kW/m².

Utilizing the expressions for mass loss rate, Tewarson (1980b) derived two additional equations relating product generation rate as the function of mass loss rate:

Product generation rate for pyrolysis ($\dot{G}''_{pj}$):

$$\dot{G}''_{pj} = (Y_j/L)(\dot{q}''_e - \dot{q}''_{rr}) = Y_j \dot{M}''_p \qquad (3.6)$$

Product generation rate for combustion ($\dot{G}''_{bj}$):

$$\dot{G}''_{bj} = (Y_j/L)(\dot{q}''_e + \dot{q}''_{fs} - \dot{q}''_{rr}) = Y_j \dot{M}''_b \qquad (3.7)$$

where Y_j is the ratio of mass generation rate of a product j to mass loss rate of the material, which is available for CO_2, CO, total gaseous hydrocarbons expressed as HC, and the mixture of soot and low vapor pressure liquids expressed as S. Table 3.11 presents all the data that enable calculation of $\dot{G}''_{pj}$ and $\dot{G}''_{bj}$ for various materials.

3.24

TABLE 3.11. Product Generation Rates for Various Materials

Combustible	Y_{CO_2}	Y_{CO}	Y_{HC}	Y_S	$\dot{M}_p''(a)$	$\dot{M}_b''(a)$	$\dot{G}_{pCO_2}''$	$\dot{G}_{pCO}''$	$\dot{G}_{pHC}''$	$\dot{G}_{pS}''$	$\dot{G}_{bCO_2}''$	$\dot{G}_{bCO}''$	$\dot{G}_{bHC}''$	$\dot{G}_{bS}''$
								Generation Rate, g/m^2 - sec						
PMMA	2.2	0.011-<0.001	<0.001	0.023	0	6-28	0	0	0	0	13.2-62	0.3-<0.03	<0.03	0.65
	1.9(b)	0.007	0.001	--	12-30	30-60	23-57	0.08-0.21	0.01-0.03	--	57-115	0.2-0.4	0.03-0.06	--
PVC	0.46	0.04-0.03	0.003-0.001	0.09-0.07	0	17-18	0	0	0	0	7.8-8.3	0.7-0.5	0.05-0.02	1.5-1.3
Polystryene	2.2	0.07-0.01	0.02-0.001	0.20	0	15-12.5	0	0	0	0	33-27.5	1.05-0.13	0.3-0.01	3-2.5
Polypropylene	2.7	0.2	0.007-0.001	0.07	0	3-24	0	0	0	0	8.1-65	0.6-4.8	0.02	0.21-1.68
	1.9(b)	0.05	0.03	--	17	45	32.5	0.85	0.51	--	86	2.25	1.35	--
Oak	1.3	0.002-0.005	<0.001	0.015	9-10	18-11	11.7-13	0.02-0.05	<0.009	0.14-0.15	23.4-14.3	0.04-0.06	<0.02	0.27-0.17

(a) Obtained from Table 3.10.
(b) With external heat flux, $\dot{q}_e''$.

3.2.2 Particle Size and Particle Size Distribution

Ranges of particulate mass median diameter (MMD) and particle size distribution (standard deviation) for cellulose and various polymers are tabulated in Table 3.12 with both normal and high ventilation air temperatures.[a] All these data were obtained from B. T. Zinn et al. of the Georgia Institute of Technology (Bankston et al. 1978; Zinn et al. 1978, 1980). Notice that in flaming combustion in both normal and highly ventilated conditions, MMD and particle size distribution data are unavailable for the polymers (except PMMA) because the large, sooty particles produced during flaming combustion tends to rapidly clog up the Cascade impactor plates used. For PMMA the quantities of smoke particulates collected were too small for reliable size distribution measurements. Only mean particle diameter is measured in these conditions by in-situ optical techniques.

3.2.3 Chemical Composition of Airborne Particles

Various polymers and a combustible hydraulic fluid were tested for the presence of PCAHs and other hydrocarbons in airborne particulates (away from the flames) by Zinn et al. Among the polymers tested, the only samples yielding significant amounts of PCAHs were the PVC samples. Some of the suspected classes of non-PCAH compounds that can be found in smoke particles generated from polymers include aldehydes and ketones, acids, bases, phenols, aliphates, aromatics, esters, ethers and chlorinated compounds. The chemical analysis schemes were developed for these studies (Zinn et al. 1978, 1980). The most recent apparatus has been developed by GIT to identify the major volatile species generated by pyrolysis.

3.2.3.1 PCAHs in Smoke Particles Generated from PVC

The PCAHs found in PVC particles are shown in Table 3.14 (Zinn et al. 1978). The PVC samples were tested individually and their various compositions are tabulated in Table 3.13. The particles analyzed were generated by exposing the sample to a heat source inside the Georgia Tech CPTC and sampling the combustion products at 30 ℓ/min through a triple-thickness glass-fiber filter. This represented ~20 of the total gas flow through the CPTC. The collected particulate smoke from nonflaming PVC combustion weighed about 20 mg, and with flaming PVC combustion, 27 mg. During flaming combustion, a propane flame was used to induce combustion. A blank run on the propane flame only showed no detectable concentration of PCAHs.

3.2.3.2 PCAHs in Smoke Particles Generated from Hydraulic Fluids

Under the thermal flux of 5 W/cm and ventilating air flow of 425 ℓ/min, smoke particles were collected to identify PCAHs in the sample. The initial

---

(a) For detailed tabulation, see the appendix (Tables A.4.1 to A.4.4, A.4.7 to A.4.12, A.5.1 to A.5.3, A.6.1 to A.6.3; Figures A.4.1 to A.4.6, A.5.2 to A.5.4, A.5.6, A.5.8 to A.5.12, A.6.1 to A.6.2).

TABLE 3.12. Particle Size and Particle Size Distribution of Fuel Materials

Fuel Material	Mass Median Diameter MMD, μm	Standard Deviation, σ	Volume Surface Mean Particle Dia at Maximum Optical Density Drs, μm	F or NF	Heat Flux, W/cm^2	Air Flow Rate, ℓ/min	Environmental Conditions
Douglas fir	0.5-0.9	1.8-2.0	0.75-0.8	NF	3.2-6.2	142-425	Normal temp. (25°C) and composition
	0.4	2.4	0.5-0.45	F	2.5-5	283-425	Normal temp. (25°C) and composition
	1.0	2.0	0.9	NF	6.2	--	Normal temp.; composition of 80% N_2, 5-10% O_2, 10% CO_2, 5% CO
	--	--	0.75-0.55	NF	5	425	Air temp. of 25-200°C, normal composition
	--	--	0.5-1.2	F	5	425-283	Air temp. of 25-200°C, normal composition
PMMA	0.7	1.9	0.6	NF	5	425	Normal temp. (25°C) and composition
	--	--	1.2	F	5	425	Normal temp. (25°C) and composition
	--	--	1.2-1.3	F	5	425	Air temp. of 25-200°C; normal composition
PS	2.6	1.9	1.4	NF	5	425	Normal temp. (25°C) and composition
	--	--	1.3	F	5	425	Normal temp. (25°C) and composition
	--	--	1.3-1.25	F	5	425	Air temp. of 25-200°C; normal composition
Polyethylene	1.5	1.75	1.1	NF	5	425	Normal temp. (25°C) and composition
	--	--	1.3	F	5	425	Normal temp. (25°C) and composition
	--	--	1.3-1.35	F	5	425	Air temp. of 25-200°C; normal composition
Polypropylene	2.05	1.8	1.6	NF	5	425	Normal temp. (25°C) and composition
	--	--	1.2	F	5	425	Normal temp. (25°C) and composition
	--	--	--	F	5	425	Air temp. of 25-200°C; normal composition
PVC	1.4	1.45	1.0	NF	5	425	Normal temp. (25°C) and composition
	--	--	1.2	F	5	425	Normal temp. (25°C) and composition
	--	--	1.1-1.15	F	5	425	Air temp. of 25-200°C; normal composition
Hydraulic fluid	--	--	1.23	NF	5	425	Normal temp. (25°C) and composition
	--	--	1.33-1.31	F	5	425	Air temp. of 25-300°C; normal composition

(a) F = Flaming combustion.
NF = Nonflaming combustion.

TABLE 3.13. Composition of PVC Samples, g

Sample	PVC Resin	Lead Stabilizer	Plasticizer 6-10 Phthalate	Plasticizer Di-Isodecyl Phthalate	$CaCO_3$	$Al_2O_3 \cdot 3H_2O$	Sb_2O_3	Lubricants
1	100	5	--	--	--	--	--	--
2	100	5	45	—	--	--	--	1.5
3	100	5	45	--	50	--	--	1.5
4	100	5	45	--	--	50	—	1.5
5	100	5	45	--	--	--	5	1.5
6	100	5	45	—	50	—	5	1.5
7	100	5	45	--	--	50	5	0.5
8	100	7.4	--	30	--	--	2	0.4

sample mass was 20 g. The amount of particulate smoke collected on the filter was 145 mg. This filtrated sample contained 20 mg of extractable organics, 2 mg of PCAHs and 18 mg of aliphatics. Table 3.15 shows the major PCAH species found in the smoke of burning hydraulic fluid. (For other materials, see Tables A.6.4 and A.6.5 of Appendix A.6.)

3.2.3.3 Volatile Compounds

Volatile species that may be generated during the process of pyrolysis often interact with airborne particles. Two types of behavior can be revealed during the interaction--volatile deposition onto and release from the particulate surface. A special apparatus has been developed at GIT to identify these volatiles. The results for hydraulic fluid and PVC are shown in Tables 3.16 and 3.17a and b. The results for polymer materials are under investigation at GIT and are unavailable at this time.

3.2.4 Particulate Concentration

Particulate concentrations in terms of mass per unit volume are not currently available in the literature for the materials of interest, but they can be estimated from mass loss data in a known chamber volume. Published data on volume fraction (volume concentration) were found for hydraulic fluid. Again, this information was determined by Zinn et al. (1980) in flaming tests on the hydraulic fluid. The Mie theory was used to calculate the soot refractive index m_e = 1.57 to 0.56i. Zinn observed that optical density ratios measured for the soot particles produced by the burning of hydraulic fluid were about 20% lower than the theoretical values for spherical particles.

TABLE 3.14. Amounts of PCAHs Found in Smoke Particles Generated from PVC Under Simulated Fire Conditions, µg of PCAH/g Pure Resin

Peak No.	Tr	Molec. Weight	Name of PCAH	PVC-0		PVC-1		PVC-2		PVC-3		PVC-4		PVC-5		PVC-1 3.5	PVC-1 7.5
				NF	F	NF	F	NF	F	NF	F	NF	F	NF	F	NF	NF
1	3.0	128	Naphthalene	--	--	--	--	--	--	--	--	--	--	--	--	--	--
2	4.6	142	1-Methylnaphthalene	--	--	--	--	--	--	--	--	--	--	--	--	--	--
3	4.9	142	2-Methylnaphthalene	--	--	--	--	--	--	--	--	--	--	--	--	--	--
4	6.4	156	2-Ethylnaphthalene	--	--	--	--	--	--	--	--	--	--	--	--	--	--
5	6.7	156	2,6-Dimethylnaphthalene 1,6-Dimethylnaphthalene	--	--	--	--	--	--	--	--	--	--	--	--	--	--
6	7.1	154	Diphenyl	--	--	--	--	--	--	--	--	--	--	--	--	--	--
7	7.5	156	2,3-Dimethylnaphthalene 1,5-Dimethylnaphthalene	--	--	--	--	--	--	--	--	--	--	--	--	--	--
8	11.4	168	Dihydrofluorene (?)														
9	12.3	165	Fluorene	13.1	--	3.6	--	5.5	--	21.6	--	16.1	--	36.0	--	--	19.3
10	10.4	178	Phenanthrene Anthracene	25.2	22.5	29.1	3.6	35.7	--	40.3	--	36.7	--	41.6	2.3	6.9	40.0
11	21.4	192	1-Methylphenanthrene 2-Methylanthracene	21.1	19.1	19.1	3.5	19.1	--	20.3	--	18.0	--	20.3	--	9.5	28.7
12	22.4	192	9-Methylanthracene	16.5	11.3	15.5	3.6	9.6	1.6	30.7	--	12.9	--	17.3	--	11.3	24.3
13	23.9	206	9,10-Dimethylanthracene	16.7	14.3	15.6	4.7	13.1	2.0	13.1	--	10.7	--	18.0	--	26.0	23.9
14	25.9	202	Fluoranthene	10.5	12.3	10.5	0	6.5	2.1	8.5	1.5	6.5	--	9.8	--	3.9	13.2
15	27.2	202	Pyrene	7.6	19.3	11.6	6.1	6.7	8.4	9.2	2.7	7.6	--	11.5	--	8.4	13.1
16	28.8	216	1,2-Benzofluorene	31.3	9.3	35.3	4.5	17.3	5.3	25.6	2.0	20.9	--	24.5	2.9	15.3	40.0
17	29.3	216	2,3-Benzofluorene	21.9	8.4	32.8	5.9	16.8	2.4	19.3	2.0	19.3	--	22.8	2.9	23.1	29.3
18-21	30.8-34.6	230	Methylbenzofluorene (?)														
22	35.5	228	Chrysene, 1,2-Benzoanthracene Triphylene	8.7	24.4	16.0	10.5	12.7	10.5	6.1	4.4	16.7	2.3	14.3	3.6	36.5	22.1
23	37.5-39.0	256	Dimethyl (MW 228) (?)														
24	39.4	256	7,12-Dimethylbenzo(a)anthracene	3.5	--	3.5	--	3.5	--	3.5	--	3.5	--	3.5	--	4.7	4.7
25	45.7	252	Benzo(a)pyrene, Benzo(e)pyrene	3.2	3.2	5.3	2.4	4.4	4.4	3.2	3.2	4.4	0	3.2	--	3.3	3.3
26	47.7	252	Perylene	3.3	3.3	7.3	2.4	4.5	2.4	2.0	2.4	3.3	0	2.0	--	5.3	5.3
			Total PCAH	182.6	149.4	205.2	47.1	155.4	39.1	203.4	18.2	176.6	2.3	224.8	11.7	154.2	275.2

(a) Heat flux = 5 W.

TABLE 3.15. Major PCAH Species Found in Particulate
Smoke of Hydraulic Fluid

PCAH	Percent
Anthracene/phenanthrene	1
Fluoranthene	29
Pyrene	45
1,2, Benzothorene, etc.	6
2,13 Benzothoranthene, etc.	12
2,4 Benzo(a)pyrene	0.7

TABLE 3.16. Mass Loss Data for Hydraulic Fluid and PVC

Sample	Sample Mass, mg	Ash Mass, mg	Particulate Mass, mg	Vapor Mass, mg
Hydraulic Fluid	22.22	0.29	0.67	21.26
PVC	10.33	2.77	0.31	7.25

Thus it appears that the soot particles produced in flaming tests of the hydraulic fluid are nonspherical. The equation used to calculate the volume fraction is:

$$\emptyset = \frac{2}{3} \left[\frac{D_{vs} \; \ell n/(I_0/I)}{\overline{Q}_{ext}(D_{vs},m)L} \right] \tag{3.8}$$

where

$\emptyset$ = volume fraction

D_{vs} = mean particle diameter

I_0 = incident light intensity

I = light intensity transmitted through smoke

$\overline{Q}_{ext}$ = mean extinction efficiency

m = refractive index

L = optical path length.

TABLE 3.17a. Major Volatile Components
from Hydraulic Fluid

Compound	Concentration,[a] mg/m³
CO	600
Air	---
CO_2	10000
Propene	700
H_2O	7000
Acetaldehyde	2000
Butene	2000
Acrolein	200
Propionaldehyde	800
Acetone	2000
1,3 Heptadiene	400
Methacrolein	300
5-Heptan-2-one	800
Cycloheptane	1000
Benzene	800

(a) Calculated on the basis of a
20-gal sample burning into a
25,000-ft³ space. The data are
for the vapor phase. Values for
compounds adsorbed onto particles
range from 1 to 4% of values shown.

The results, presented in Figure 3.9 and Table 3.18, were corrected to the standard flow rate (425 ℓ/min) with the following equation:

$$\emptyset_{corr} = \emptyset_{meas} \frac{\dot{V}_t}{\dot{V}_{25}} = \emptyset_{meas} \left[\frac{T + 273}{298} \right] \qquad (3.9)$$

where $\dot{V}_t$ is the volumetric flow rate at temperature T and $\dot{V}_{25}$ is at 25°C.

TABLE 3.17b. Major Volatile Components from PVC

Compound[a]	Concentration,[b] mg/m^3
CO	3
Air	--
CO_2	53
H_2O	32
1,3 Butadiene	3
Acetone	3
3-Chloro-2-methylpropene	3
1,4 Dichlorobutane	1
Benzene	9
Acetic acid	1
Toluene	2

(a) HCl was identified separately using a
    nonchromatographic method.
(b) Calculated on the basis of a 3-ft length of
    cable burning into a 25,000-ft^3 space. The
    data are for the vapor phase. Values for
    compounds adsorbed onto particles range from
    1 to 4% of the values shown.

3.2.5 Summary

    Studies of combustion products found in smoke have been reviewed and data
on the characteristics of these materials, collected under simulated fire con-
ditions, are tabulated.

    Table 3.9a presents the percentages of smoke particles becoming airborne
for most of the materials of interest (except cellulosic materials and
kerosene); the corresponding experimental methods and approximate fire condi-
tions are given in Table 3.9b. Tables 3.10 and 3.11 show mass loss rates and
product generation rates, respectively, for many polymeric materials as a
function of external heat flux and O_2 availability. Particle size and distri-
bution can be found in Table 3.12 in terms of mass mean diameter, volume sur-
face mean particle diameter and standard deviation. (The particle size and
distribution were also measured under approximate fire conditions.) Chemical
analysis for particulate materials collected from burning hydraulic fluid and
various compositions of PVC samples are shown in Tables 3.14 through 3.18.
There is little information on particulate concentration for the materials of
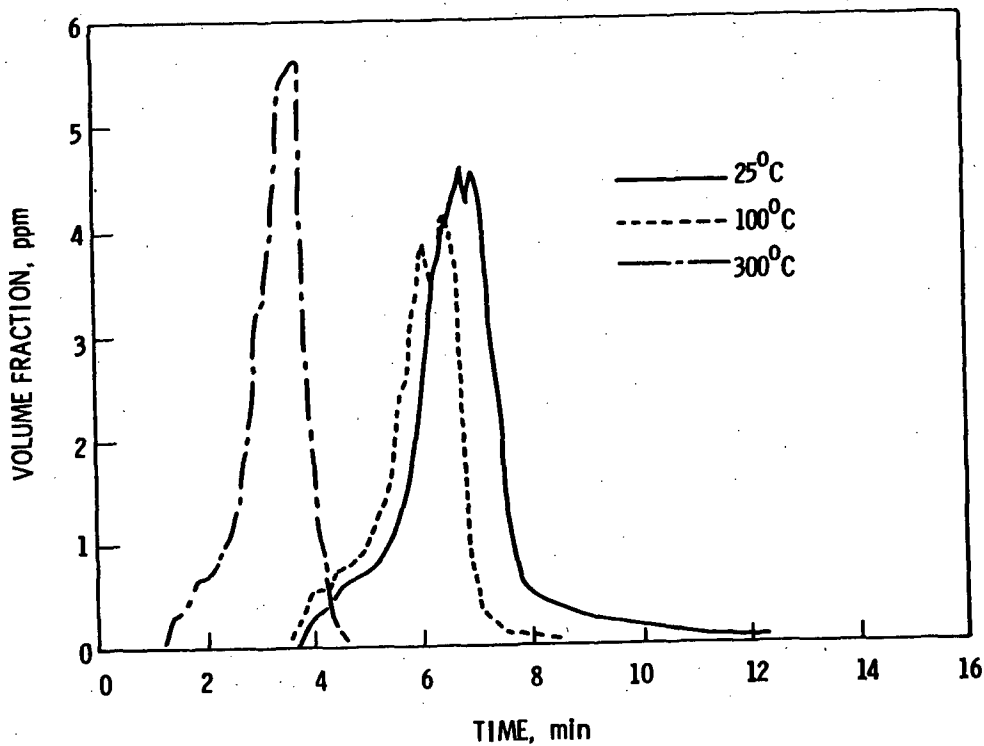
FIGURE 3.9. Effect of the Ventilation Air Temperature on the Particulate
Volume Fraction for Flaming Combustion of Hydraulic Fluid
Exposed to a Radiant Flux of 5 W/cm²

TABLE 3.18. Sample Weight Loss and Smoke Concentration Data
for Hydraulic Fluid

Mode	Ventilation Air Temperature, °C	Peak Volume[a] Fraction, ppm
Nonflaming[b]	25	0.83
Flaming	25	4.54
Flaming	100	4.11
Flaming	300	5.58

(a) Based on m_R = 1.50 - 0.0i for nonflaming
    combustion and m_R = 1.57 - 0.56i for
    flaming combustion at a standard flow rate
    of 425 ℓ/min.
(b) During the initial nonflaming phase,
    spontaneous ignition occurred 5.9 min after
    initiation of exposure.

3.33

interest in terms of mass concentration as a function of time. Nonetheless, from the available mass loss data in a known chamber volume, mass density as a function of time can be estimated.

3.3 ENERGY RELEASE RATE

The expression for energy release rate (Tewarson 1980b) is:

$$\dot{Q}_a'' = X_a(H_t/L)(\dot{q}_e'' + \dot{q}_{fs}'' - \dot{q}_{rr}'') \qquad (3.10)$$

where $\dot{q}_{fs}''$ is equal to the sum of flame convective and radiative heat flux to the surface, respectively:

$$\dot{q}_{fs}'' = \dot{q}_{fc}'' + \dot{q}_{fr}'' \qquad (3.11)$$

Table 3.19 presents energy release rates (using Equation 3.10) for the fuel materials we have been considering. Energy release rate is a function of external heat flux $\dot{q}_e''$, volumetric flow rate of air into the apparatus $\dot{V}_a$ and

TABLE 3.19. Energy Release Rates for Various Combustible Materials

Combustible	$\dot{q}_e''$ kW/m²	$\dot{V}_a$ m³/sec×10³	M_{O_2}	H_t kJ/g	L kJ/g	$\dot{q}_{rr}''$ kW/m²	X_a	$\dot{q}_{fs}''$ kW/m²	$\dot{Q}_a''$ kW/m²
PMMA	0	1.4	0.183-0.531	25.2	1.63	11	0.99-0.98	21-56	150-680
	31[a]-60[b]	N[b]	0.233	25.2	1.63	11	0.86	29-45	650-1250
PVC	0	2.0	0.671-0.874	16.4	2.47	21	0.35	63-65	95-100
Granular PS	0	1.4	0.233-0.524	39.2	1.70	14	0.68-0.67	39-35	390-320
Polypropylene	0	1.4	0.196-0.507	43.3	2.03	18	0.99-0.91	23-66	100-930
	52[a]	0.86	0.233	43.3	2.03	18	0.63	58	1250
Oak[a]	31[a]-71	1.4	0.233	17.7	1.7[c] 5.5[d]	16	0.68 0.71	16-7	220-140

(a) Data taken from Tewarson's previous studies.
(b) Natural air flow.
(c) For $\dot{q}_e'' < 46$ kW/m².
(d) For $\dot{q}_e'' > 46$ kW/m².

3.34

mass fraction of O_2. Note that H_t and L are material properties and are expected to be independent of fire environment, while Q_a'' depends on both material properties and fire environment. Figure 3.10 shows the Factory Mutual small-scale apparatus that Tewarson has been using to obtain the data for the calculation of energy release rates.
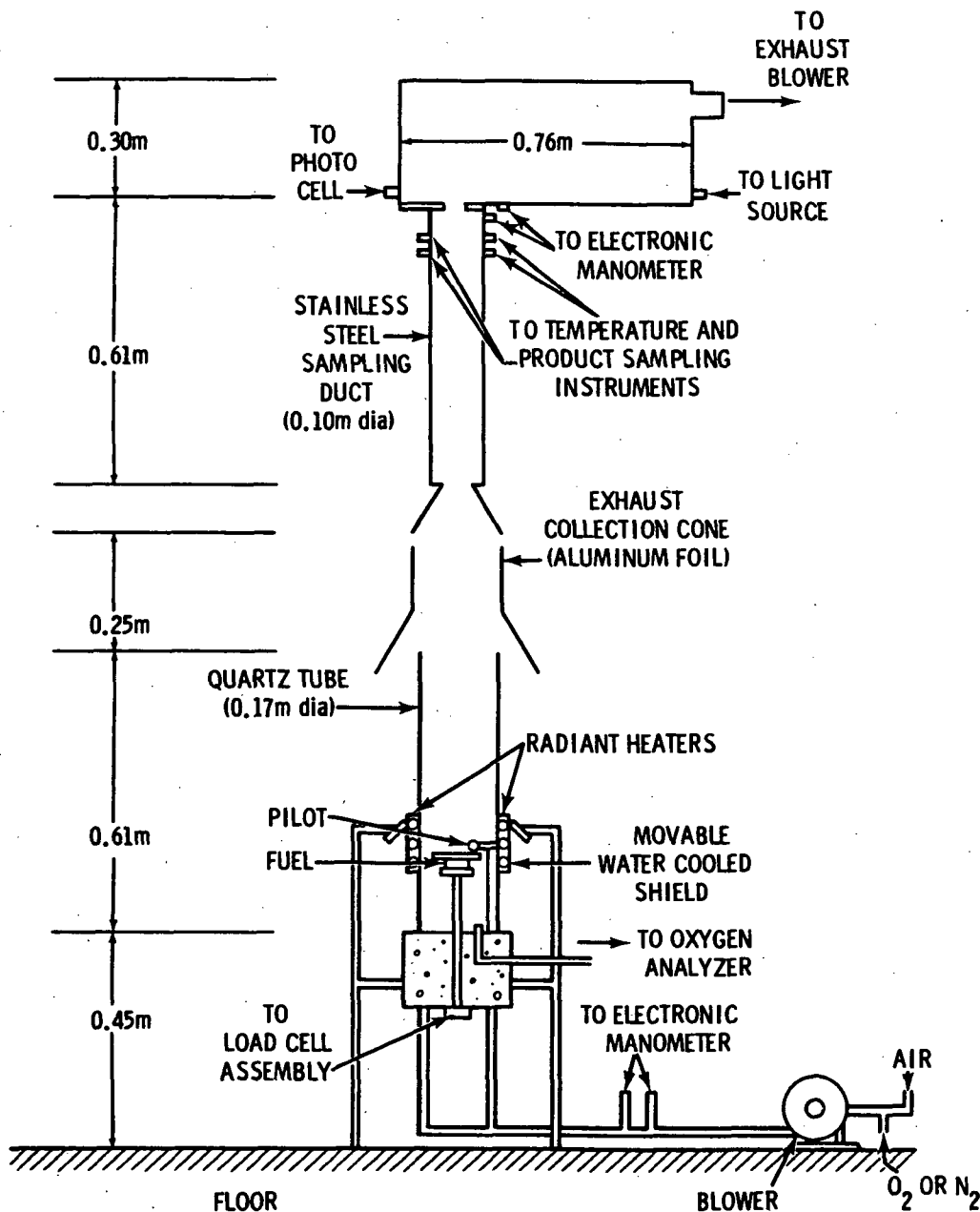
FIGURE 3.10. Factory Mutual Combustibility Apparatus

According to Tewarson, $\dot{q}''_{fc}$ and $\dot{q}''_{fr}$ are accurate to about ± 30 and $\pm 20\%$, respectively. Therefore, the calculation of energy release rates with this equation could have an uncertainty of 50%. Based on the data shown in Table 3.19, the energy release rate of the given combustibles increases with increasing availability of O_2 and presence of external heat flux $\dot{q}''_e$. This is true for all the materials considered except PS, which has a lower heat release rate at a higher fraction of O_2 concentration. Tewarson (1980b) stated that this is due to the char-forming nature of PS. Also, with the high-charring behavior, the mass loading rate of PS is suppressed.

In the study of high-pressure spray flammability, Roberts and Brooks (1981) determined the heat output of various types of hydraulic fluids. The experiments were performed in a ventilated test chamber with two axial fans mounted near the floor. The chamber, housed in a laboratory, was constructed from 0.8 mm sheet steel and was 12 ft long x 8 ft wide x 8 ft high with a door at one end and a Perspex window on the other. Figure 3.11 is a cutaway drawing of the chamber, showing the position of the equipment.

A metering pump capable of delivering up to 0.5 ℓ/min of fluid against a back pressure of 6.9 MPa (1000 lb/in.^{2}) was used to disperse the fluid. A
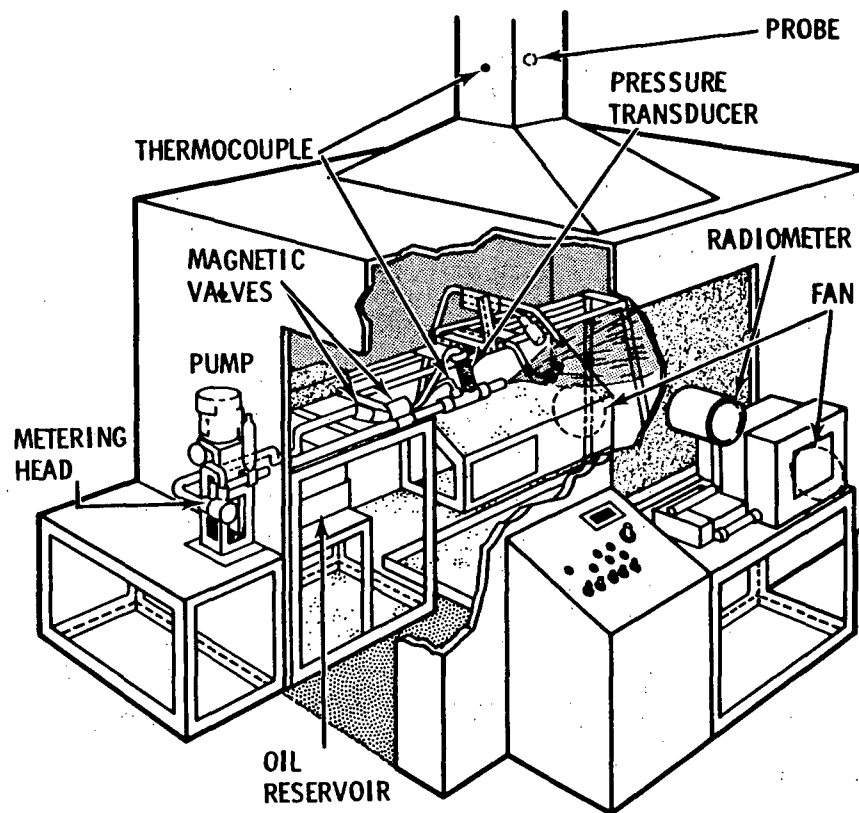
FIGURE 3.11. Chamber for High Pressure Spray Flammability Tests

premixed propane/air flame was used to ignite the hydraulic fluid spray and to stabilize the flame throughout the test. The equipped instrumentation is capable of measuring pressure and temperature of the spray, thermal radiation of the flame, oxygen concentration from the stack, and temperature rise of the exhaust gases.

The results in average values are summarized in Table 3.20. For more detailed tabulation, refer to Table A.7.1 of Appendix A.7. The calorific values of each fluid were determined in a standard high-pressure oxygen bomb. The comparison of energy outputs from various hydraulic fluids can be made directly from the table. A comparison between the sets of data obtained for mineral oil and water-in-oil emulsion is of interest, since the latter consists of about 60% mineral oil, 40% water, with traces of anti-corrosion and stabilizing additives.

3.4 RATE EQUATIONS OF COMBUSTION PROCESSES

Tewarson et al. (1978, 1980) of Factory Mutual Research Corporation has derived the following three rate equations which describe the amount of material loss, heat release and product generation in a fire as a function of material properties and fire conditions.

3.4.1 Mass Loss Rate ($\dot{M}''$)

The mass loss rate of various combustible materials depends on the available net heat flux received by the material in a fire and the heat requirement to generate a unit mass of combustible vapors (Tewarson 1980a):

$$\dot{M}'' = \dot{q}''_n/L \tag{3.12}$$

where

$\dot{M}''$ = mass loss rate of the material

$\dot{q}''_n$ = net heat flux received by the fuel material per unit fuel surface area

L = heat required to generate a unit mass of the fuel vapors.

Mass loss rates for the two phenomena, pyrolysis and combustion, are defined as follows (Tewarson 1980b):

● mass loss rate in pyrolysis ($\dot{M}''_p$)

$$\dot{M}''_b = (\dot{q}''_e - \dot{q}''_{rr})/L \tag{3.13}$$

TABLE 3.20. Results of Heat Output Tests on Various Types of Hydraulic Fluid

Fluid Type	Average Fluid Temperature, °C	Average Spraying Rate, g/sec	Calorific Value	Average Total Heat Output, kJ/g	Combustion Efficiency,%	Radiative Contribution,%	Average Air Consumption, kg/kg of fluid
Mineral oil	48	3.7	44.9	27.8	62	43	14.1
Water-in-oil emulsion	48	4.2	25.7	17.9	70	26	8.5
Phosphate ester	46	5.2	30.8	19.4	63	45	6.7
Water-glycol	40	4.9	14.7	5.3	36	13	2.7

where

$$(\dot{q}_e'' - \dot{q}_{rr}'') = \text{the net heat flux}$$

$$\dot{q}_e'' = \text{external heat flux}$$

$$\dot{q}_{rr}'' = \text{surface reradiation loss.}$$

● mass loss rate in combustion ($\dot{M}_b''$)

$$\dot{M}_b'' = (\dot{q}_e'' + \dot{q}_{fs}'' - \dot{q}_{rr}'')/L \tag{3.14}$$

where $\dot{q}_e'' + \dot{q}_{fs}'' - \dot{q}_{rr}''$ is the net heat flux, and the total flame heat flux $\dot{q}_{fs}''$ is included in the net heat transfer because of the flaming combustion. Value $\dot{q}_{fs}''$ is the summation of flame convective heat flux $\dot{q}_{fc}''$ and radiative heat flux $\dot{q}_{fr}''$.

(Equations 3.13 and 3.14 are the final forms which were used in Section 3.2.1 for calculation of mass loss rate in pyrolysis and combustion.)

3.4.2 Heat Release Rate ($\dot{Q}_a''$)

To be able to describe the rate of fire growth and the size of the fire, heat release rate must be considered. The measurement of heat release rates in fires can be expressed as follows (Tewarson 1980a):

$$\dot{Q}_i'' = H_i \dot{M}_b'' \tag{3.15}$$

where

$$H_i = \text{the heat of combustion}$$

$$\dot{M}_b'' = \text{mass loss rate in combustion}$$

$$\dot{Q}_i'' = \text{the heat release rate.}$$

When all the fuel vapors burn completely, H_i of Equation (3.15) is defined as heat of complete combustion of the fuel H_t (original discussion of H_t can be found in Section 2.1.4). In an actual fire, where both material pyrolysis and combustion often coexist and oxygen is not always available, fuel vapors generated from pyrolysis do not often burn completely. Therefore, H_i is defined as the actual heat of combustion of fuel H_a, and $\dot{Q}_a''$ is the actual heat release rate. Thus Equation (3.15) can be rewritten as

$$\dot{Q}_a'' = H_a \dot{M}_b'' \tag{3.16}$$

3.39

Furthermore, the ratio of actual to complete heat of combustion (H_a/H_t) is defined as combustion efficiency of the fuel X_a. Therefore,

$$\dot{Q}''_a = X_a H_t \dot{M}''_b \qquad (3.17)$$

or from Equation (3.14) and Equation (3.17), the heat release rate is written as

$$\dot{Q}''_a = X_a (H_t/L) (\dot{q}''_e + \dot{q}''_{fs} - \dot{q}''_{rr}) \qquad (3.18)$$

(Equation 3.18 is the final expression which was used in Section 3.3 for the calculation of energy release rates.)

Notice that $\dot{Q}''_a$ depends on the material properties and fire environment (Tewarson 1980b); i.e., thermal environment $\dot{q}''_e$ and $\dot{q}''_{fs}$, availability of oxygen, X_a, and material X_a, H_t/L, and $\dot{q}''_{rr}$.

Heat release rate (Tewarson 1980b) deals with a) the combustion efficiency of combustible materials, b) the ratio of heat of complete combustion to heat required to generate a unit mass of vapors and c) the net heat flux absorbed by the surface. Tewarson studied the dependency of heat release rate on thermal and over- or underventilated fire environment and various materials. He found that the combustion efficiency for an overventilated fire environment becomes approximately constant for each generic type of material tested. The combustion efficiency X_a may be classified as shown in Table 3.21. According to Tewarson, combustion efficiency can decrease if:

- the ratio of carbon relative to H,O, etc., in the vapors decreases

- the gas-phase reactions are quenched or retarded by lack of available oxygen, chemical retardants in the materials, or decrease in temperature

- soot-forming reactions are preferred in the gas phase (i.e., PS).

3.4.3 Product Generation Rate $\dot{G}''_j$

The combustion product (i.e., CO_2, CO, H_2O, smoke, and low volatile hydrocarbons) generation rate is equal to the fractional yield of the product times the mass loss rate, according to Tewarson (1080b). This is expressed as:

$$\dot{G}''_j = Y_j \dot{M}'' \qquad (3.19)$$

TABLE 3.21. Combustion Efficiency, X_a

Non-aromatic polymers[a]

    PMMA   High $(0.81 < X_a < 0.97)$

    Polypropylene

Aromatic compounds[b]

    Red oak   Medium $(0.51 < X_a < 0.7)$

    PS

Chlorinated compound

    PVC   Low $(X_a \sim 0.35)$

(a) non-charring materials.
(b) charring materials.

where

    j = combustion product

    $\dot{G}''$ = is the mass generation rate of product j per unit surface area j

    $\dot{M}''$ = the mass loss rate by pyrolysis or combustion

    Y_j = the yield of product j, which can be expressed as the multiple of the yield of product j expected from stoichiometry kj, and the product generation efficiency f_j:

$$Y_j = f_j k_j \qquad (3.20)$$

Thus product generation rate for pyrolysis of certain species can be written as

$$\dot{G}''_{pj} = f_j (k_j/L) (\dot{q}''_e - \dot{q}''_{rr}) \qquad (3.21)$$

Product generation rate for combustion is (using Equation 3.14)

$$\dot{G}''_{bj} = f_j (k_j/L) (\dot{q}''_e + \dot{q}''_{fs} = \dot{q}''_{rr}) \qquad (3.22)$$

Notice that, like $\dot{Q}''_a$, $\dot{G}''_j$ depends on both material properties and fire conditions. (Equations 3.21 and 3.22 are the final expressions that were used in Section 3.2.1 for the calculation of product generation rates.)
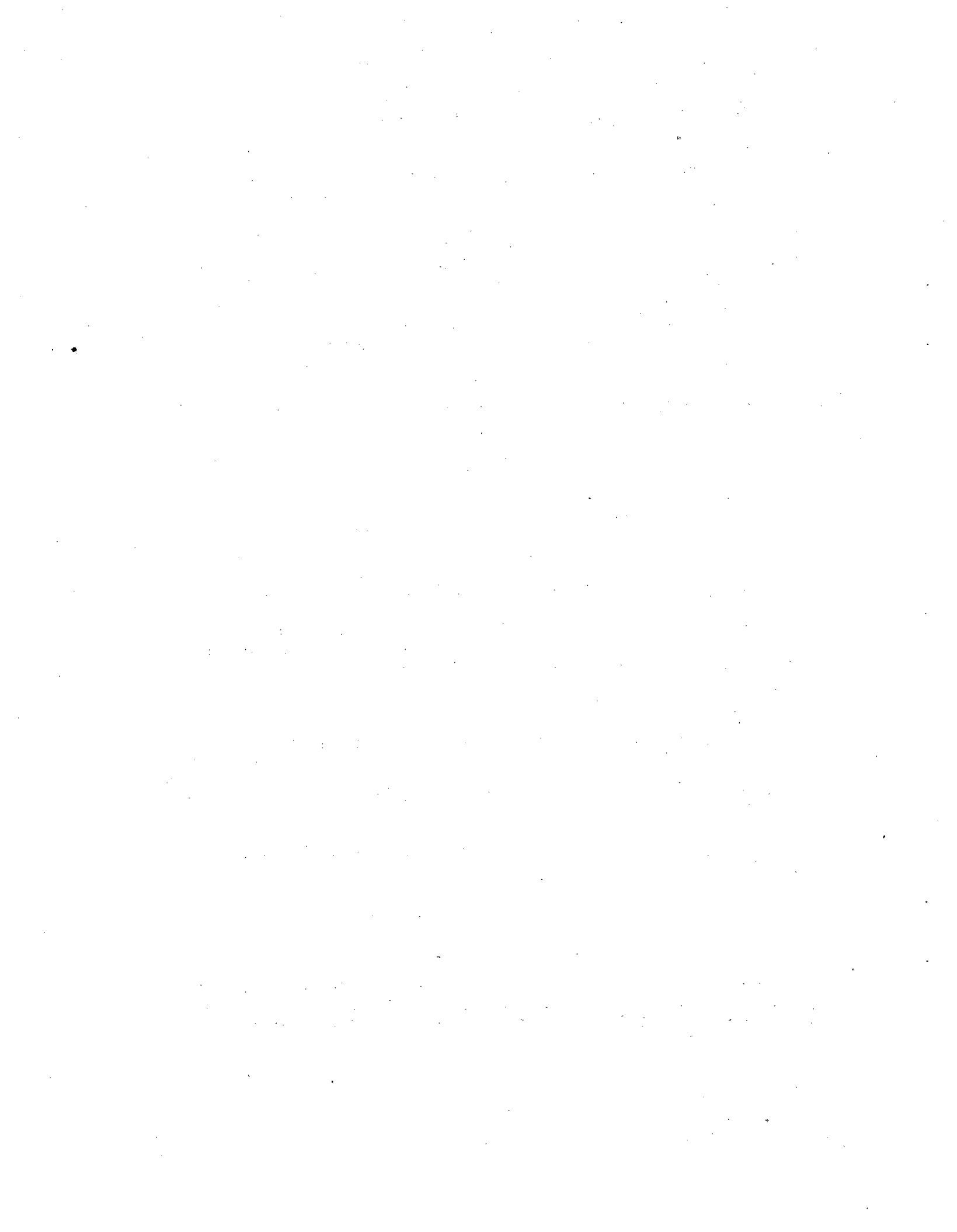
4.0 DISCUSSION

The discussion below is followed by examples that illustrate the use of the available data. Information gaps are then identified based on this literature review.

4.1 THE STUDY OF COMBUSTION PRODUCTS

The combustion products generated have been the main subject in fire research due to their threat to public health and safety in the event of an enclosure fire. Today, the characteristics of fire-generated products are examined by conducting laboratory tests. During the past few years, small-scale fire tests of all types have come under considerable criticism because of the growing evidence that they are not good predictors of actual fire performance and because the quoting of small-scale test data can be misleading to fire-safety regulatory officials and the public. Still, large-scale tests are costly and time-consuming, and a philosophy is needed on the relevant roles of both large- and small-scale tests. According to Punderson (1981), there seems to be a developing consensus as follows:

- The best test methods for judging acceptability of materials and for public fire-safety standards are based on full-scale, end-use simulations related to realistic fire scenarios. (Note that an end-use simulation generally requires that the test specimen be in the form of an end-use product rather than a small specimen of material.)

- Small-scale tests are essential for guidance of research programs that are developing new materials and products.

At the present time, only small-scale test data are readily available for various sets of approximate fire conditions. Unfortunately, a real fire is not a set of time and temperature conditions; nonetheless, the combination of the discrete small-scale data, under different sets of fire conditions, can be used carefully, based on the current stage of combustion technology, to approximate the outcome of the combustion process in a well-defined fire scenario of interest.

4.2 APPLICATION OF THE DATA

The characteristic data of fire-generated products (mass and energy) measured by Factory Mutual Research and GIT are the best available today for fire accident analysis inside a nuclear fuel cycle facility. The data are limited to combustible materials normally found in fuel cycle facilities. In this section examples are given to demonstrate general usage of the data collected in Tables 3.9, 3.10, 3.11, 3.12, and 3.19.

Major fire consequences such as elevated room temperature and pressure resulting from the generation of heat, smoke particles, toxic gases and unburned vapors are the important parameters for enclosure fire analysis. Both

temperature and pressure gradients govern the dynamics of fluid motion and the thermodynamics of gas interaction, as well as particle behavior. To estimate these parameters, fire source terms such as the rates of mass and energy generation in the fire, and the particulate characteristics are necessary.

Mass loss rate (sometime referred as generation or burning rate) of a fuel depends strongly on the chemical and physical properties of the material itself, its surface area, heat fluxes from the external source such as burning objects nearby, and the availability of oxygen (see Sections 2.4 and 3.2 for details). Table 3.10 may be used to estimate mass loss rates for materials of interest. For example, assuming 1000 g of a PMMA slab burning in an overventilated room with no external heat source, a steady state mass loss rate (flowing combustion) of 28 g/sec can be used, provided that the slab has a constant burning surface area of 1 m^2. If the burning conditions do not change significantly, the time required to consume 1000 g (at 1000 g/28 g/sec) is approximately 35 sec.

From Table 3.11, the generation rates of gases, smoke, and hydrocarbons (in the form of unburnt vapor) can be obtained for the flaming combustion of PMMA. For example, under the above burning conditions, the steady state generation rate for CO_2 is 62 g/sec; for CO and hydrocarbons, less than 0.03 g/sec each; and for smoke, 0.65 g/sec. During the PMMA fire, particles with a volume diameter of 1.2 μm at maximum optical density (from Table 3.12) can be generated.

Energy generation rate is a strong function of mass loss rate. The actual energy generated from a burning episode is composed of convective and radiative fractions. The convective fraction of energy is responsible for the heating of the combustion gases. Actual energy generation rates can be obtained from Table 3.19, while the convective and radiative fractions can be calculated using Table A.1.2 in the appendix. For example, assuming the same PMMA slab is burning, the steady state energy generation rate is 680 kW. From Table A.1.2 the convective fraction is 0.64/0.94 (defined as X_c/X_a) under a normal air conditions in a room, while the radiative fraction is 0.30/0.94 (defined as X_r/X_a). Therefore the steady state convective energy release rate is

$$680 \text{ kW}(0.64/0.94) = 217 \text{ kW}$$

and the steady state radiative energy release rate is

$$680 \text{ kW}(0.30/0.94) = 463 \text{ kW}.$$

The above examples are applicable for a specific fire condition. Since fire is a dynamic process, a set of discrete mass and energy rates under different fire conditions are rquired to realistically predict the outcome of an enclosure fire. It must be further understood that the data are mainly for overventilated fire and independent burning of material. Smoldering combustion, which is responsible for the increased generation rate of flammable vapor, is the characteristic of underventilated fires.

Besides the characteristics found in the examples above, additional information that may be obtained in Section 3.0 (and the appendix) includes:

- product generation rates of CO, CO_2, and total gas hydrocarbon (Figures A.1.3 to A.1.5)

- product generation efficiencies (Tables A.1.2 and A.1.4)

- actual heat release rates (Figures A.1.1 and A.1.6)

- heat required to generate a unit mass of vapor (Table A.1.1 and A.1.5)

- convective and radiative heat release rates per unit surface area of the material [Equation (3.17) of Section 3.4 with replacement of X_a by X_c and X_r, respectively]

- combustion efficiency (Tables A.1.2 and A.1.4)

- convective and radiative fractions of heat of complete combustion (Table A.2.6)

- surface reradiation loss (Tables A.1.2 and A.1.4)

- flame height (see Tewarson 1980b)

- excess pyrolysate (see Tewarson 1980b).

4.3 IDENTIFICATION OF INFORMATION GAPS

The numerous assumptions required to arrive at an estimate of the characteristics of airborne combustion products for the examples indicate the lack of usable data for certain materials of interest in this study. Data on the energy release rate (derived from the mass loss rate and combustion efficiency), fraction of mass loss rates generated as particles, size distribution of the airborne particulate materials, and chemical composition of the airborne materials are estimated by conducting laboratory-scale fire experiments. This available information must be used carefully in a postulated fire scenario inside a real-scale enclosure. There are, in fact, some information gaps which must be filled in order to predict and describe the characteristics of airborne materials in a nuclear facility fire. The gaps are identified below:

- lack of combustion product data for cellulosic materials (i.e., paper and rags)

- lack of combustion product data for elastomers (i.e., both synthetic and natural rubber materials used in glovebox and surgeons' gloves)

- lack of some combustion data for organic fluids that are possibly found as working fluids in fuel processing (i.e., kerosene--as fuel for heating requirements of some process equipment). The information found for kerosene is solely for jet spray combustion.

- lack of combustion data for mixtures of the combustible materials of interest

- lack of information on how radioactive particles have influenced the characteristics of the airborne combustion products, and vice versa.

- lack of information on a "scaling factor" which can be used to approximately convert the data obtained from small-scale combustion experiments to an actual fire

- Lack of energy information on significantly reduced oxygen levels that would cover underventilated burn modes.

5.0 REFERENCES

Alpert et al. 1981. Modeling of Ceiling Fire Spread and Thermal Radiation. Factory Mutual Research, Norwood, Massachusetts.

Alvares et al. 1980. Fire Protection Countermeasures for Containment Ventilation Systems. UCID-1878, Lawrence Livermore National Laboratory, Livermore, California.

Bankston, C. P. et al. 1978. Review of Smoke Particulate Properties Data for Natural and Synthetic Materials. NBS-GCR-78-147, Georgia Institute of Technology, Atlanta, Georgia.

Bittner, J. D. 1978. "Formation of Soot and Polycyclic Aromatic Hydrocarbons in Combustion Systems." In Combustion Research on the Characterization of Particulate Organic Matter from Flames, eds. R. A. Hites and J. B. Howard, pp. 21-40. PB-291 314, National Technical Information Service, Springfield, Virginia.

Boisdron, Y. and J. R. Brock. 1972. "Particle Growth Processes and Initial Size Distribution." In Assessment of Airborne Particles: Fundamentals, Applications, and Implications to Inhalation Toxicity, pp. 129-150. Charles C. Thomas, pub., Springfield, Illinois.

Bonne, U., K. H. Homann, and H. G. Wagner. 1965. "Carbon Formation in Premixed Flames." In Tenth Symposium (International) on Combustion, pp. 503-512. The Combustion Institute, Pittsburgh, Pennsylvania.

Burge, S. J. and C. F. H. Tipper. 1969. "The Burning of Polymers." Combustion and Flame 13:495-505.

Burgess, W. A., R. D. Treitmar and A. Gold. 1979. Air Contaminants in Structural Fires--Final Report. PB299017, Harvard School of Public Health, Cambridge, Massachusetts.

Cheng, J., N. W. Ryan and A. D. Baer. 1969. "Oxidative Decomposition of PBAA Polymers at High Heating Rates." In Twelfth Symposium (International) on Combustion, pp. 525-532. The Combustion Institute, Pittsburgh, Pennsylvania.

Chien, W. P. and J. D. Seader. 1975. Smoke Measurement in a Modified NBS Smoke Density Chamber. FRC/UU-44 (UTEC 75-055), Flammability Resources Center, University of Utah, Salt Lake City, Utah.

Chippet, S. and W. A. Gray. 1978. "The Size and Optical Properties of Soot Particles." Combustion and Flame 31:149-159.

Currin, Myron L. 1974. Physics of Smoke Formation. Colorado State University, Fort Collins, Colorado.

D'Alessio, A. et al. 1974. "Soot Formation in Methane-Oxygen Flames." In Fifteenth Symposium (International) on Combustion, pp. 1427-1438. The Combustion Institute, Pittsburgh, Pennsylvania.

Driscoll, J. F. et al. 1978. "Submicron Particle Size Measurements in an Acetylene-Oxygen Flame." Combustion Science and Technology 20:41-47.

Edwards, J. B. 1974. Combustion-Formation and Emission of Trace Species. Ann Arbor Science Publishers, Michigan.

Emmons, Howard W. 1980. The Growth of Fire Science. Harvard University, Cambridge, Massachusetts.

Fenimore, C. P. and G. W. Jones. 1966. "Modes of Inhibiting Polymer Flammability." Combustion and Flame 10:245-301.

Gaydon, A. G. and H. G. Wolfhard. 1970. Flames--Their Structure, Radiation and Temperature. Chapman and Hall, London.

Gross, D., J. J. Loftus and A. F. Robertson. 1969. "Method for Measuring Smoke from Burning Materials." In ASTM Special Technical Publication 422. American Society for Testing and Materials, Philadelphia, Pennsylvania.

Hilado, C. J. 1969. Flammability Handbook for Plastics. Technomic Publications, Stamford, Connecticut.

Huggett, Clayton. 1978. "Oxygen Consumption Calorimetry." Paper presented at the 1978 Fall Technical Meeting of the Eastern Section of Center for Fire Research, National Bureau of Standards, Washington, D.C. The Combustion Institute, Miami, Florida, November 29-December 1.

King, T. V. 1979. Smoke and Carbon Monoxide Formation from Materials Tested in the Smoke Chamber. NBSIR 75-901, Center for Fire Research, National Bureau of Standards, Washington, D.C.

Krause, F. R. et al. 1980. LWR Fire Protection Design Verification by Thermodynamic Simulation. SAND80-1020, Sandia National Laboratory, Albuquerque, New Mexico.

Kunngi, M. and H. Tinno. 1974. "Determination of Size and Concentration of Soot Particles in Diffusion Flames by a Light Scattering Technique." In Fifteenth Symposium (International) on Combustion, pp. 257-266. The Combustion Institute, Pittsburgh, Pennsylvania.

Long, R. 1972. Studies on Polycyclic Aromatic Hydrocarbon in Flames. EPA-R3-92-020, University of Burmingham, Burmingham, England.

Magnussen, B. F. et al. 1978. "Effects of Turbulent Structure and Local Concentrations on Soot Formation and Combustion in C_2H_2 Diffusion Flames." In Seventeenth Symposium (International) on Combustion, pp. 1383-1393. The Combustion Institute, Pittsburgh, Pennsylvania.

McCaffrey, Bernard J. 1979. Purely Buoyant Diffusion Flames: Some Experimental Results. Center for Fire Research, National Bureau of Standards, Washington, D.C.

McHale, E. T. and E. G. Skolnik. 1979. Final Technical Report--Chemistry of Combustion of Fuel Water Mixtures. AD-A076958, Atlantic Research Corporation, Alexandria, Virginia.

Morrison, R. T. and R. N. Boyd. 1977. Organic Chemistry. 3rd ed. Allyn and Bacon, Boston, Massachusetts.

Murty, Kanuary A. 1978. Introduction to Combustion Phenomena. Gordon and Breach Science Publications, New York.

Pagni, P. J. and B. Bard. 1978. "Particulate Volume Fractions in Diffusion Flames." In Seventeenth Symposium (International) on Combustion, pp. 326-343. The Combustion Institute, Pittsburgh, Pennsylvania.

Palmer, H. B. and C. F. Cullis. 1965. "The Formation of Carbon from Gas." In Chemistry and Physics of Carbon, ed. P. L. Walker, Jr., Marcel Dekker, Inc., New York.

Parker, W. G. and H. G. Wolfhard. 1953. "Some Characteristics of Flames Supported by NO and NO_2." In Fourth Symposium (International) on Combustion, pp. 420-428. The Combustion Institute, Pittsburgh, Pennsylvania.

Pauling, L. ed. 1964. College Chemistry. 3rd ed., p. 315, W. H. Freeman and Company, San Francisco, California.

Pourprix, M. et al. 1978. "Size Distribution of Combustion Aerosols." Gosselachaft Fur Aerosol Forchung (GAF):76-78.

Powell, E. A. et al. 1979. "The Effects of Environmental Temperature Upon the Physical Characteristics of the Smoke Produced by Burning Wood and PVC Samples." Fire and Materials 3(1):12-15.

Prado, G. P. et al. 1978. "Soot and Hydrocarbon Formation in a Turbulent Diffusion Flame." In Combustion Research on Characterization of Particulate Organic Matter from Flames, ed. R. A. Hites and J. B. Howard, pp. 6-18. PB-291 314, National Technical Information Service, Springfield, Virginia.

Punderson, J. O. 1981. "A Closer Look at Cause and Effect in Fire Fatalities--The Role of Toxic Fumes." Fire and Materials 5(1):41-46.

Roberts, A. F. and F. R. Brooks. 1981. Hydraulic Fluids: An Approach to High Pressure Spray Flammability Testing Based on Measurement of Output. Explosion and Flame Laboratory, Harper Hill, Buxton, Derbyshire, England.

Rummel, K. and P. O. Veh. 1941. Arch Eisenhutten Wesen 14:489.

Saito, F. 1974. "Smoke Generation from Building Materials." In Fifteenth Symposium (International) on Combustion, pp. 1383-1393. The Combustion Institute, Pittsburgh, Pennsylvania.

Seader, J. D. and I. N. Einhorn. 1976. Some Physical, Chemical, Toxicological, and Physiological Aspects of Fire Smokes. Flammability Research Center, University of Utah, Salt Lake City, Utah.

Tesner, P. A. 1959. "Formation of Dispersed Carbon by Thermal Decomposition of Hydrocarbons." In Seventh Symposium (International) on Combustion, pp. 546-553. The Combustion Institute, Pittsburgh, Pennsylvania.

Tewarson, A. 1980a. "Heat Release Rate in Fires." Fire and Materials 4(4):185-191.

Tewarson, A. 1980b. Physico-Chemical and Combustion/Pyrolysis Properties of Polymeric Materials--Technical Report. PMRC J. I. OEON 6.RC, National Bureau of Standards, Washington, D.C.

Tewarson, A. and R. F. Pion. 1976. "Flammability of Plastics - I. Burning Intensity." Combustion and Flame 26:85-103.

Tewarson, A. et al. 1980. The Influence of Oxygen Concentration on Fuel Parameters. Factory Mutual Research Corporation, Norwood, Massachusetts.

Tsuchiya, Y. and G. W. Leir. 1975. "Equilibrium Composition of Fire Atmospheres." J. of Fire and Flammability 6:5-16.

Wagner, H. G. 1978. "Soot Formation in Combustion." In Seventeenth Symposium (International) on Combustion, pp. 3-18. The Combustion Institute, Pittsburgh, Pennsylvania.

Weast, Robert C., ed. 1981. CRC Handbook of Chemistry and Physics. 62nd ed. CRC Press, Cleveland, Ohio.

Williams, A. and D. B. Smith. 1970. Chem. Rev. 69:267.

Zinn, B. T. and R. A. Cassanova. 1976. "Properties of Combustion Products from Building Fires." Paper presented at the Annual Conference on Fire Research of National Fire Prevention and Control Administration, July 14-16, U.S. Dept. of Commerce, The Johns Hopkins University, Laurel, Maryland.

Zinn, B. T. et al. 1978. Investigation of the Properties of the Combustion Products Generated by Building Fires--Final Report of National Bureau of Standards. School of Aerospace Engineering, Georgia Institute of Technology, Atlanta, Georgia.

Zinn, B. T. et al. 1980. The Smoke Hazards Resulting from the Burning of Shipboard Materials Used by the U.S. Navy. NRL 8414, Georgia Institute of Technology, Atlanta, Georgia.

Zukoski et al. 1981. <u>Entrainment in Fire Plumes.</u> California Institute of Technology, Pasadena, California.

APPENDIX A

COLLECTION OF LITERATURE DATA

COLLECTION OF LITERATURE DATA

This appendix contains copies of data collected from the literature on the characteristics of combustion products. (Much of the tabulated material from Section 3.0 is derived from here.) Each section (Appendix A.1 through A.7) is a collection of tables and figures from one source. At the beginning of each section, this source is identified and the tables and figures are listed. A list of nomenclature is also provided if necessary.

LITERATURE

Tewarson, A. 1980. Physico-Chemical and Combustion/Pyrolysis Properties of Polymeric Materials--Technical Report. PMRC J.I. OEON 6.RC. National Bureau of Standards, Washington, D.C.

TABLES

A.1.1   Physicochemical Properties of Nonaromatic Materials

A.1.2   Combustion Properties of Nonaromatic Materials

A.1.3   Physicochemical Properties of Polystyrenes

A.1.4   Combustion Properties of Polystyrenes

FIGURES

A.1.1   Actual Heat Release Rate as a Function of Heat Released in the Complete Combustion of Material Vapors, $\dot{q}''_n + \dot{q}''_e + \dot{q}''_{fs} - \dot{q}''_{rr}$

A.1.2   Ratio of Yields of CO and CO_2 for Heptane as a Function of Oxygen-to-Fuel Stoichiometric Fraction (ϕ) ($\phi > 1$ for overventilated environment, $\phi < 1$ for underventilated environment)

A.1.3   Experimental Mass Generation Rate of CO_2 as a Function of Rate Expected from Stoichiometry, $\dot{q}''_n = \dot{q}''_e + \dot{q}''_{fs} - \dot{q}''_{rr}$

A.1.4   Experimentally Measured Mass Generation Rate of CO as a Function of Rate Expected from Stoichiometry, $\dot{q}''_n = \dot{q}''_e + \dot{q}''_{fs} - \dot{q}''_{rr}$

A.1.5   Experimentally Measured Mass Generation Rate of Soot and Low Vapor Pressure Liquids as a Function of Mass Loss Rate of the Material, $\dot{q}''_n = \dot{q}''_e + \dot{q}''_{fs} - \dot{q}''_{rr}$

A.1.6   Actual Heat Release Rate Calculated from CO and CO_2 as a Function of Actual Heat Release Rate Calculated from O_2 Depletion

NOMENCLATURE

$\dot{q}''_n$ Net heat flux per unit surface area of the material, kW/m^2

$\dot{q}''_e$ External heat flux per unit surface area of the material, kW/m^2

$\dot{q}''_{fs}$ Total flame heat flux per unit surface area of the material, kW/m^2

$\dot{q}''_{rr}$ Surface reradiation heat flux per unit surface area of the material

H_t Heat of complete combustion, kJ/g

L Heat required to generate a unit mass of vapor, kJ/g

$\dot{Q}''_A$ Actual heat release rate per unit surface area of the material, kW/m^2

Y_{CO} Mass fractional yield of CO

Y_{CO_2} Mass fractional yield of CO_2

G''_{CO_2} Generation rate of product CO_2 per unit surface area of the material, g/m^2-sec

kCO_2 Yield of CO_2 expected from stoichiometry

G''_s Generation rate of soot per unit surface area of the material, g/m^2-sec

T_s Material surface temperature

$\dot{V}_a$ Volumetric flow rate of air into the apparatus, m^3/sec

m_{O_2} Mass fraction of oxygen

X_A Combustion efficiency

X_C Convective fraction of heat of complete combustion

X_R Radiative fraction of heat of complete combustion

Y_{HC} Mass fractional yield of hydrocarbon

$\dot{q}''_{fc}$ Flame convective heat flux per unit surface area of the material

$\dot{q}''_{fr}$ Flame radiative heat flux per unit surface area of the material

σ Light obscuration parameter, m^2/g

TABLE A.1.1. Physicochemical Properties of Nonaromatic Materials[a]

Sample	Chemical Formula	Stoichiometric Air/Fuel Ratio	H_T, kJ/g	L, kJ/g	$\dot{q}_{rr}''$, kW/m²	T_s, K
Oak	$CH_{1.60}O_{0.71}N_{0.00}$	5.8	17.7	1.7[a] 5.5[b]	16	730
Polyoxymethylene (POM)	CH_2O	4.6	15.4	2.43	13	690
PMMA	$CH_{1.60}O_{0.40}$	8.2	25.2	1.63	11	660
Polypropylene (PP)	CH_2	15	43.3	2.03	18	750
PVC	$CH_{1.5}Cl_{0.50}$	5.5	16.4	2.47	21	780

(a) For $\dot{q}_e'' < 46$ kW/m².

(b) For $\dot{q}_e'' > 46$ kW/m².

TABLE A.1.2. Combustion Properties of Nonaromatic Materials

Sample	$\dot{q}_e''$, kW/m²	$\dot{v}_a$ (m³/sec) ×10³	m_{O_2}	X_A	X_C	X_R	Y_{CO_2}	Y_{CO}	Y_{HC}	Y_S	σ, m²/g	$\dot{q}_{fc}''$, kW/m²	$\dot{q}_{fr}''$, kW/m²
Oak	31	1.4	0.233	0.68	0.49	0.19	1.2	0.002	< 0.001	---	0.135	11	5
	37	1.4	0.233	0.63	0.43	0.20	1.2	0.004	< 0.001	0.017	0.108	8	10
	42	1.4	0.233	0.64	0.43	0.21	1.2	0.003	< 0.001	0.013	0.095	8	5
	46	1.4	0.233	0.72	0.45	0.27	1.2	0.003	< 0.001	0.013	0.081	7	6
	52	1.4	0.233	0.77	0.49	0.28	1.4	0.006	< 0.001	---	0.104	9	
	60	1.4	0.233	0.74	0.43	0.31	1.3	0.004	< 0.001	0.018	0.137	8	
	71	1.4	0.233	0.71	0.37	0.34	1.4	0.005	< 0.001	---	0.128	7	
POM	0	1.4	0.233	0.93	0.76	0.17	1.4	< 0.001	< 0.001	< 0.001	---	25	2
			0.303	0.93	0.77	0.16	1.4	< 0.001	< 0.001	< 0.001	---	28	8
			0.404	0.93	0.76	0.17	1.4	< 0.001	< 0.001	< 0.001	---	37	6
			0.445	0.93	0.65	0.28	1.4	< 0.001	< 0.001	< 0.001	---	33	12
			0.521	0.96	0.70	0.26	1.4	< 0.001	< 0.001	< 0.001	---	38	12
	39	0.86	0.233	0.82	0.53	0.29	1.2	0.001	< 0.001	< 0.001	---	11	7
	52	0.86	0.233	0.71	0.45	0.25	1.0	0.001	< 0.001	< 0.001	---	8	17
PMMA	0	1.4	0.183	0.99	0.76	0.23	2.2	0.011	< 0.001	---	---	17	4
			0.195	0.98	0.74	0.24	2.2	0.011	< 0.001	---	---	16	7
			0.207	0.98	0.70	0.28	2.1	0.012	< 0.001	---	---	17	7
			0.233	0.94	0.64	0.30	2.1	0.011	< 0.001	0.021	0.225	15	15
			0.318	0.95	0.54	0.41	2.1	< 0.001	< 0.001	0.023	0.111	13	26
			0.404	0.96	0.48	0.48	2.2	< 0.001	< 0.001	0.024	0.055	12	38
			0.491	0.97	0.49	0.48	2.2	< 0.001	< 0.001	0.020	0.029	13	43
			0.531	0.98	0.45	0.53	2.2	< 0.001	< 0.001		0.012	12	44
	0	N(a)	0.233										
	31	N(a)	0.233	0.86	0.57	0.29	1.9	0.008	< 0.001	---	0.232	8	21
	46	N(a)	0.233	0.86	0.49	0.37	1.9	0.007	0.001	---	0.282	3	32
	46	1.4	0.233	0.82	0.51	0.31	1.8	0.007	< 0.001	---	0.247	4	28
	60	N(a)	0.233	0.86	0.49	0.37	1.9	0.006	< 0.001	---	0.257	2	43
PP	0	1.4	0.196	0.99	0.82	0.16	3.1	0.021	0.007	---	---	20	3
			0.208	0.92	0.63	0.29	2.9	0.032	0.002	---	---	15	14
			0.233	0.86	0.58	0.28	2.7	0.034	0.001	0.083	---	17	14
			0.266	0.86	0.53	0.33	2.7	0.023	0.001	0.090	---	15	23
			0.310	0.88	0.46	0.42	2.8	0.021	< 0.001	0.064	0.390	12	37
			0.370	0.88	0.47	0.41	2.8	0.014	< 0.001	0.070	0.437	20	41
			0.427	0.91	0.46	0.45	2.9	0.012	< 0.001	---	0.265	18	44
			0.507	0.91	0.43	0.48	2.9	0.014	< 0.001	---		13	53
	52	0.86	0.233	0.63	0.41	0.22	1.9	0.054	0.03	---	0.429	2	56
PVC	0	2.0	0.671	0.35	0.17	0.18	0.46	0.039	0.003	0.091	0.656	26	37
			0.757	0.35	0.19	0.16	0.47	0.034	0.002	0.093	0.489	24	37
			0.874	0.35	0.20	0.14	0.46	0.029	0.001	0.074	0.398	26	39

(a) Natural air flow.

TABLE A.1.3. Physicochemical Properties of Polystyrenes

Rigid-Foam Sample[a]	Density, kg/m^3	Chemical Formula	Stoichiometric Air/Fuel Ratio, g/g	H_T, kJ/g	L, kJ/g	$\dot{q}''_{rr}$, kW/m^2	T_s, K
GM-47	16	$CH_{1.01}$	13	38.1	3.00	10	650
GM-49/FR	16	$CH_{1.05}O_{0.004}$	13	38.2	3.10	13	690
GM-51	34	$CH_{1.01}O_{0.021}$	13	35.6	2.50	12	680
GM-53	29	$CH_{1.05}O_{0.012}$	13	37.6	2.25	13	690
Granular polystyrene	1,051	CH	13	39.2	1.70	14	700
Liquid styrene	---	CH	13	40.5	0.64	2	420

(a) GM-sample designation by the National Bureau of Standards, Center for Fire Research, Washington, D.C.

TABLE A.1.4. Combustion Properties of Polystyrenes

Rigid Foam Sample	$\dot{q}''_e$, kW/m²	$\dot{v}_a$ (m³/sec) x10³	$\dot{m}_{O_2}$	X_A	X_C	X_R	Y_{CO_2}	Y_{CO}	Y_{HC}	Y_S	σ, m²/g	$\dot{q}''_{fc}$, kW/m²	$\dot{q}''_{fr}$, kW/m²
GM-47[a]	0	2.0	0.371	0.62	0.13	0.49	2.1	0.031	0.002	0.27	1.08	6	30
			0.501	0.57	0.11	0.46	1.9	0.023	0.008	0.31	0.951	8	30
			0.564	0.55	0.10	0.45	1.8	0.014	0.007	0.36	0.572	9	29
			0.631	0.60	0.14	0.46	2.0	0.012	0.004	0.37	0.793	14	23
	40	0.86	0.233	0.59	0.14	0.45	1.6	0.052	0.006	---	1.32	1	54
GM-49/FR[a]	0	2.0	0.422	0.55	0.11	0.45	1.8	0.033	0.003	0.37	0.681	6	38
			0.503	0.54	0.091	0.45	1.8	0.024	0.001	0.33	0.762	6	36
			0.555	0.54	0.082	0.46	1.8	0.021	0.008	0.37	0.771	6	41
			0.615	0.57	0.11	0.45	1.9	0.014	0.005	0.38	0.543	10	40
GM-51[a]	0	2.0	0.445	0.53	0.12	0.41	1.7	0.032	0.004	0.27	0.731	6	41
			0.498	0.54	0.13	0.41	1.8	0.033	0.002	0.27	0.724	9	29
			0.568	0.51	0.11	0.40	1.7	0.031	0.002	0.26	0.632	9	34
			0.619	0.54	0.15	0.39	1.8	0.024	0.002	0.21	0.560	16	18
GM-53[a]	0	2.0	0.445	0.51	0.13	0.38	1.7	0.031	0.004	0.30	0.811	8	31
			0.498	0.52	0.13	0.39	1.7	0.030	0.004	0.25	0.732	9	30
			0.565	0.48	0.10	0.38	1.6	0.030	0.003	0.29	0.660	9	28
			0.628	0.51	0.090	0.42	1.7	0.033	0.003	0.24	1.10	8	32
Granular polystyrene	0	1.4	0.233	0.68	0.40	0.28	2.2	0.071	0.02	0.15	0.73	11	27
			0.264	0.67	0.34	0.33	2.2	0.053	0.01	0.21	0.63	8	41
			0.313[a]	0.68	0.35	0.33	2.2	0.032	0.005	---	---	10	37
			0.334[a]	0.68	0.34	0.34	2.3	0.032	0.002	---	1.1	14	23
			0.375[a]	0.66	0.32	0.34	2.2	0.022	0.003	0.20	1.0	12	32
			0.420[a]	0.64	0.22	0.42	2.2	0.024	0.001	---	---	11	28
			0.524[a]	0.67	0.21	0.46	2.3	0.010	[a]	---	---	15	20
Liquid styrene	0	0.86	0.233	0.50	0.18	0.32	1.7	0.062	0.0041	0.33	0.783	6	13

(a) Extensive deposition of flame soot on the surface; mass loss rate suppressed; combustion similar to the combustion for char-forming materials.
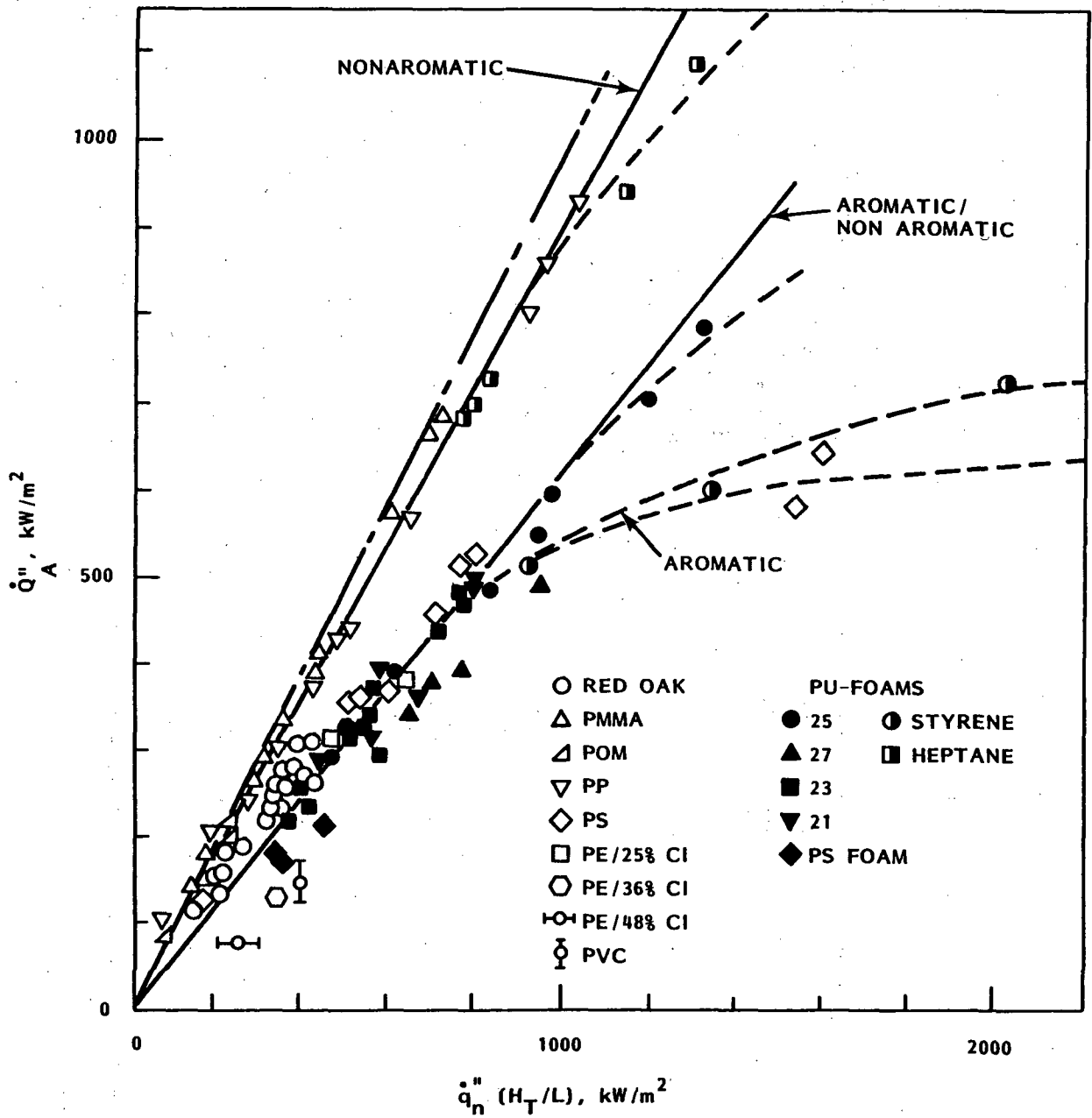
FIGURE A.1.1. Actual Heat Release Rate as a Function of Heat Released in the Complete Combustion of Material Vapors, $\dot{q}_n'' = \dot{q}_e'' + \dot{q}_{fs}'' - \dot{q}_{rr}''$
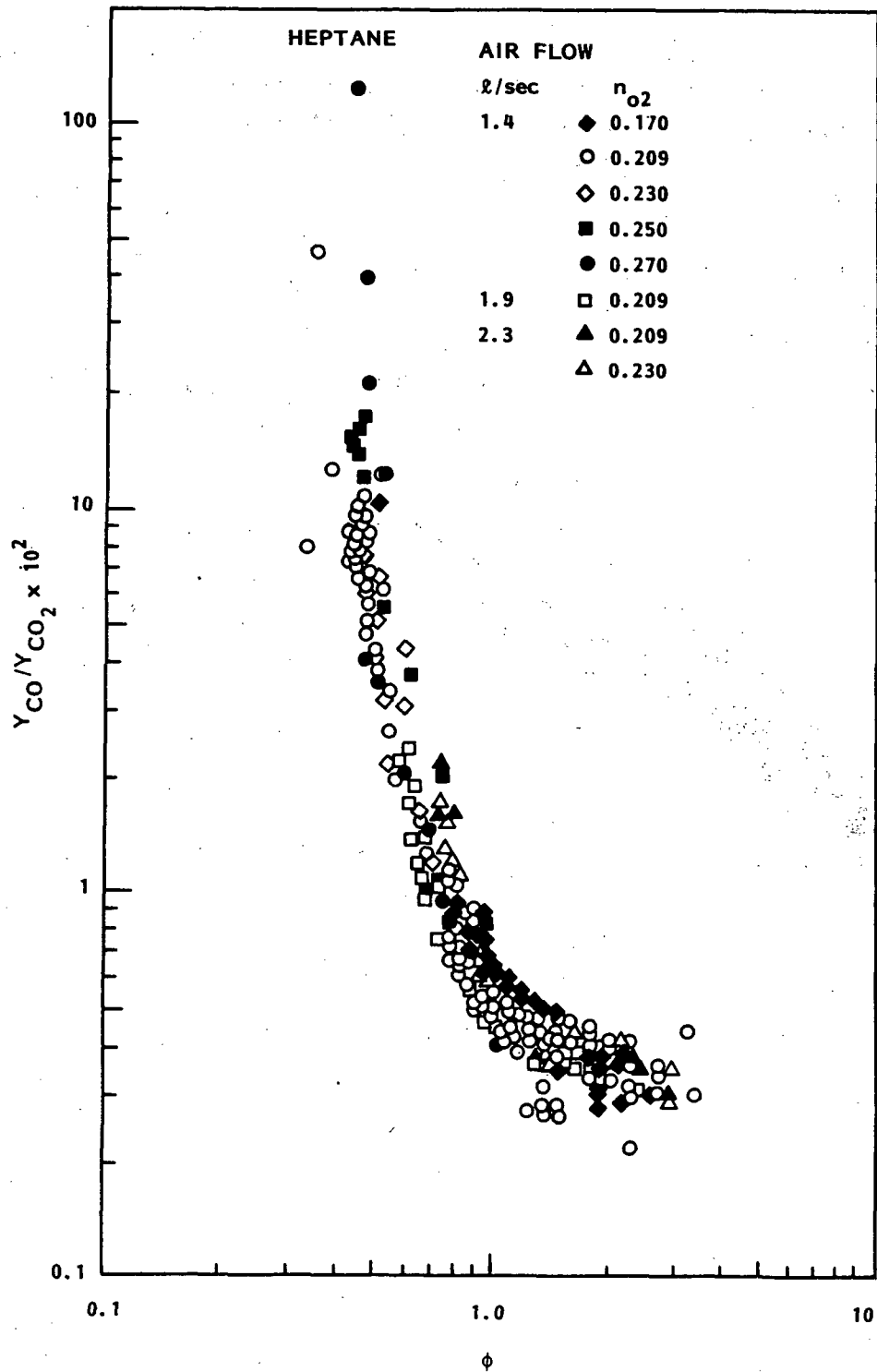
FIGURE A.1.2. Ratio of Yields of CO and CO_2 for Heptane as a Function of Oxygen-to-Fuel Stoichiometric Fraction (ϕ) ($\phi > 1$ for overventilated environment, < 1 for underventilated environment)
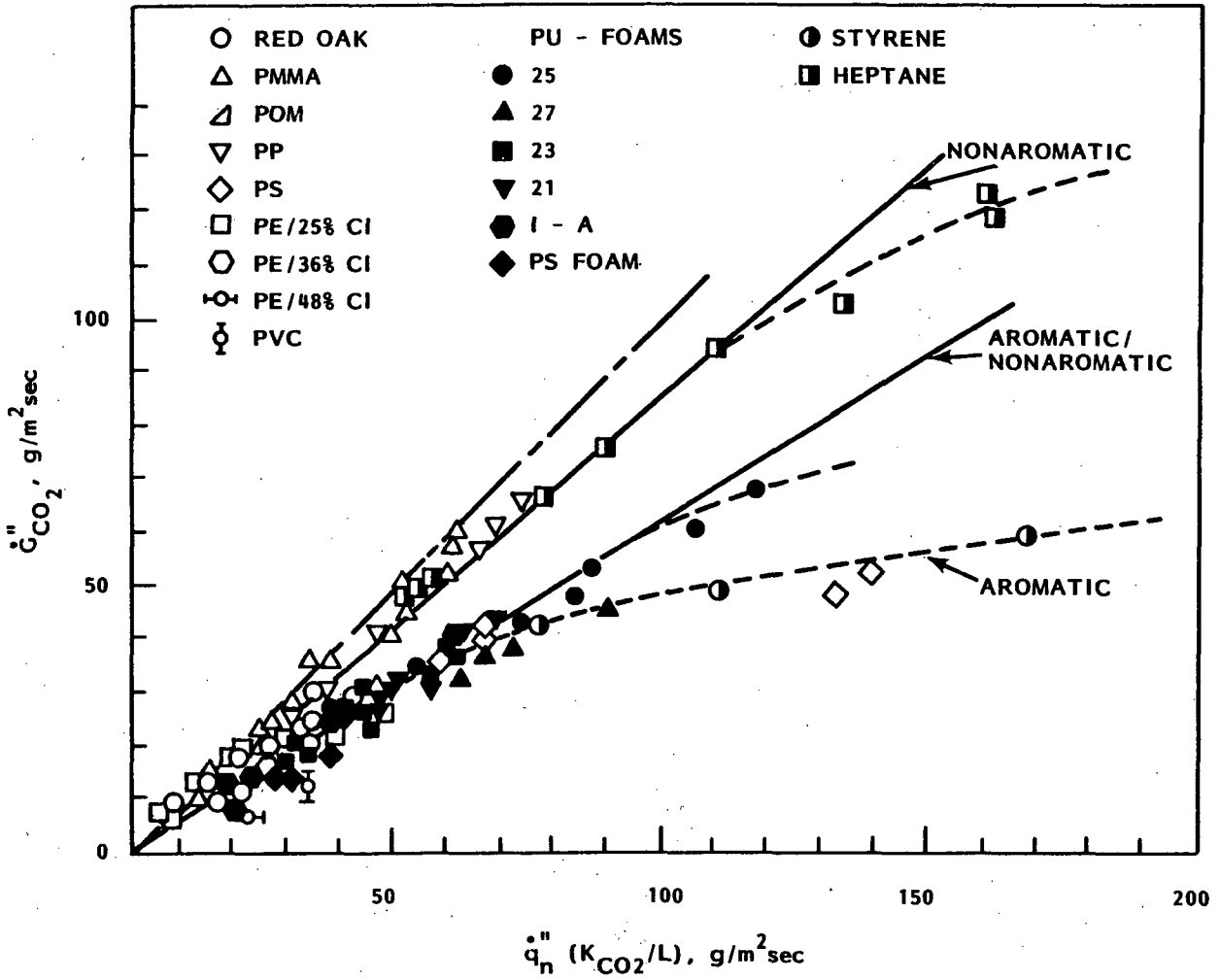
A.9

FIGURE A.1.3. Experimental Mass Generation Rate of CO_2 as a Function of Rate Expected from Stoichiometry, $\dot{q}_n'' = \dot{q}_e'' + \dot{q}_{fs}'' - \dot{q}_{rr}''$
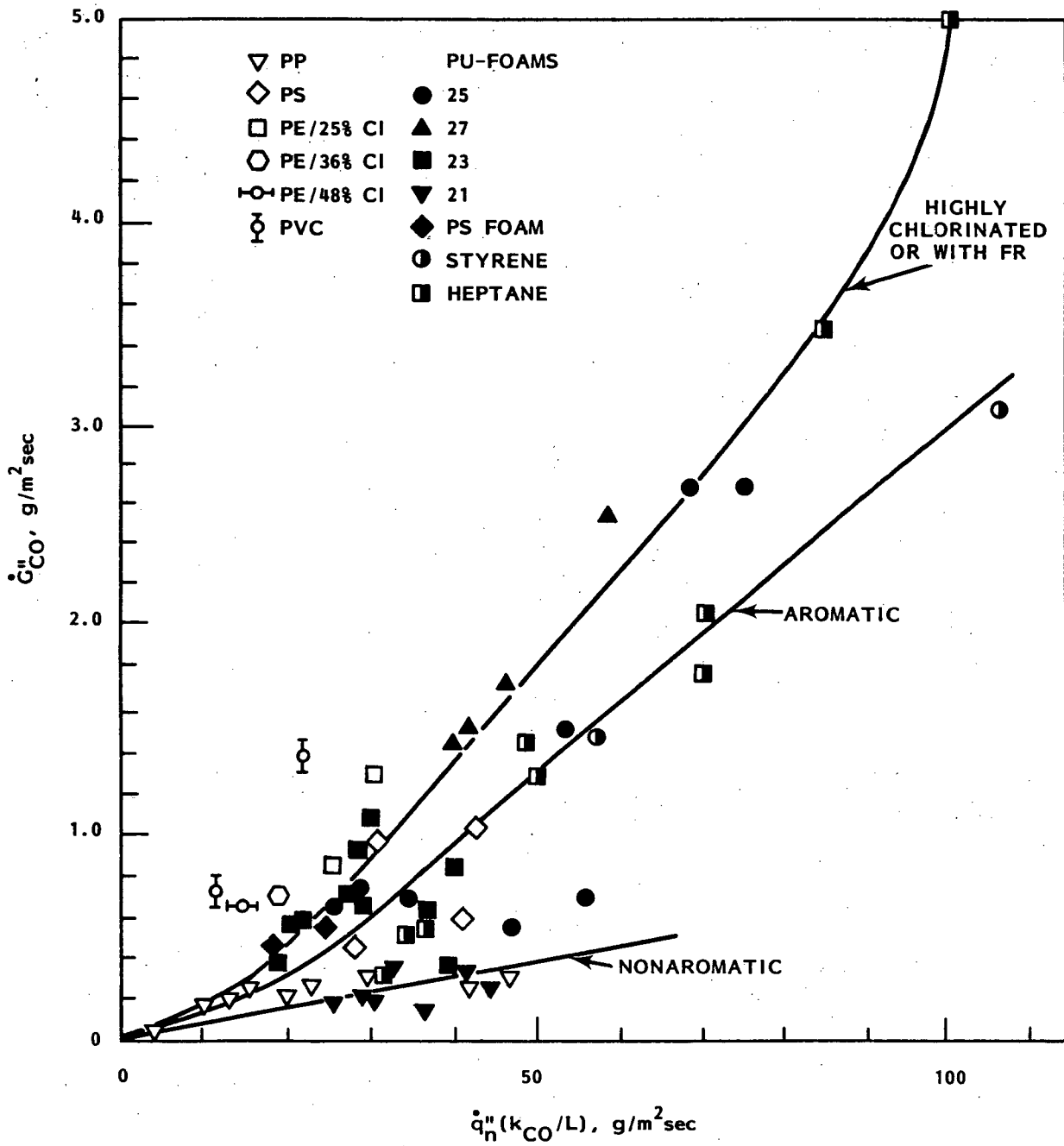
FIGURE A.1.4. Experimentally Measured Mass Generation Rate of CO as a Function of Rate Expected from Stoichiometry, $\dot{q}_n'' = \dot{q}_e'' + \dot{q}_{fs}'' - \dot{q}_{rr}''$
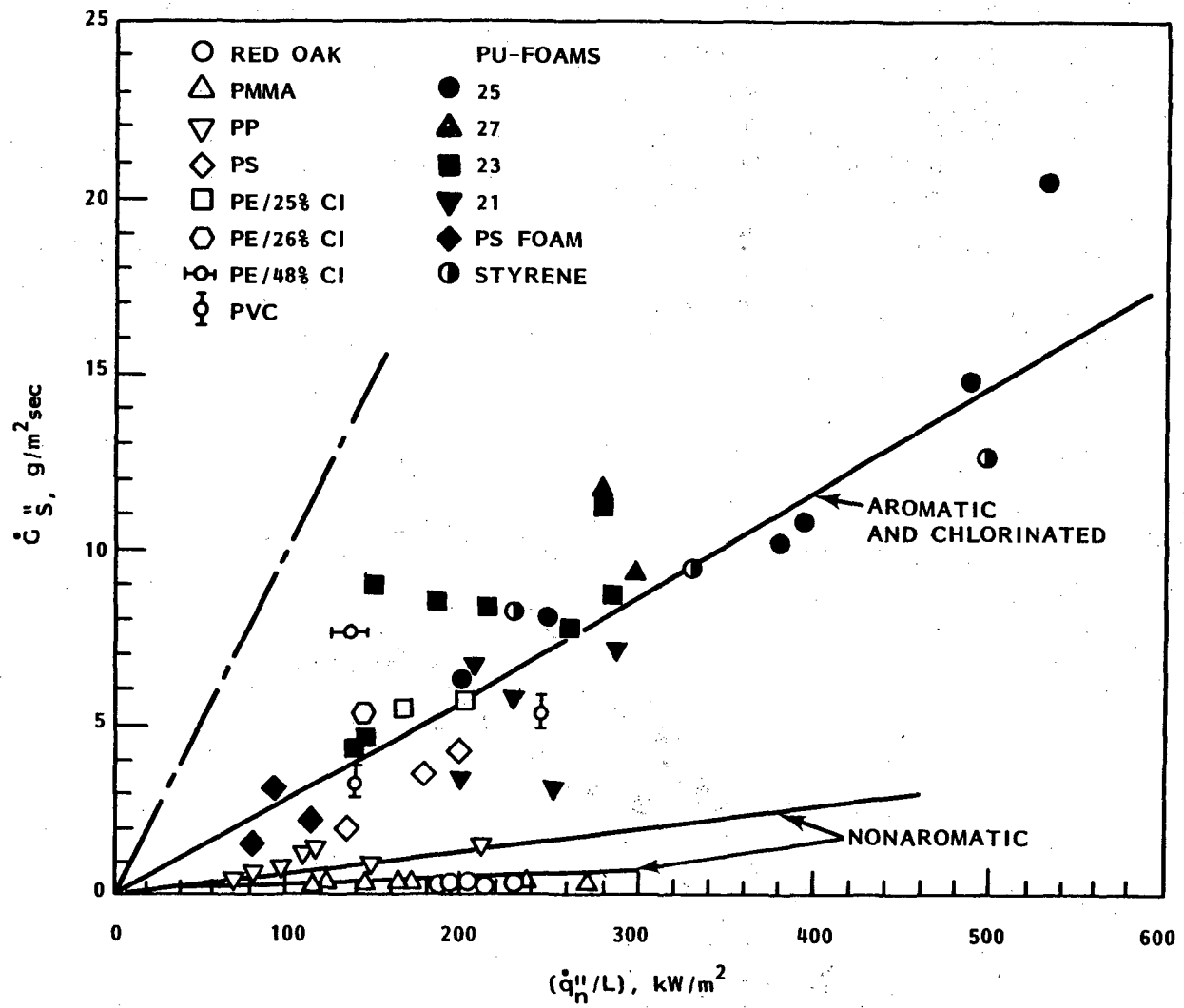
FIGURE A.1.5. Experimentally Measured Mass Generation Rate of Soot and Low Vapor Pressure Liquids as a Function of Mass Loss Rate of the Material, $\dot{q}_n'' = \dot{q}_e'' + \dot{q}_{fs}'' - \dot{q}_{rr}''$
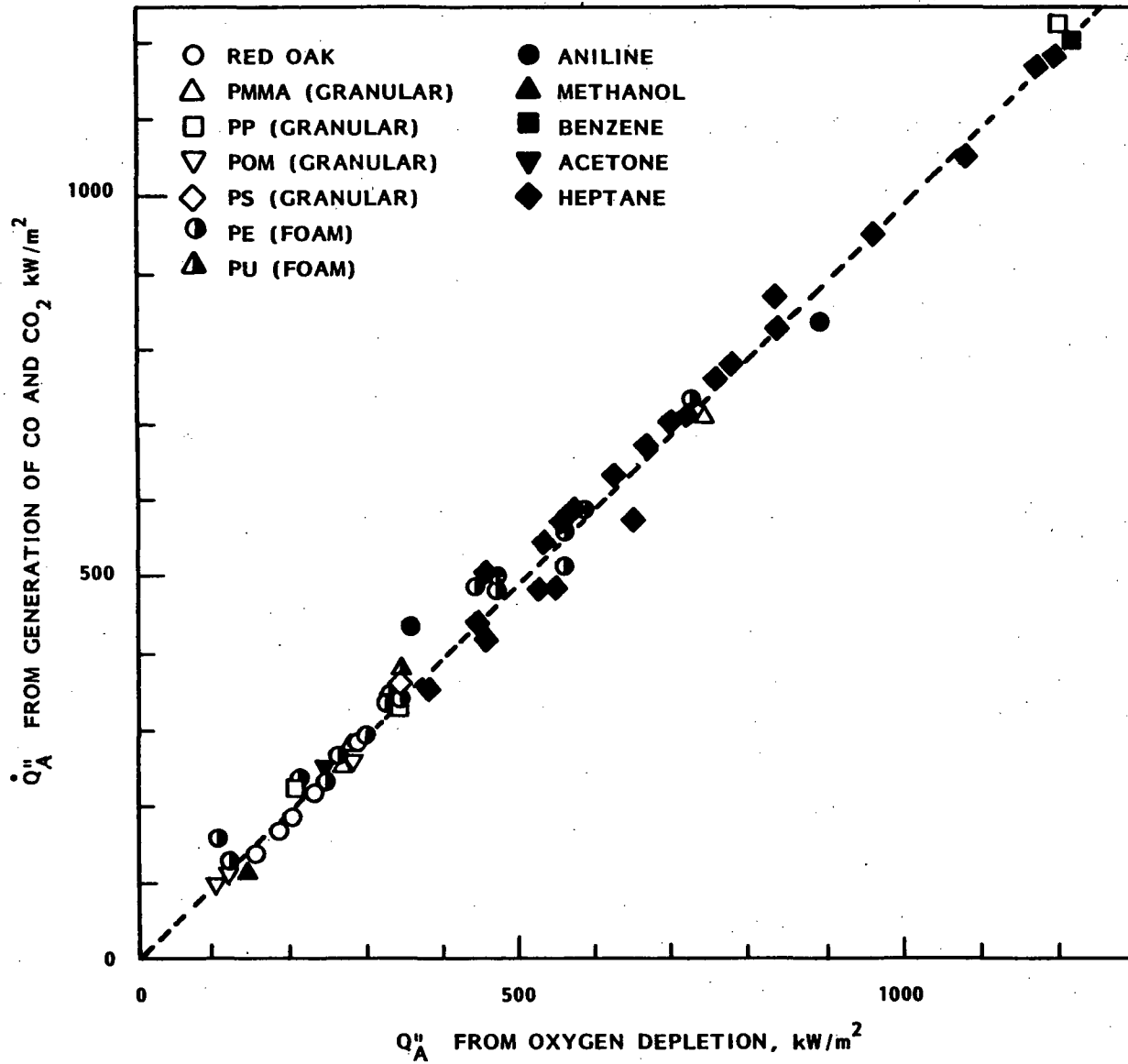
FIGURE A.1.6. Actual Heat Release Rate Calculated from CO and CO_2 as a Function of Actual Heat Release Rate Calculated from O_2 Depletion

APPENDIX A.2

LITERATURE SOURCE

Tewarson, A. 1980. "Heat Release Rate in Fires." Fire and Materials 4(4):185-191.

TABLES

A.2.1   Components of Heat of Combustion

A.2.2 H_T/L Values for Fuels

NOMENCLATURE

See Appendix A.1.

TABLE A.2.1. Components of Heat of Combustion

Fuel	Heat of Combustion, kJ g^{-1}			
	Complete	Actual	Convective	Radiative
Rigid polyethylene foam	40.84	22.83	18.79	4.04
Rigid polyurethane foam	26.02	11.84	3.85	7.99
PMMA	25.20	17.89	10.33	7.56
Flexible polyurethane foam	26.64	14.41	4.46	9.95
Red oak	17.78	12.69	6.65	6.04
Cellulose	16.48	11.80	5.78	6.02
PVC	16.44	5.89	2.43	3.46

TABLE A.2.2. H_T/L Values for Fuels

Fuel[a]	H_T/L[b]
Red oak (solid)	2.96
Cellulose (filter paper)	4.64
Rigid PI foam (43)	5.14
Rigid PI foam (41)	6.04
POM (granular)	6.37
Rigid PU foam (37)	6.54
Flexible PU foam (1-A)	6.63
PVC (granular)	6.66
PE/48% Cl (granular)	6.72
Rigid PU foam (31)	8.05
Rigid PU foam (29)	8.37
PE/36% Cl (granular)	8.91
Flexible PU foam (23)	10.02
Flexible PU foam (27)	12.26
Nylon (granular)	13.10
Flexible PU foam (21)	13.34
Epoxy/FR/glass fiber (solid)	13.38
PE/25% Cl (granular)	14.90
Rigid PE foam (1)	15.15
PMMA (granular)	15.46
Rigid PE foam (2)	15.65
Methanol (liquid)	16.50
Flexible PU foam (25)	20.03
Rigid PS foam (47)	20.51
PP (granular)	21.37
Rigid PE foam (3)	22.82
PS (granular)	23.04
PE (granular)	24.84
Rigid PS foam (51)	26.79
Rigid PE foam (4)	27.23

TABLE A.2.2. (contd)

Fuel[a]	H_T/L[b]
Rigid PS foam (53)	30.02
Rigid PS foam (49)	30.30
Aniline (liquid)	44.69
Acetone (liquid)	47.48
Styrene (liquid)	63.30
Benzene (liquid)	80.60
Heptane (liquid)	92.83

(a) Numbers in parentheses are PRC sample numbers.

(b) H_T measured in an oxygen bomb calorimeter and corrected for water as a vapor for fuels for which data are not available; L is obtained by measuring the mass loss rate of the fuel in pyrolysis in N_2 environment as a function of external heat flux for fuels for which data are not available.

APPENDIX A.3

LITERATURE SOURCE

Seader, J. P. and I. N. Einhorn. 1976. Some Physical, Chemical, Toxicological, and Physiological Aspects of Fire Smokes. Flammability Research Center, University of Utah, Salt Lake City, Utah.

TABLE

A.3.1   Smoke Particulates Generated from Several Woods and Polymers

TABLE A.3.1. Smoke Particulates Generated from Several Woods and Polymers

Material	% Converted to	
	Residue	Smoke Particulate
Red oak	0.2	0.2
White oak	0.7	0.2
Black walnut	1.0	0.3
Marine plywood (Douglas fir)	1.0	0.4
Redwood	0.2	0.4
PMMA	0	0.6
Nylon 6/6	2.5	5.5
Polyethylene terephthalate	9.8	5.8
Polyethylene	0.05	8.3
PVC	7.9	10.2
Polyisoprene	0	19.4
PS	0.2	21.0

APPENDIX A.4

LITERATURE SOURCE

Bankston, C. P. et al. 1978. Review of Smoke Particulate Properties Data for Natural and Synthetic Materials. NBS-GCR-78-147, Georgia Institute of Technology, Atlanta, Georgia.

TABLES

A.4.1   Wood Smoke Properties at different radiant heating rates--Nonflaming Conditions

A.4.2   Wood Smoke Properties Compared for Flaming and Nonflaming Conditions

A.4.3   Wood Smoke Properties in Different Atmospheric Compositions-- Nonflaming Conditions

A.4.4   Wood Smoke Properties at Different Environmental Temperatures-- Nonflaming Conditions

A.4.5   Wood Smoke Properties at Different Environmental Temperatures--Flaming Conditions

A.4.6   Composition (in PHR) of PVC Samples

A.4.7   Effect of Sample Composition on PVC Smoke Properties--Nonflaming Conditions

A.4.8   Rigid PVC Smoke Properties at Different Radiant Heating Rates-- Nonflaming Conditions

A.4.9   Rigid PVC Smoke Properties Compared for Flaming and Nonflaming Conditions

A.4.10 Rigid PVC Smoke Properties in Different Atmospheric Compositions-- Nonflaming Conditions

A.4.11 Rigid PVC Smoke Properties at Different Environmental Temperatures-- Nonflaming Conditions

A.4.12 Rigid PVC Smoke Properties at Different Environmental Temperatures-- Flaming Conditions

FIGURES

A.4.1   Particle Size Distributions for Wood Smoke Generated Under Nonflaming Conditions

A.4.2 Particle Size Distributions for Wood Smoke Generated Under Flaming and Nonflaming Conditions

A.4.3 Smoke Particle Size Distribution for PVC Compositions 1 Through 4 Generated Under Nonflaming Conditions

A.4.4 Smoke Particle Size Distributions for PVC Compositions 5 Through 7 Generated Under Nonflaming Conditions

A.4.5 Particle Size Distributions for Rigid PVC Smoke Generated Under Nonflaming Conditions

A.4.6 Particle Size Distributions for Rigid PVC Smoke Generated Under Flaming and Nonflaming Conditions

NOMENCLATURE

Γ Fraction of sample weight loss converted to smoke particulates

OD_{max} Maximum optical density per meter at 0.458 m (blue) and 0.633 m (red)

D_{32} Volume-surface mean particle diameter at maximum optical density

F Flaming

NF Nonflaming

TABLE A.4.1. Wood Smoke Properties at Different Radiant Heating Rates--Nonflaming Conditions

	Γ	D_{MMD}, m	σ, µm	OD (Blue), m^{-1}	OD (Red), m^{-1}	D_{32}, µm
Douglas fir Nonflaming (3.2 W/cm^2) Air (142 /min)	0.031	0.5	1.86	NM	NM	NM
Douglas fir Nonflaming (5 W/cm^2) Air (425 ℓ/min)	0.154	0.82	1.98	1.57	1.07	0.75
Douglas fir Nonflaming (6.2 W/cm^2) Air (425 ℓ/min)	0.165	0.90	1.96	2.48	2.04	0.80
Douglas fir Nonflaming (5 W/cm^2)(a) Air (425 ℓ/min)	0.108	1.80	1.83	3.87	3.46	0.77

(a) Horizontal sample mount
NM = Not measured

TABLE A.4.2. Wood Smoke Properties Compared for Flaming and Nonflaming Conditions

	Γ	D_{MMD}, m	σ, µm	OD (Blue), m^{-1}	OD (Red), m^{-1}	D_{32}, µm
Douglas fir Flaming (2.5 W/cm^2) Air (283 ℓ/min)	0.025	0.43	2.37	0.61	0.32	0.52
Douglas fir Flaming (5 W/cm^2) Air (425 ℓ/min)	<0.01	NM	NM	NG	NG	0.47
Douglas fir Nonflaming (5 W/cm^2) Air (425 ℓ/min)	0.154	0.82	1.98	1.57	1.07	0.75

NM = Not measured
NG = Negligible values

TABLE A.4.3. Wood Smoke Properties in Different Atmospheric Compositions--Nonflaming Conditions

	Γ	D_{MMD}, µm	σ, µm	OD (Blue), m^{-1}	OD (Red), m^{-1}	D_{32}, µm
Douglas fir Nonflaming (6.2 W/cm²) Air (425 ℓ/min)	0.165	0.90	1.96	2.48	2.04	0.80
Douglas fir Nonflaming (6.2 W/cm²) 80% N_2, 10% O_2, 10% CO_2	0.221	1.05	1.93	1.95	2.09	1.00
Douglas fir Nonflaming (6.2 W/cm²) 80% N_2, 5% O_2, 10% CO_2, 5% CO	0.237	0.92	2.28	1.48	1.18	0.75

TABLE A.4.4. Wood Smoke Properties at Different Environment Temperatures--Nonflaming Conditions

	OD (Blue), m^{-1}	OD (Red), m^{-1}	D_{32}, µm
Douglas fir Nonflaming (5 W/cm²) Air (25°C, 425 ℓ/min)	1.57	1.07	0.75
Douglas fir Nonflaming (5 W/cm²) Air (100°C, 425 ℓ/min)	0.97	0.86	0.74
Douglas fir Nonflaming (5 W/cm²) Air (200°C, 425 ℓ/min)	0.96	0.74	0.54

TABLE A.4.5. Wood Smoke Properties at Different Environmental Temperatures--Flaming Conditions

	OD (Blue), m^{-1}	OD (Red), m^{-1}	D_{32}, μm
Douglas fir Flaming (5 W/cm^2) Air (25°C, 425 ℓ/min)	NM	NM	0.47
Douglas fir Flaming (5 W/cm^2) Air (100°C, 425 ℓ/min)	NM	NM	0.89
Douglas fir Flaming (5 W/cm^2) Air (200°C, 283 ℓ/min)	0.13	0.09	1.08
Douglas fir Flaming (5 W/cm^2) Air (300°C, 283 ℓ/min)	0.24	0.19	1.20

NM = Not measured

TABLE A.4.6. Composition (in PHR) of PVC Samples

Sample	PVC Resin	Lead Stabilizer	Plasticizer (6-10) (Phthalate)	CaCO$_3$	Al$_2$O$_3$·3H$_2$O	Sb$_2$O$_3$	Lubricants
1	100	5					
2	100	5	45				1.5
3	100	5	45	50			1.5
4	100	5	45			5	1.5
5	100	5	45	50		5	1.5
6	100	5	45		50	5	0.5
7	Rigid, commercially available "standard-impact" formulation; composition unknown.						

TABLE A.4.7. Effect of Sample Composition on PVC Smoke Properties--
Nonflaming Conditions

	Γ	D_{MMD}, μm	σ, μm	OD (Blue), m^{-1}	OD (Red), m^{-1}	D_{32}, μm
PVC-1 Nonflaming (5 W/cm^2) Air (425 ℓ/min)	0.093	1.40	1.45	2.08	2.24	0.99
PVC-2 Nonflaming (5 W/cm^2) Air (425 ℓ/min)	0.123	1.49	1.61	3.30	3.55	1.05
PVC-3 Nonflaming (5 W/cm^2) Air (425 ℓ/min)	0.085	1.14	1.78	NM	NM	NM
PVC-4 Nonflaming (5 W/cm^2) Air (425 ℓ/min)	0.125	1.37	1.61	4.54	4.99	1.10
PVC-5 Nonflaming (5 W/cm^2) Air (425 ℓ/min)	0.095	1.15	1.83	NM	NM	NM
PVC-6 Nonflaming (5 W/cm^2) Air (425 ℓ/min)	0.079	0.91	1.85	2.19	1.92	0.80
PVC-7 Nonflaming (5 W/cm^2) Air (425 ℓ/min)	0.070	1.20	1.86	1.49	1.42	0.84

NM = Not measured.

TABLE A.4.8. Rigid PVC Smoke Properties at Different Radiant Heating Rates--
Nonflaming Conditions

	Γ	D_{MMD}, μm	σ, μm	OD (Blue), m^{-1}	OD (Red), m^{-1}	D_{32}, μm
PVC-7 Nonflaming (3.2 W/cm^2) Air (142 ℓ/min)	0.012	0.42	1.90	NM	NM	NM
PVC-7 Nonflaming (5 W/cm^2) Air (425 ℓ/min)	0.030	0.85	1.79	0.55	0.30	0.62
PVC-7 Nonflaming (6.2 W/cm^2) Air (425 ℓ/min)	0.072	0.73	2.00	1.17	0.95	0.73
PVC-7 Nonflaming (5 W/cm^2)[a] Air (425 ℓ/min)	0.070	1.20	1.86	1.49	1.42	0.84

(a) Horizontal sample mount.
NM = Not measured.

TABLE A.4.9. Rigid PVC Smoke Properties Compared for Flaming and Nonflaming
Conditions

	Γ	D_{MMD}, μm	σ, μm	OD (Blue), m^{-1}	OD (Red), m^{-1}	D_{32}, μm
PVC-7 Flaming (2.5 W/cm^2) Air (425 ℓ/min)	0.012	0.41	2.22	0.95	0.56	0.58
PVC-7 Flaming (2.5 W/cm^2) 80% N_2, 10% CO_2, 10% O_2	0.012	0.44	2.02	1.39	0.68	0.33
PVC-7 Nonflaming (6.2 W/cm^2) Air (425 ℓ/min)	0.072	0.73	2.00	1.17	0.95	0.73

TABLE A.4.10. Rigid PVC Smoke Properties in Different Atmospheric Compositions--Nonflaming Conditions

	Γ	D_{MMD}, μm	σ, μm	OD (Blue), m^{-1}	OD (Red), m^{-1}	D_{32}, μm
PVC-7 Nonflaming (6.2 W/cm^2) Air (425 ℓ/min)	0.072	0.73	2.00	1.17	0.95	0.73
PVC-7 Nonflaming (6.2 W/cm^2) 80% N_2, 10% O_2, 10% CO_2	0.076	0.70	1.94	1.61	1.16	0.67
PVC-7 Nonflaming (6.2 W/cm^2) 80% N_2, 5% O_2, 10% CO_2, 5% CO	0.064	0.77	2.04	1.14	0.85	0.70

TABLE A.4.11. Rigid PVC Smoke Properties at Different Environmental Temperatures--Nonflaming Conditions

	OD (Blue), m^{-1}	OD (Red), m^{-1}	D_{32}, μm
PVC-7 Nonflaming (5 W/cm^2) Air (25°C, 425 ℓ/min)	0.55	0.30	0.62
PVC-7 Nonflaming (5 W/cm^2) Air (100°C, 425 ℓ/min)	0.42	0.34	1.01
PVC-7 Nonflaming (5 W/cm^2) Air (200°C, 425 ℓ/min)	0.45	0.32	1.11
PVC-7 Nonflaming (5 W/cm^2) Air (300°C, 425 ℓ/min)	0.66	0.37	0.90

TABLE A.4.12. Rigid PVC Smoke Properties at Different Environmental Temperatures--Flaming Conditions

	OD (Blue), m^{-1}	OD (Red), m^{-1}	D_{32}, μm
PVC-7 Flaming (5 W/cm^2) Air (25°C, 425 ℓ/min)	2.04	1.53	0.73
PVC-7 Flaming (5 W/cm^2) Air (100°C, 425 ℓ/min)	1.78	1.45	0.76
PVC-7 Flaming (5 W/cm^2) Air (200°C, 425 ℓ/min)	2.07	1.67	0.95
PVC-7 Flaming (5 W/cm^2) Air (300°C, 425 ℓ/min)	2.69	2.11	1.20
PVC-7 Flaming[a] Air (400°C, 425 ℓ/min)	2.93	2.29	1.22

(a) No radiant heating.
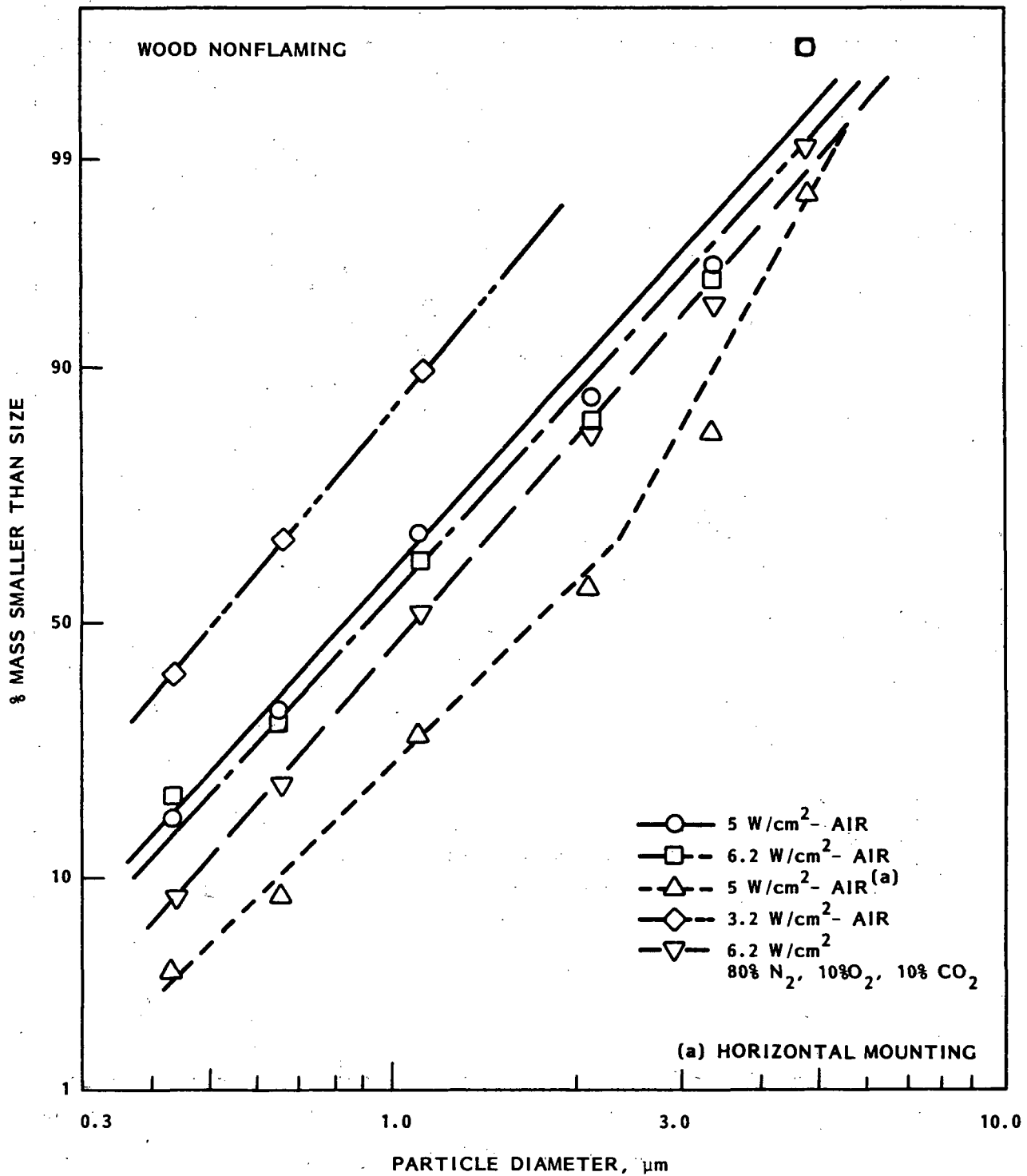
FIGURE A.4.1. Particle Size Distributions for Wood Smoke Generated Under Nonflaming Conditions.
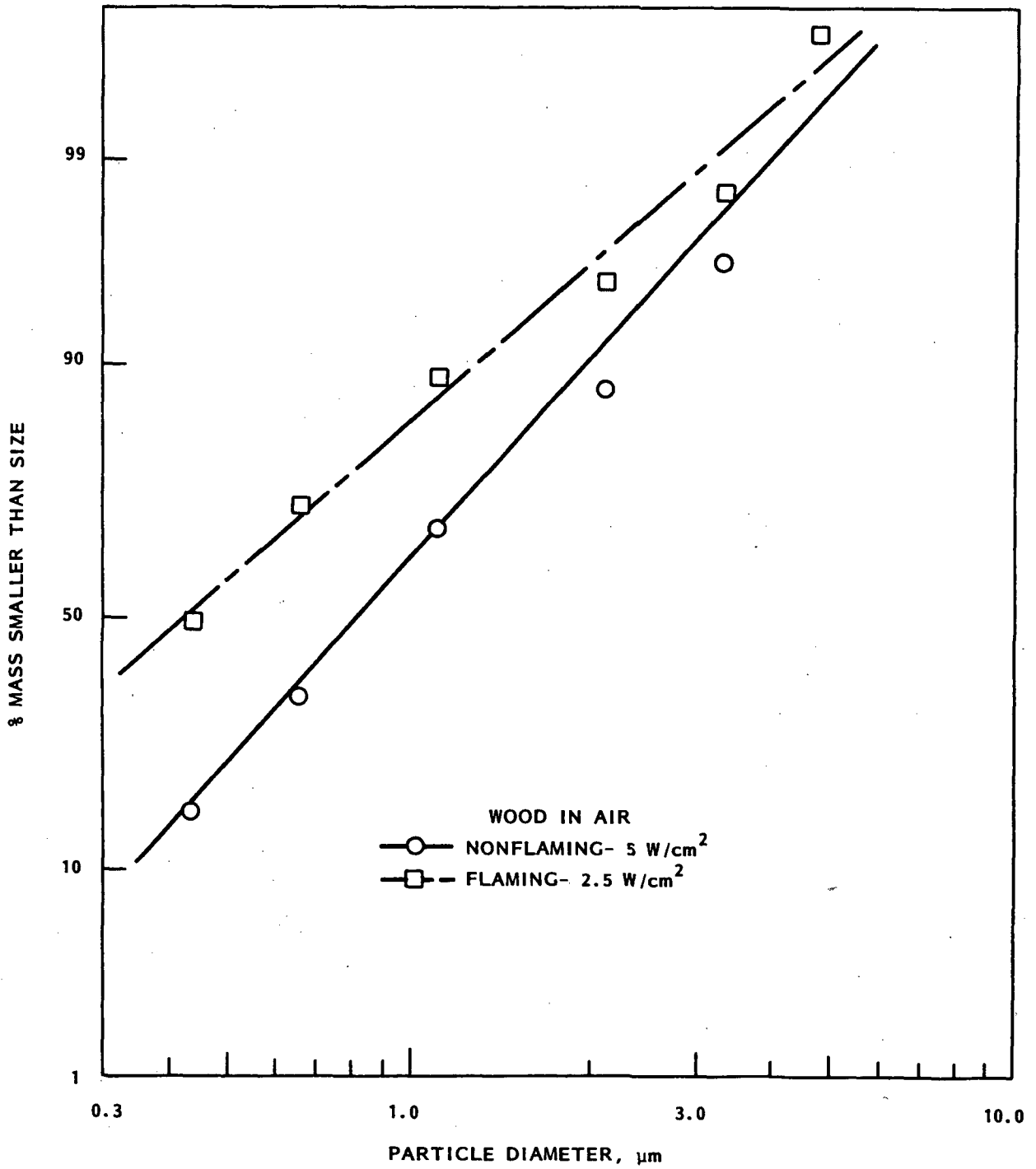
FIGURE A.4.2. Particle Size Distributions for Wood Smoke Generated Under Flaming and Nonflaming Conditions
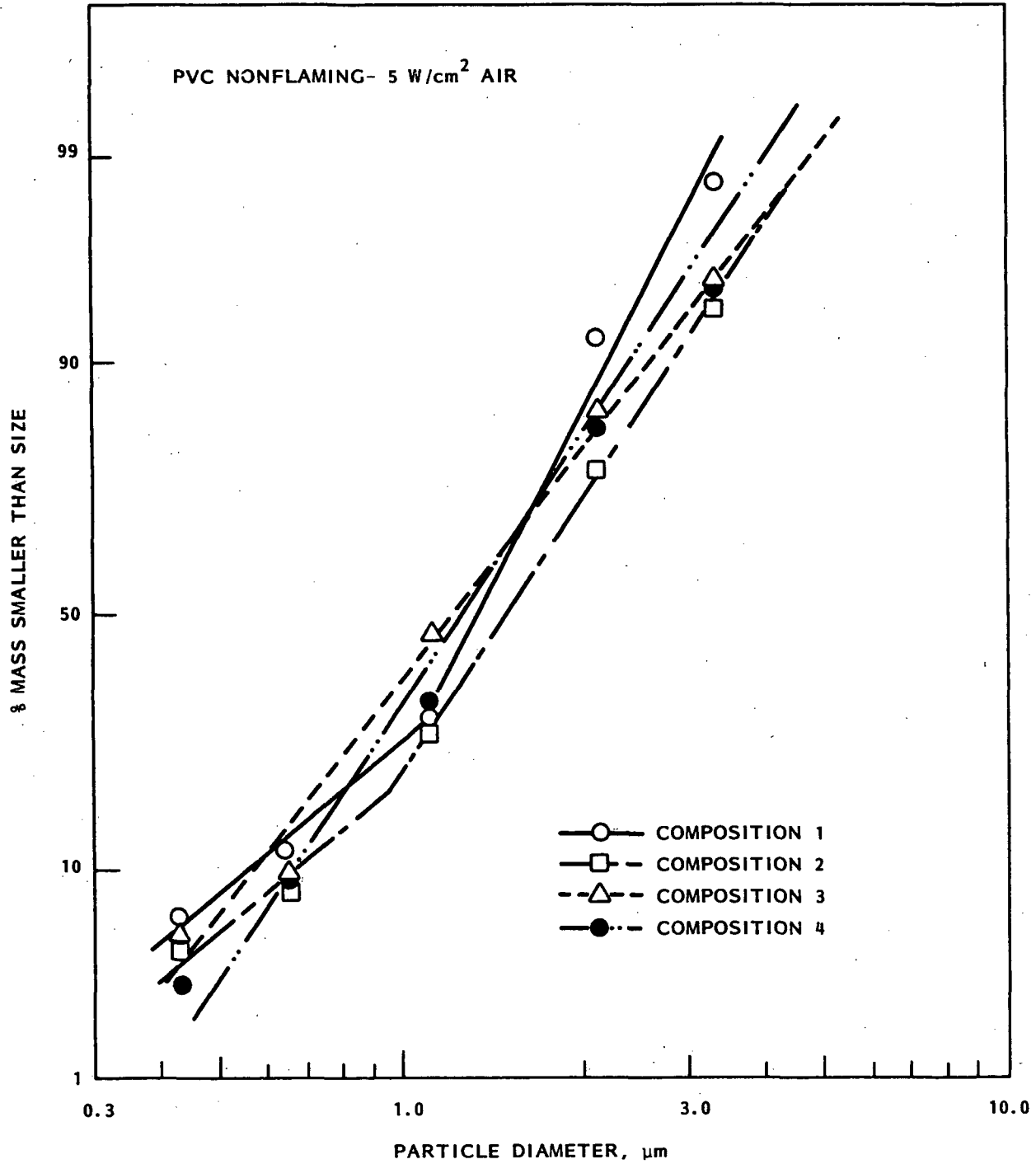
FIGURE A.4.3. Smoke Particle Size Distributions for PVC Compositions 1 Through 4 Generated Under Nonflaming Conditions
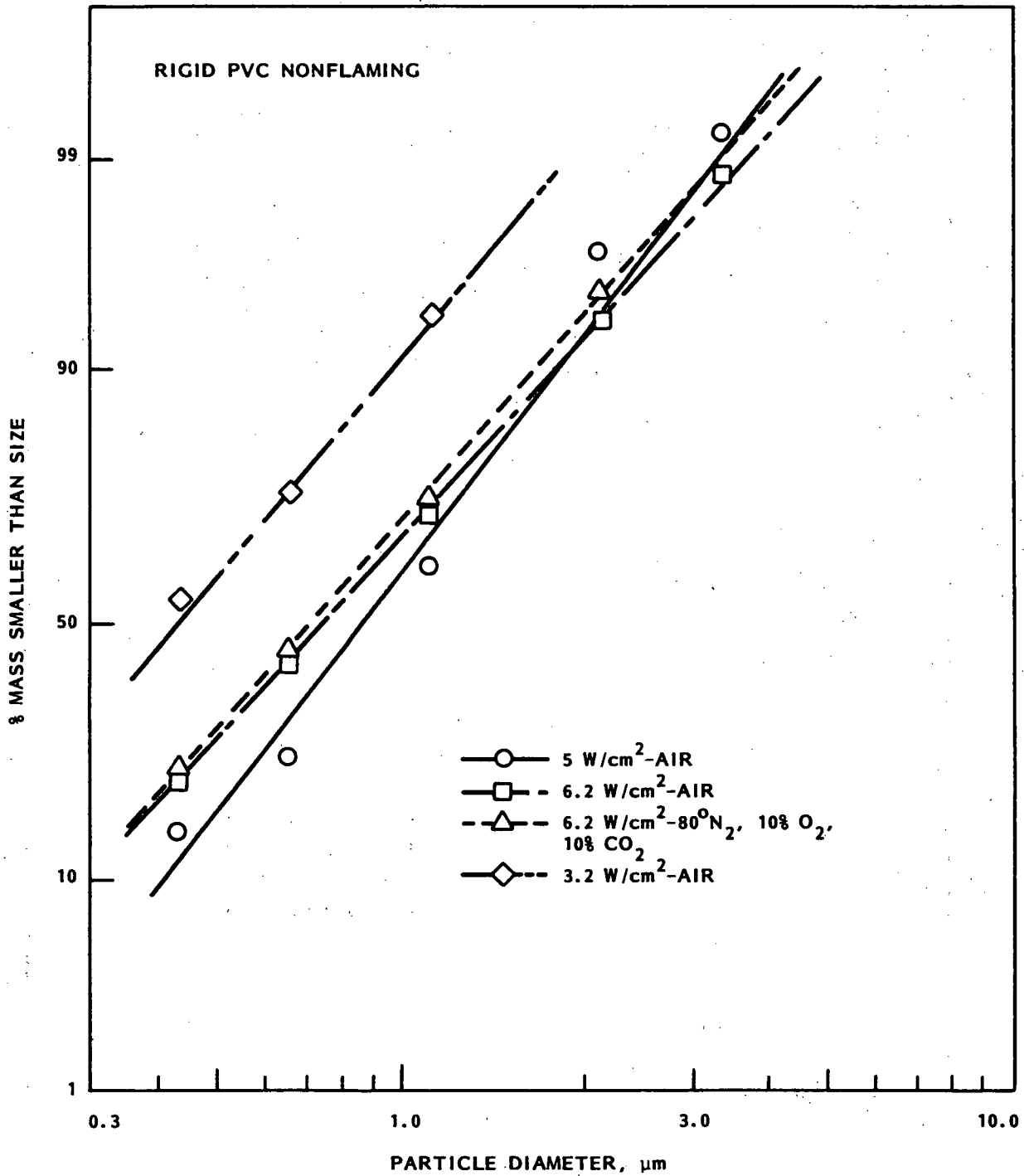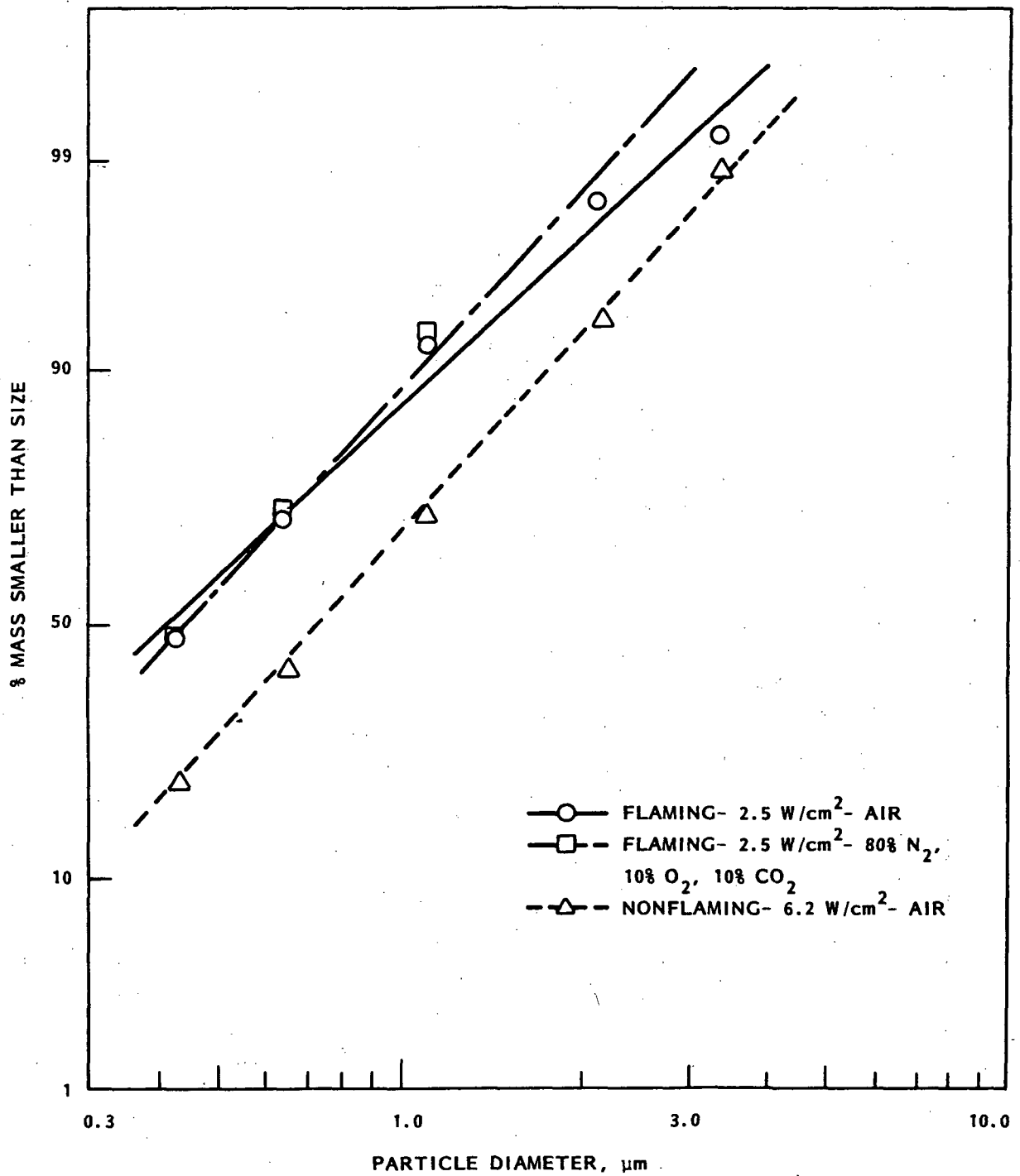
A.31
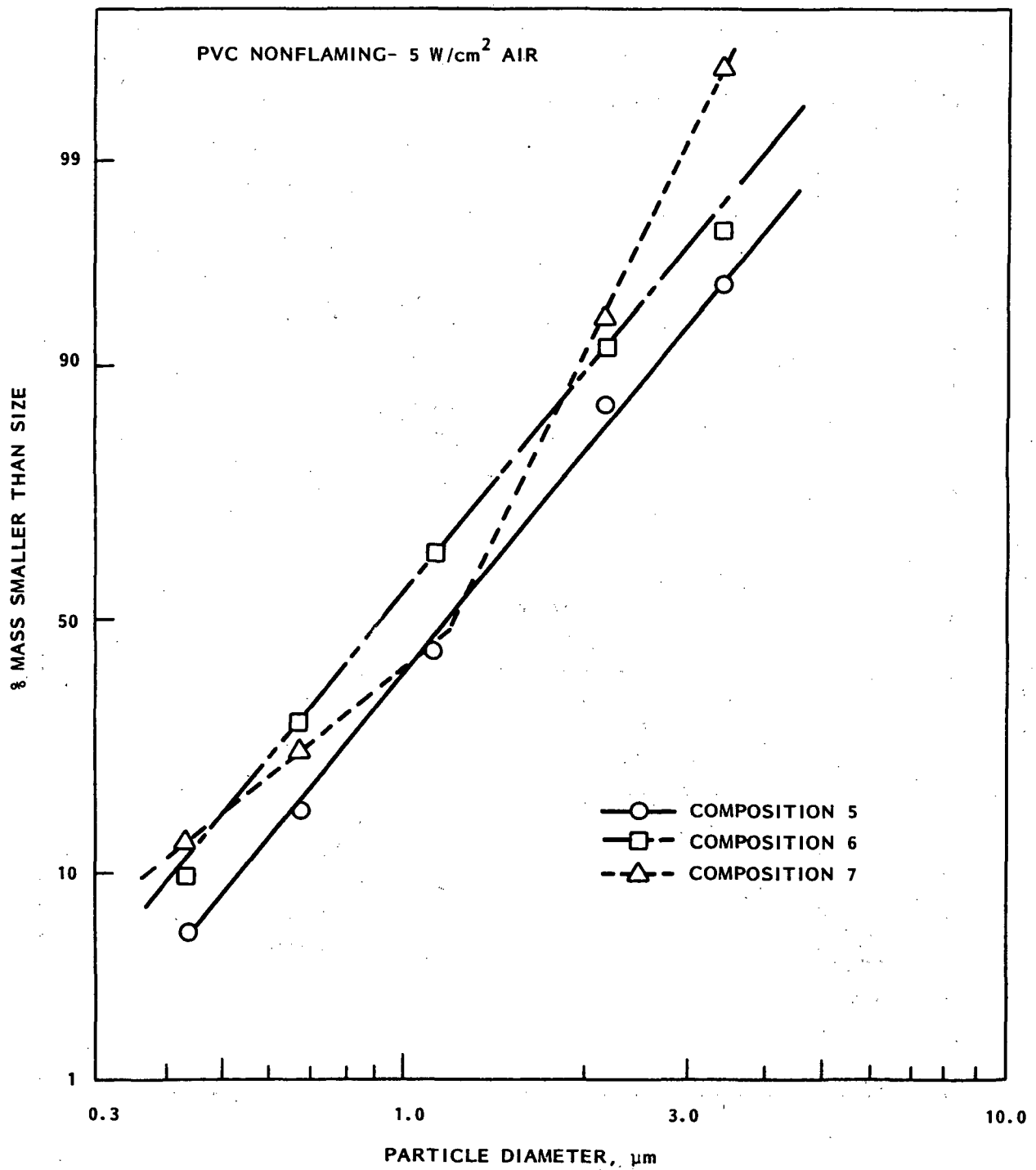
FIGURE A.4.4.   Smoke Particle Size Distributions for PVC Compositions 5
Through 7 Generated Under Nonflaming Conditions

A.32

FIGURE A.4.5. Particle Size Distributions for Rigid PVC Smoke Generated Under Nonflaming Conditions

FIGURE A.4.6. Particle Size Distribution for Rigid PVC Smoke Generated Under Flaming and Nonflaming Conditions

APPENDIX A.5

LITERATURE SOURCE

Zinn, B. T. et al. 1978. Investigation of the Properties of the Combustion Products Generated by Building Fires--Final Report of National Bureau of Standards. School of Aerospace Engineering, Georgia Institute of Technology, Atlanta, Georgia.

TABLES

A.5.1   Smoke Property Data Under Nonflaming Conditions at 5 W/cm^2 and 25°C (Materials--PS, PVC, Polypropylene, Polyethylene, and PMMA)

A.5.2   Smoke Property Data in Room Temperature Air at 5 W/cm^2

A.5.3   Smoke Property Data Under Flaming Conditions at 5 W/cm^2

FIGURES

A.5.1   Sample Weight Loss in Nonflaming Combustion in Room Temperature Air for Polystyrene, PVC, Polyethylene, and PMMA

A.5.2   Smoke Particle Size Distributions for Five Substrate Polymers Generated Under Low Temperature, Nonflaming Conditions

A.5.3   Smoke Mean Particle Size for Five Substrate Polymers in Nonflaming Combustion in Room Temperature Ventilation Air

A.5.4   Effect of Ventilation Gas Temperature Upon Mean Particle Diameter for a PVC Sample in Nonflaming Combustion at 5 W/cm^2

A.5.5   Sample Weight Loss in Flaming Combustion in room Temperature Air for Polystyrene, Polypropylene, Polyethylene, and PMMA

A.5.6   Smoke Mean Particle Diameter for Five Substrate Polymers in Flaming Combustion in Room Temperature Ventilation Air

A.5.7   Effect of Ventilation Gas Temperature Upon Sample Weight Loss for Polyethylene and Polystyrene Under Flaming Conditions

A.5.8   Effect of Ventilation Gas Temperature Upon Smoke Mean Particle Diameter for Flaming Polystyrene at 5 W/cm^2

A.5.9   Effect of Ventilation Gas Temperature Upon Smoke Mean Particle diameter for Flaming PVC at 5 W/cm^2

NOMENCLATURE

Γ Fraction of sample weight loss converted to smoke particulates

D_{MMD} Mass median diameter

OD_{MAX} Maximum optical density per meter at 458 nm (blue) and 633 nm (red)

D_{32} Volume-surface mean particle diameter at maximum optical density

F   Flaming

NF   Nonflaming

TABLE A.5.1. Smoke Property Data Under Nonflaming Conditions at 5 W/cm^2 and 25°C

Material	Γ	D_{MMD}, μm	σ, μm	OD_{MAX} Blue	OD_{MAX} Red	D_{32}, μm	Time to Peak OD, min
PS	0.084	2.60	1.84	0.58	0.63	1.42	11.3
PVC	0.093	1.40	1.45	2.08	2.24	0.98	13.5
Polypropylene	0.121	2.05	1.77	2.12	2.08	1.55	6.4
Polyethylene	NA	1.50	1.73	1.41[a]	1.51[a]	1.06[a]	9.9
PMMA	<0.01	0.68	1.87	0.07	0.05	0.58	10.7

(a) Measured during nonflaming phase, spontaneous ignition occurred 10 min after initiation of exposure.

TABLE A.5.2. Smoke Property Data in Room Temperature Air at 5 W/cm^2

Material	Type of Combustion	Γ	OD_{MAX} Blue	OD_{MAX} Red	D_{32}, μm	Time to Peak OD, min
PS	F	0.032	11.29	8.84	1.30	5.1
	NF	0.084	0.58	0.63	1.42	11.3
PVC	F	0.025	2.55	2.02	1.06	5.7
	NF	0.093	2.08	2.24	0.98	13.5
Polypropylene	F	0.018	3.34	2.53	1.21	4.5
	NF	0.121	2.12	2.08	1.55	6.4
Polyethylene	F	0.012	2.70	2.05	1.26	6.9
	NF	---	1.41	1.51	1.06	9.9
PMMA	F	<0.01	1.43	1.05	1.17	5.3
	NF	<0.01	0.07	0.05	0.58	10.7

TABLE A.5.3. Smoke Property Data Under Flaming Conditions at 5 W/cm^2

Material	Temperature, °C	Γ	OC_{MAX} Blue	Red	D_{32}, μm	Time to Peak OD, min
PS	25	0.032	11.29	8.84	1.30	5.1
	200	---	12.21	9.99	1.35	3.7
PVC	25	0.025	2.55	2.02	1.06	5.7
	200	---	3.45	2.64	1.14	5.7
Polypropylene	25	0.018	3.34	2.53	1.21	4.5
	200	---	4.46	3.57	1.33	3.9
Polyethylene	25	0.012	2.70	2.05	1.26	6.9
	200	---	4.07	3.22	1.33	5.1
PMMA	25	<0.01	1.43	1.05	1.17	5.3
	200	---	1.60	1.30	1.29	3.6
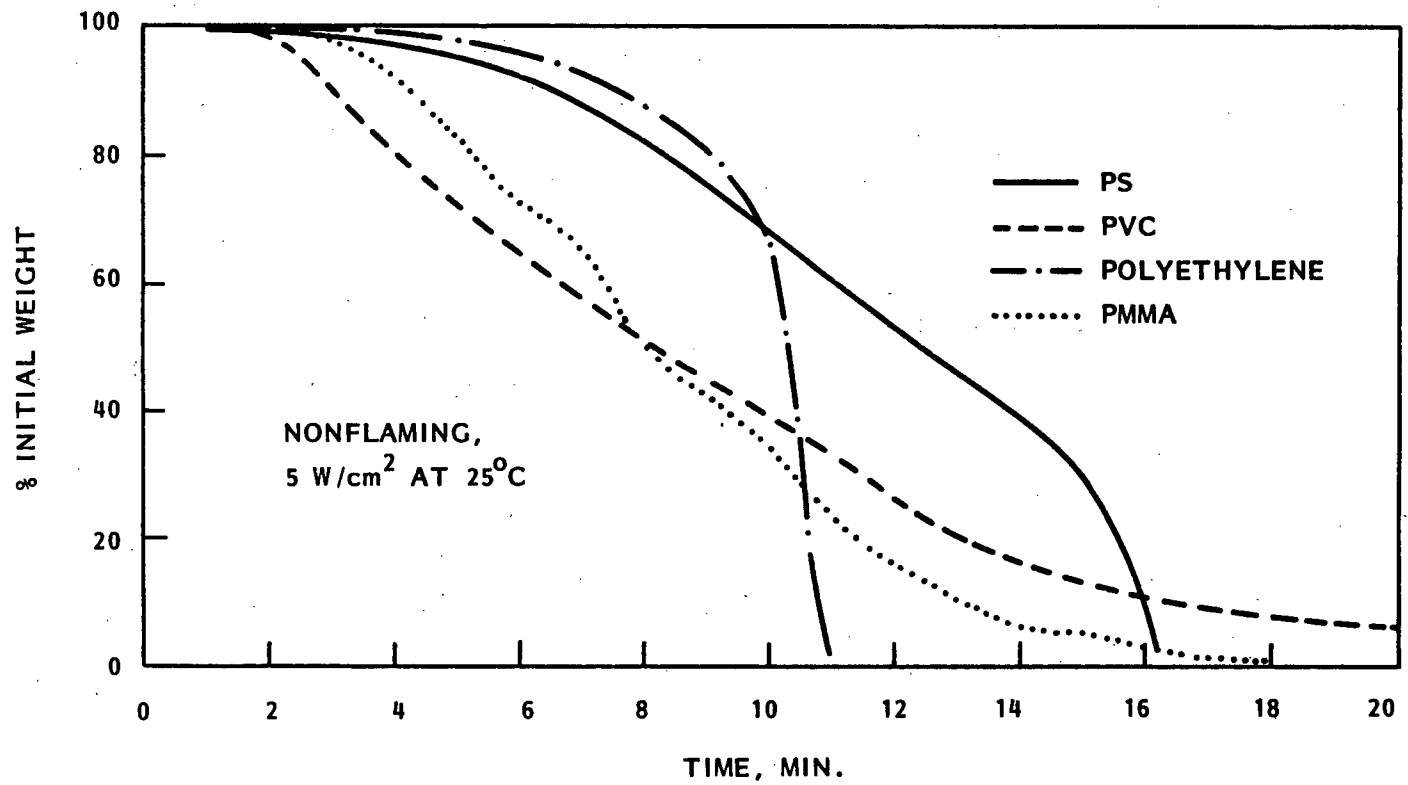
FIGURE A.5.1. Sample Weight Loss in Nonflaming Combustion in Room Temperature Air for Polystyrene, PVC, Polyethylene, and PMMA
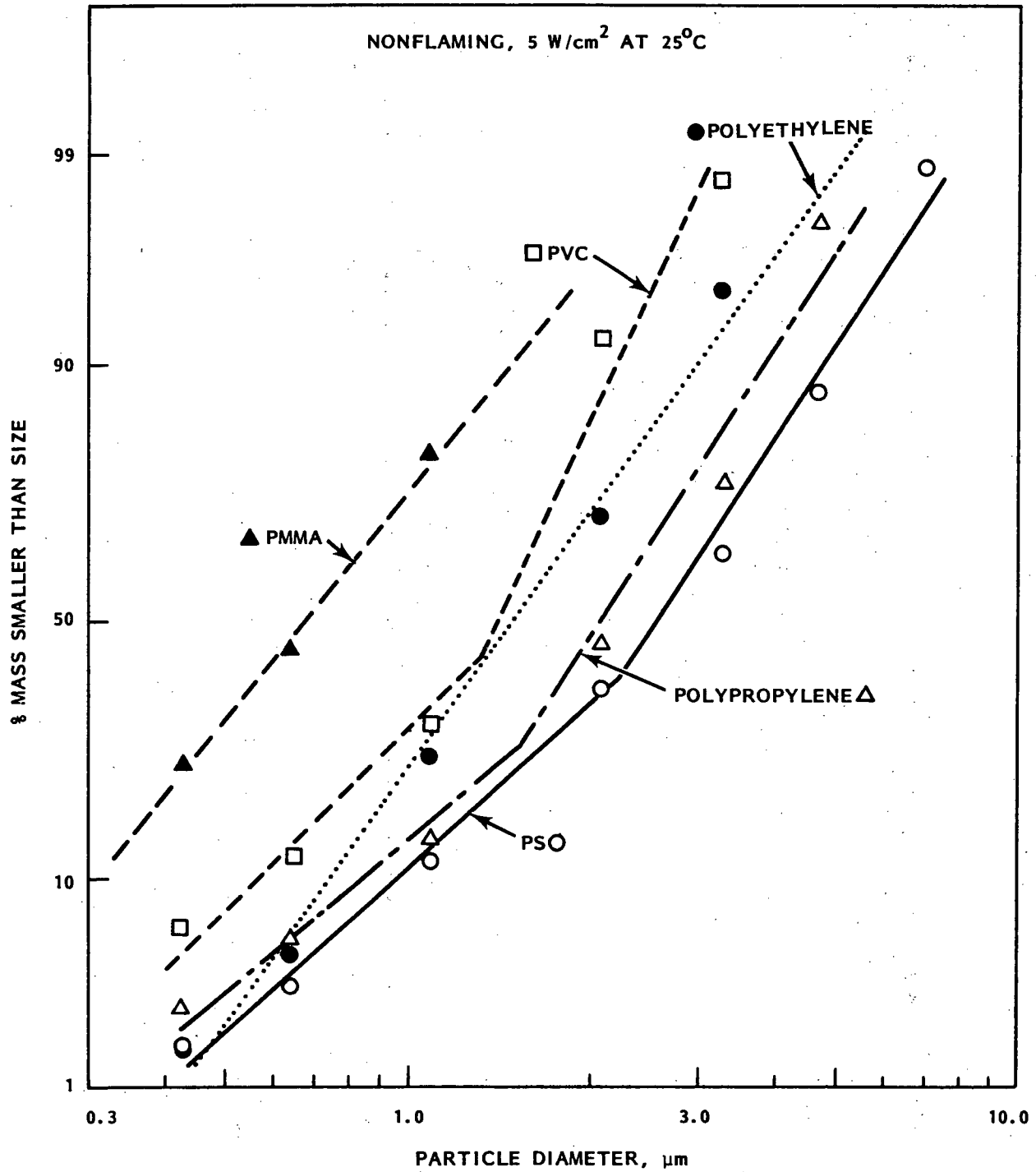
FIGURE A.5.2. Smoke Particle Size Distributions for Five Substrate Polymers Generated Under Low Temperature, Nonflaming Conditions
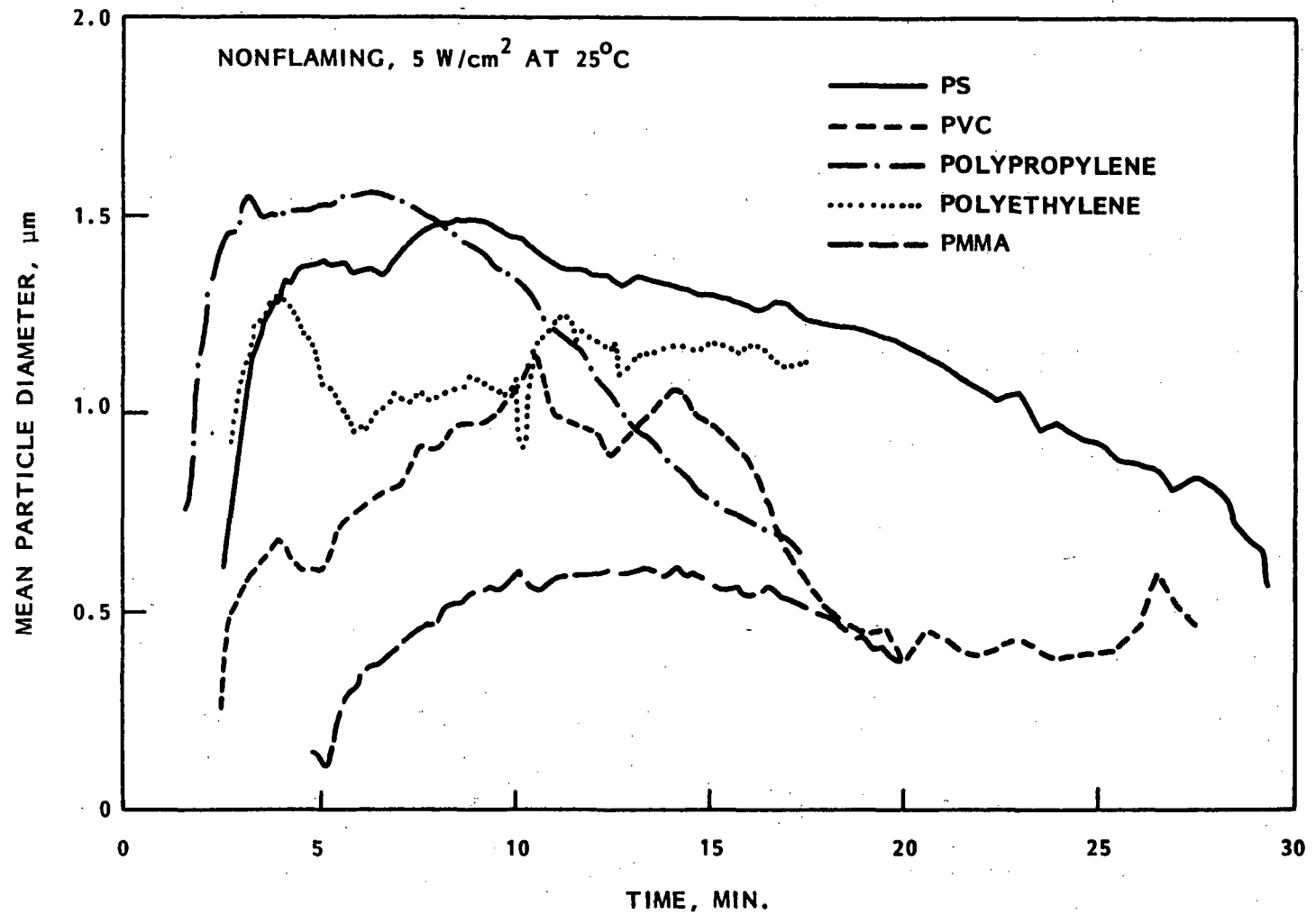
A.40

FIGURE A.5.3. Smoke Mean Particle Size for Five Substrate Polymers in Nonflaming Combustion in Room Temperature Ventilation Air
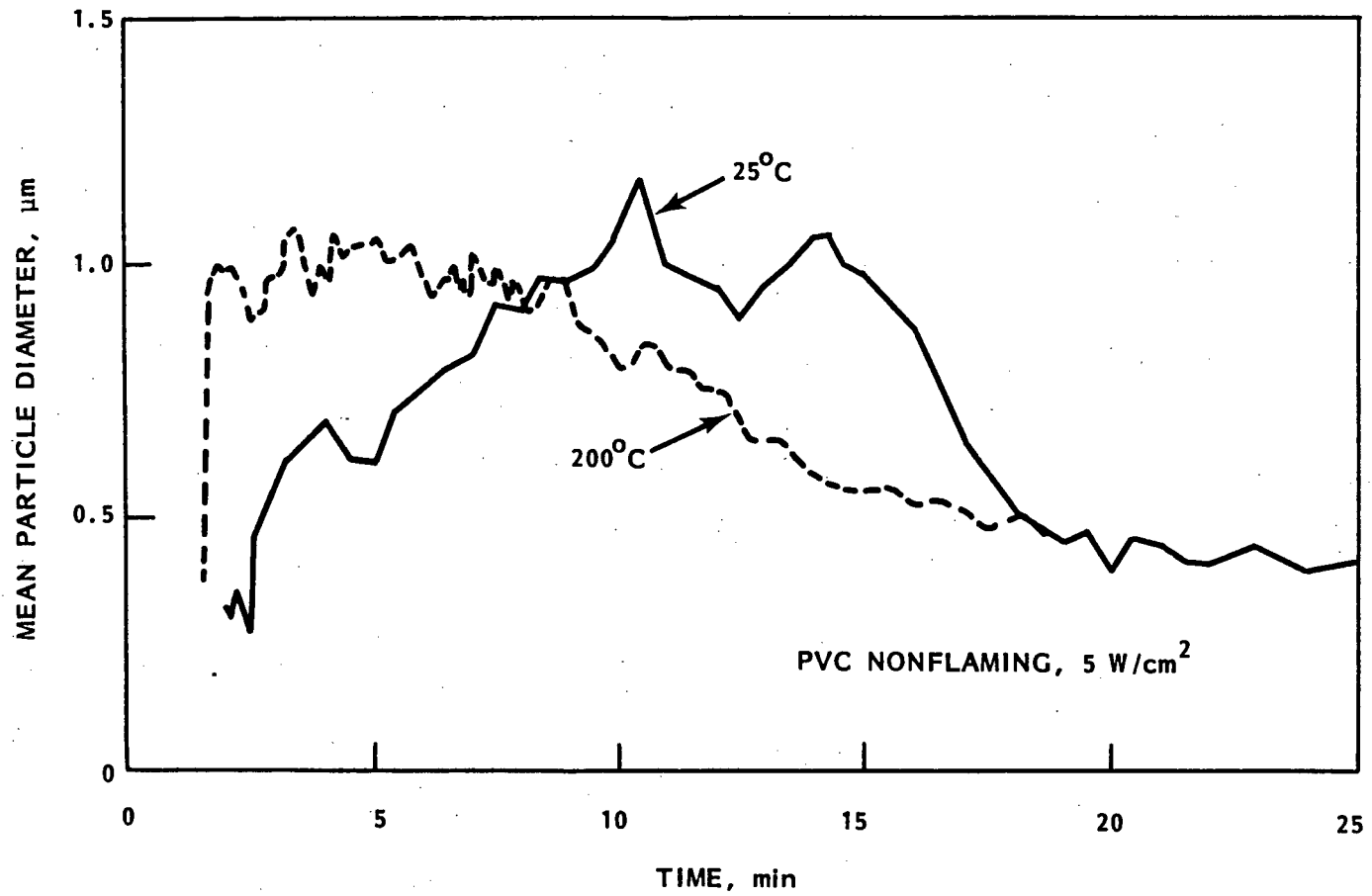
A.41

FIGURE A.5.4. Effect of Ventilation Gas Temperature Upon Mean Particle Diameter for a PVC Sample in Nonflaming Combustion at 5 W/cm^2
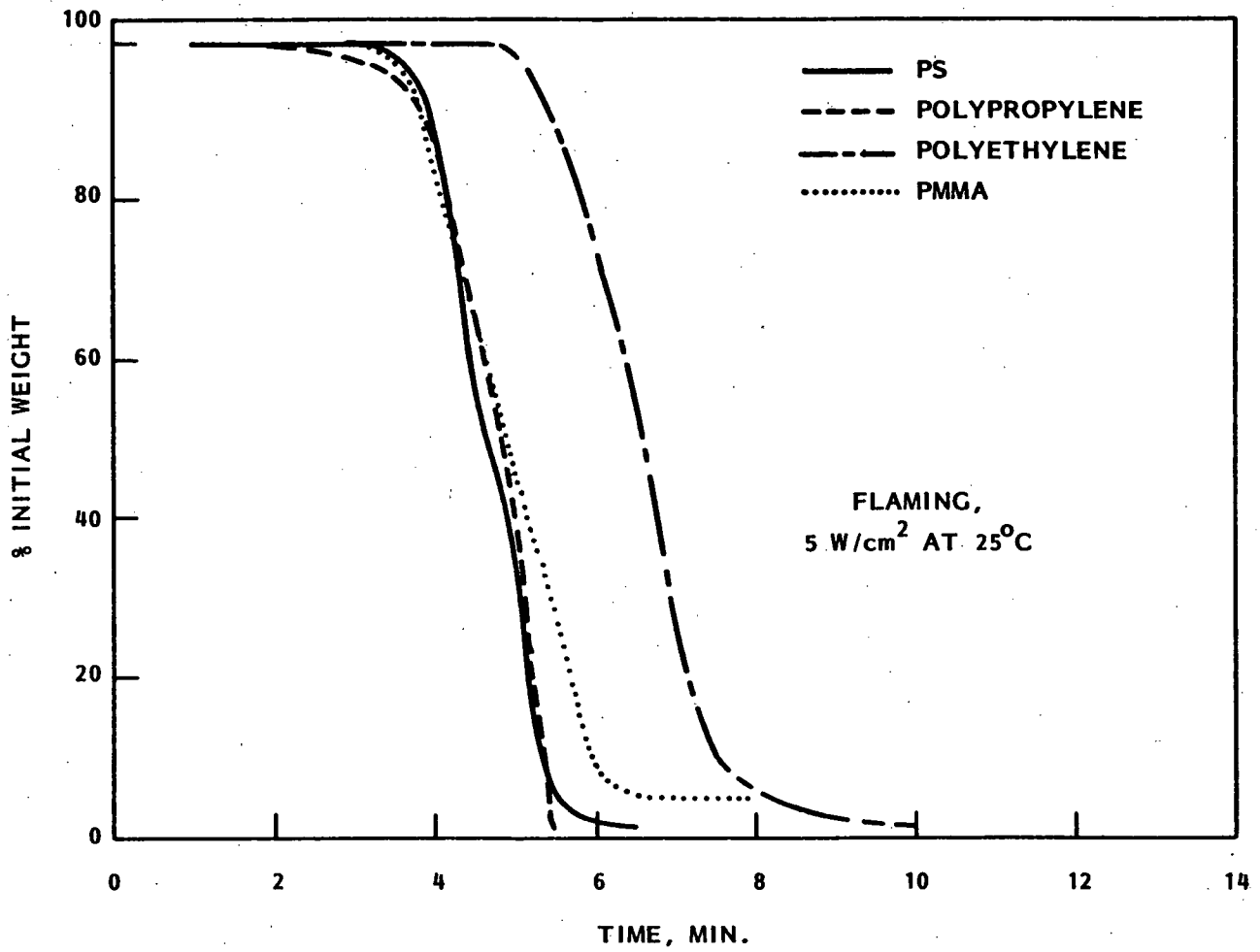
FIGURE A.5.5.   Sample Weight Loss in Flaming Combustion in Room Temperature
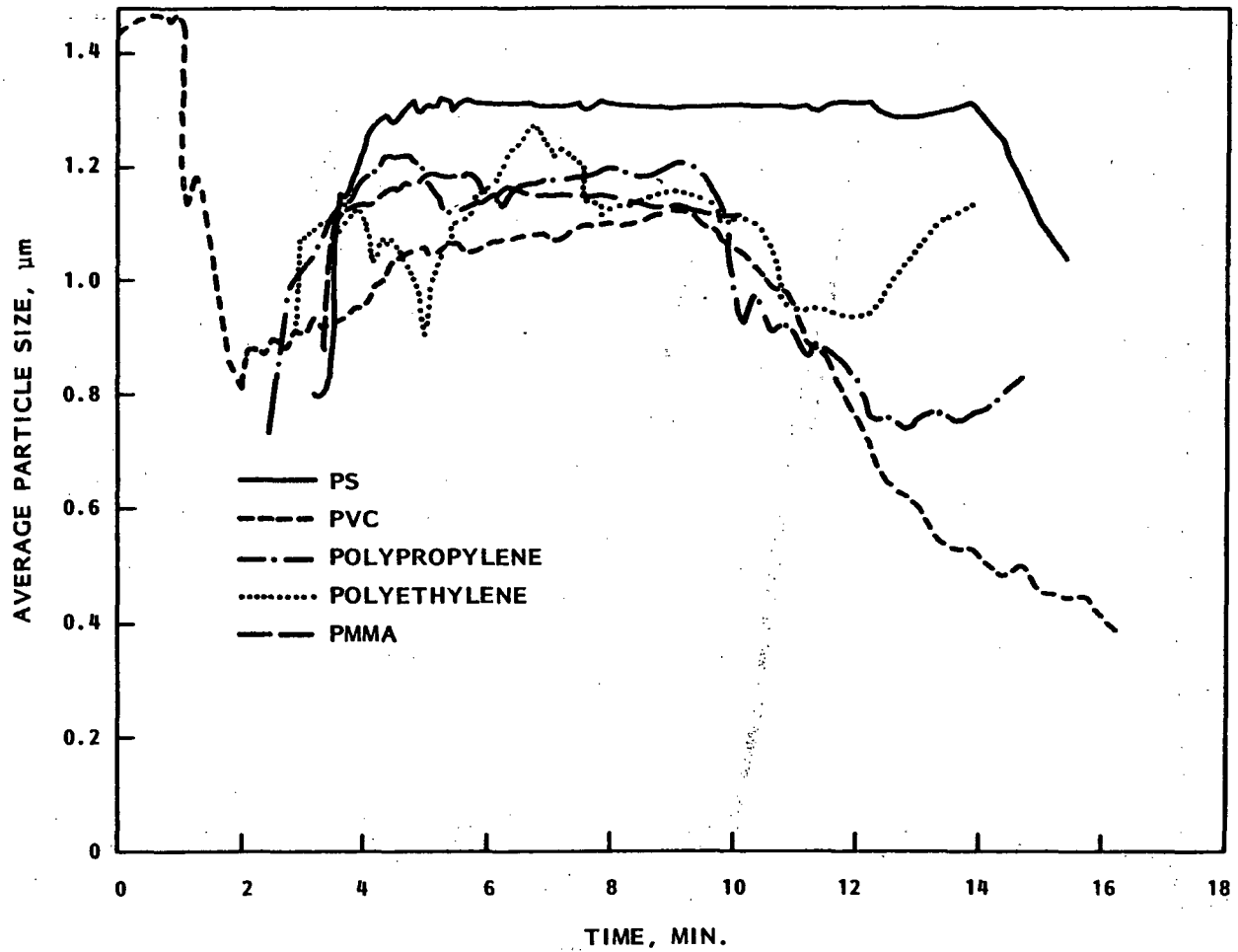Air for Polystyrene, Polypropylene, Polyethylene, and PMMA

FIGURE A.5.6. Smoke Mean Particle Diameter for Five Substrate Polymers in Flaming Combustion in Room Temperature Ventilation Air
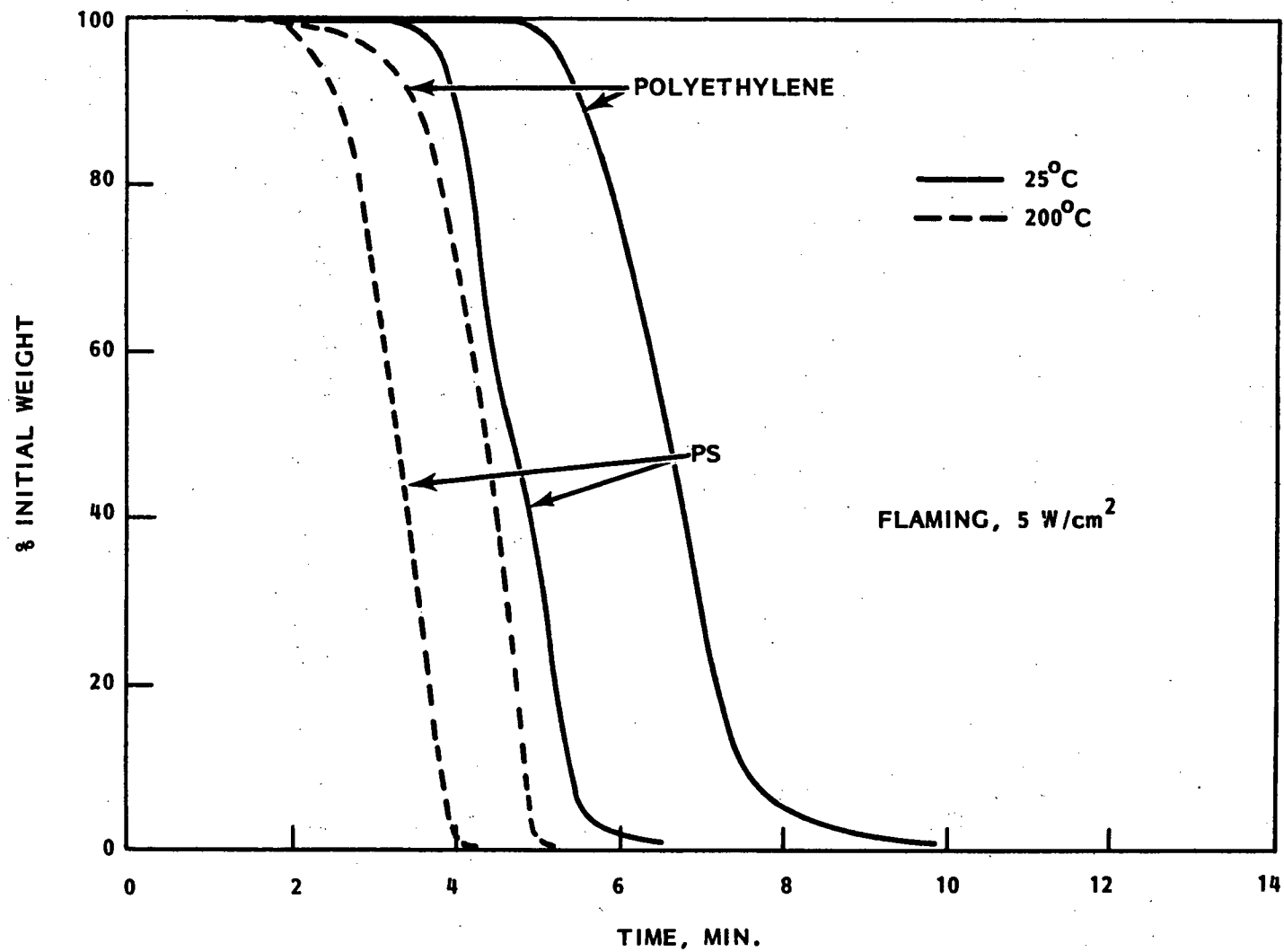
A.44

FIGURE A.5.7. Effect of Ventilation Gas Temperature Upon Sample Weight Loss for Polyethylene and Polystyrene Under Flaming Conditions
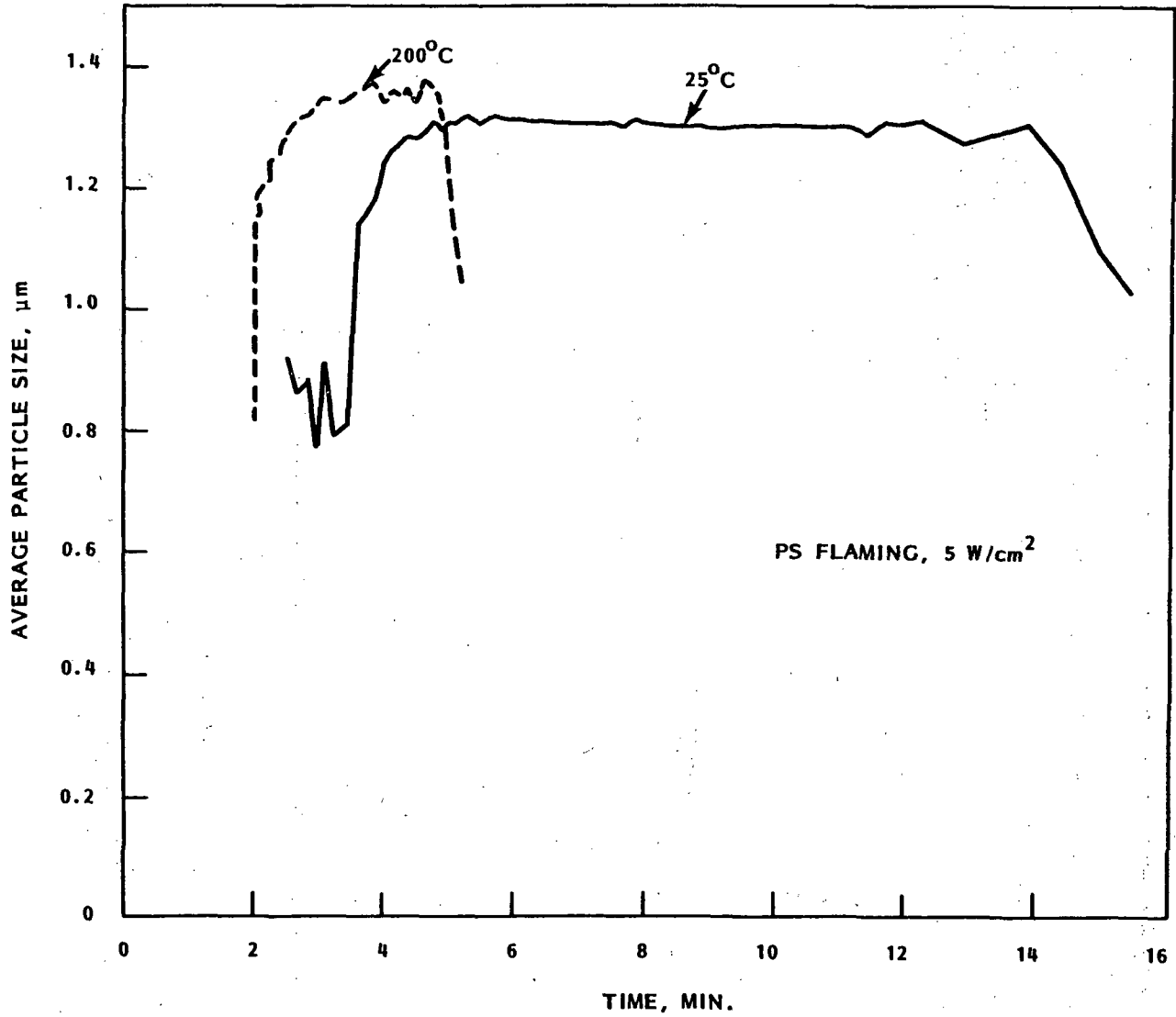
FIGURE A.5.8. Effect of Ventilation Gas Temperature Upon Smoke Mean Particle Diameter for Flaming Polystyrene at 5 W/cm²
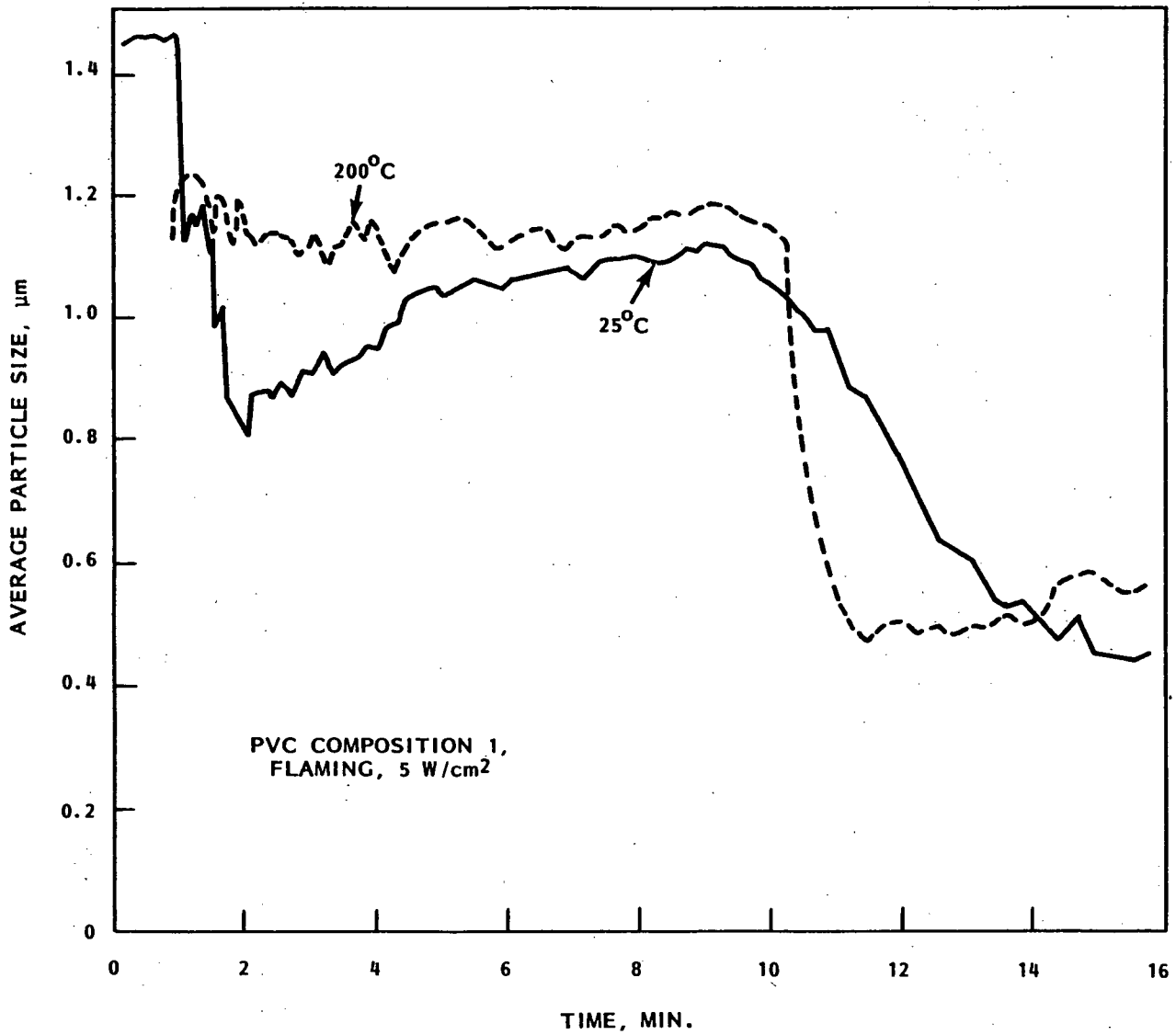
FIGURE A.5.9. Effect of Ventilation Gas Temperature Upon Smoke Mean Particle Diameter for Flaming PVC at 5 W/cm^2
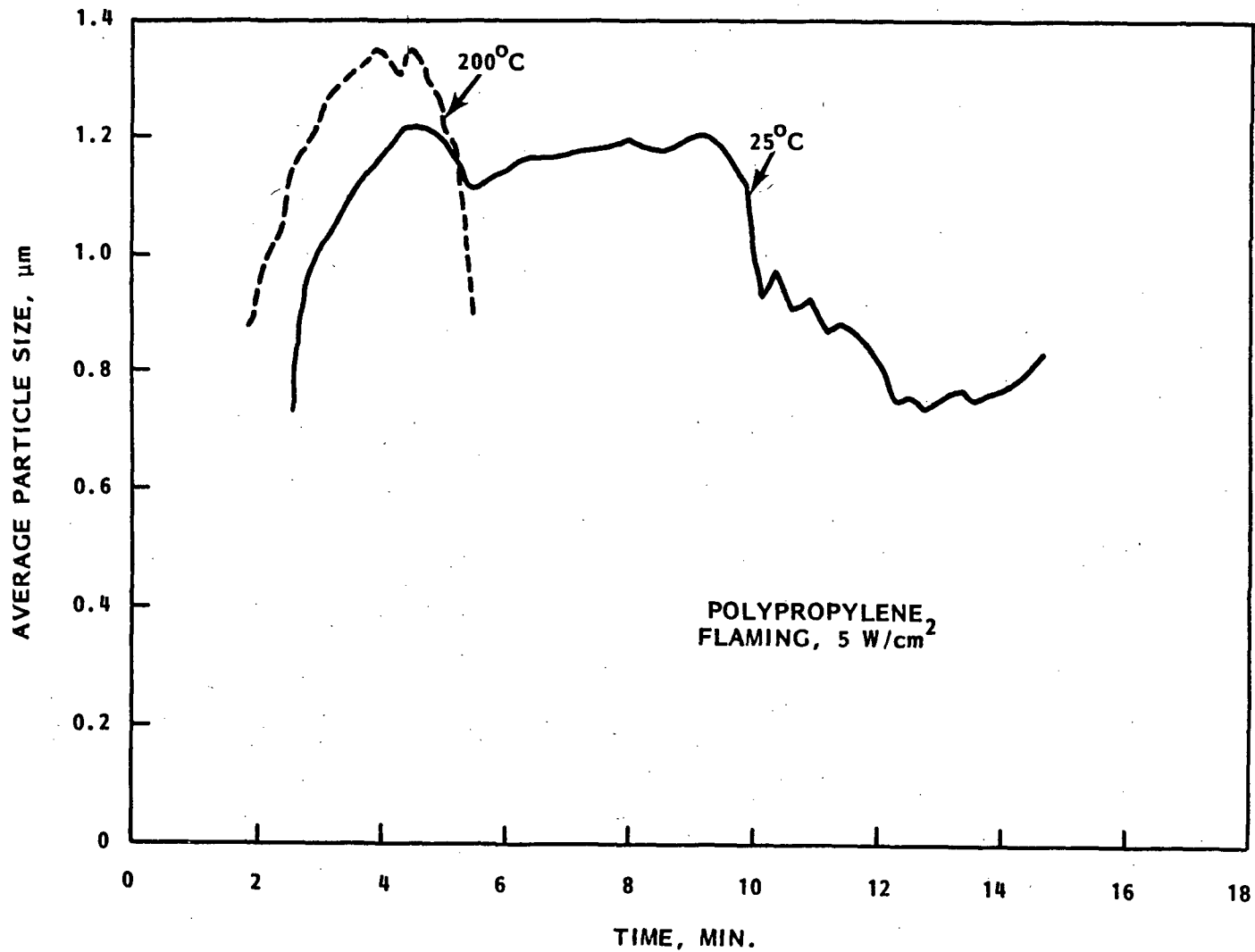
FIGURE A.5.10. Effect of Ventilation Gas Temperature Upon Smoke Mean Particle Diameter for Flaming Polypropylene at 5 W/cm^2
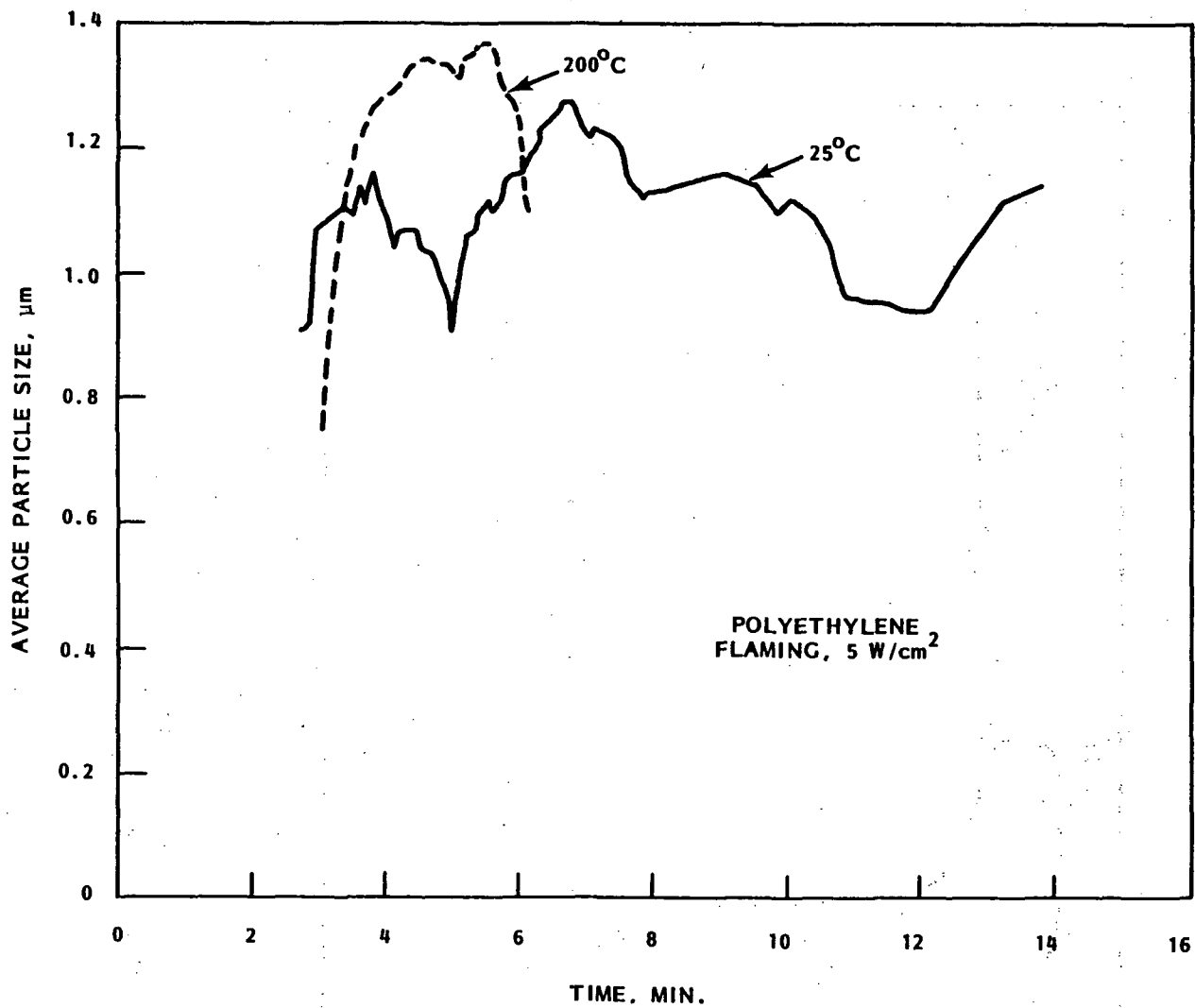
FIGURE A.5.11. Effect of Ventilation Gas Temperature Upon Smoke Mean
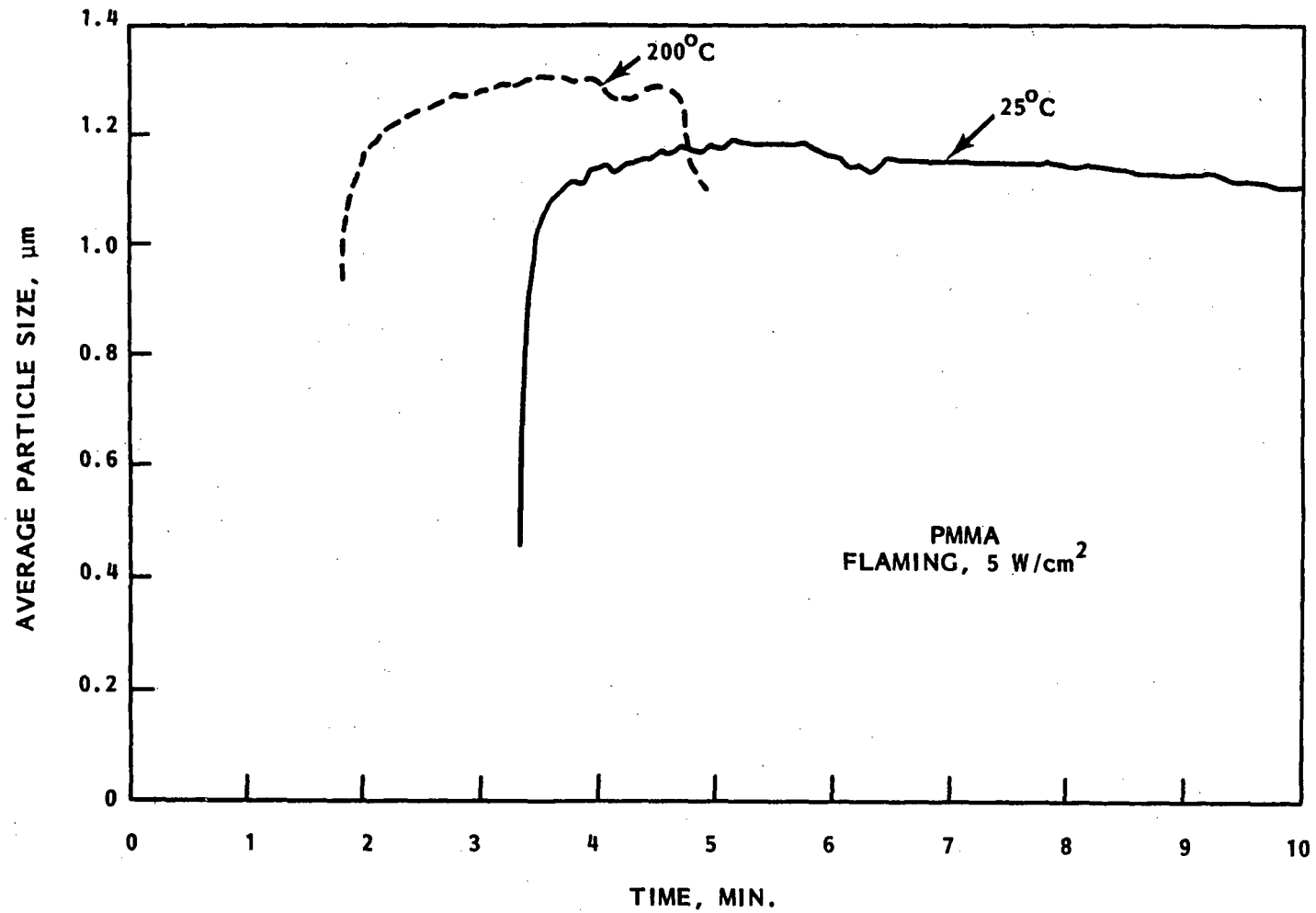Particle Diameter for Flaming Polyethylene at 5 W/cm²

FIGURE A.5.12. Effect of Ventilation Gas Temperature Upon Smoke Mean Particle Diameter for Flaming PMMA at 5 W/cm^2

APPENDIX A.6

LITERATURE SOURCE

Zinn, B. T. et al. 1980. The Smoke Hazards Resulting from the Burning of Shipboard Materials Used by the U.S. Navy. NRL Report 8414, Georgia Institute of Technology, Atlanta, Georgia.

TABLES

A.6.1   Smoke Property Data for Hydraulic Fluid

A.6.2   Sample Weight Loss and Smoke Concentration Data for Hydraulic Fluid

A.6.3   Mass Loss Data

A.6.4   Particulate Combustion Products of the Tested Materials

A.6.5   Major PCAH Species Found in Particulate Smoke of the Samples

FIGURES

A.6.1   Effect of the Ventilation Air Temperature on the Sample Weight Loss for Flaming Combustion of Hydraulic Fluid Exposed to a Radiant Flux of 5 W/cm^2

A.6.2   Effect of the Ventilation Air Temperature on the Smoke Mean Particle Size for Flaming Combustion of Hydraulic Fluid Exposed to a Radiant Flux of 5 W/cm^2

NOMENCLATURE

See Appendix A.4

TABLE A.6.1. Smoke Property Data for Hydraulic Fluid

Mode	Ventilation Air Temperature, °C	Γ	OD_{MAX} Blue	OD_{MAX} Red	D_{32},[a] μm	Time to Peak OD, min
Nonflaming[b]	25	---	1.23	1.27	1.23	5.9
Flaming	25	0.028	7.18	5.49	1.33	6.9
Flaming	100	---	6.73	5.10	1.31	6.5
Flaming	300	---	9.41	7.02	1.31	3.7

(a) Averages for data points near the time of maximum optical density.
(b) During the initial nonflaming phase; spontaneous ignition occurred 5.9 min after initiation of exposure.

TABLE A.6.2. Sample Weight Loss and Smoke Concentration Data for Hydraulic Fluid

Mode	Ventilation Air Temperature, °C	Peak Mass Loss Rate, mg/cm^2 sec	Peak Volume Fraction,[a] ppm	Total Particulate Volume,[a] cm^3	$\dfrac{\Gamma}{\Gamma_{25}}$
Nonflaming[b]	25	0.14	0.83	0.32	---
Flaming	25	5.6	4.54	3.61	1.00
Flaming	100	9.8	4.11	2.60	0.72
Flaming	300	11.1	5.58	2.68	0.74

(a) Based on m_R = 1.50 - 0.0i for nonflaming combustion and m_R 1.57 - 0.56i for flaming combustion at a standard flow rate of 425 ℓ/min.
(b) During the initial nonflaming phase; spontaneous ignition occurred 5.9 min after initiation of exposure.

TABLE A.6.3. Mass Loss Data

Sample Type	Sample Mass, mg	Ash Mass, mg	Particulate Mass, mg	Vapor Mass, mg
Wall insulation material	27.34	15.71	0.41	11.22
Cable jacket	10.33	2.77	0.31	7.25
Hydraulic fluid	22.22	0.29	0.67	21.26

TABLE A.6.4. Particulate Combustion Products of the Tested Materials

Test	Sample Mass, g	Particulate Smoke, mg	Extractable Organics, mg	PCAHs, mg	Aliphatic and Others, mg
Wall insulation material:					
nonflaming	7.50	35	34	0.5	33.5
flaming	7.60	41	11.5	1.5	10
Cable jacket, flaming	16.4	128	17.5	2.5	15
Hydraulic fluid, flaming	20	145	20	2	18

TABLE A.6.5. Major Polynuclear-Aromatic-Hydrocarbon Species Found in Particulate Smoke of the Samples

| Sample	Major PCAH Identified	%
Wall insulation	Anthracene/phenanthrene (178)[a] Pyrne (202)	
Cable jacket	Anthracer.e (178)	0.5
	Fluoranthene (202)	27
	Pyrene (202)	44
	1,2 Benzotheorene or methyl pyrene (216)	4
	2,13 Benzothoranthene (226)	8
	Chrysene, benzoanthracene triphenylene (228)	16
	2,4 Benzo(a)pyrene (252)	0.3
Hydraulic fluid	Anthracene/phenanthrene	1
	Fluoranthene	29
	Pyrene	45
	1,2 Benzothorene, etc.	6
	2,13 Benzothoranthene, etc.	12
	2, 4 Benzo(a)pyrene	0.7

(a) Molecular weight.
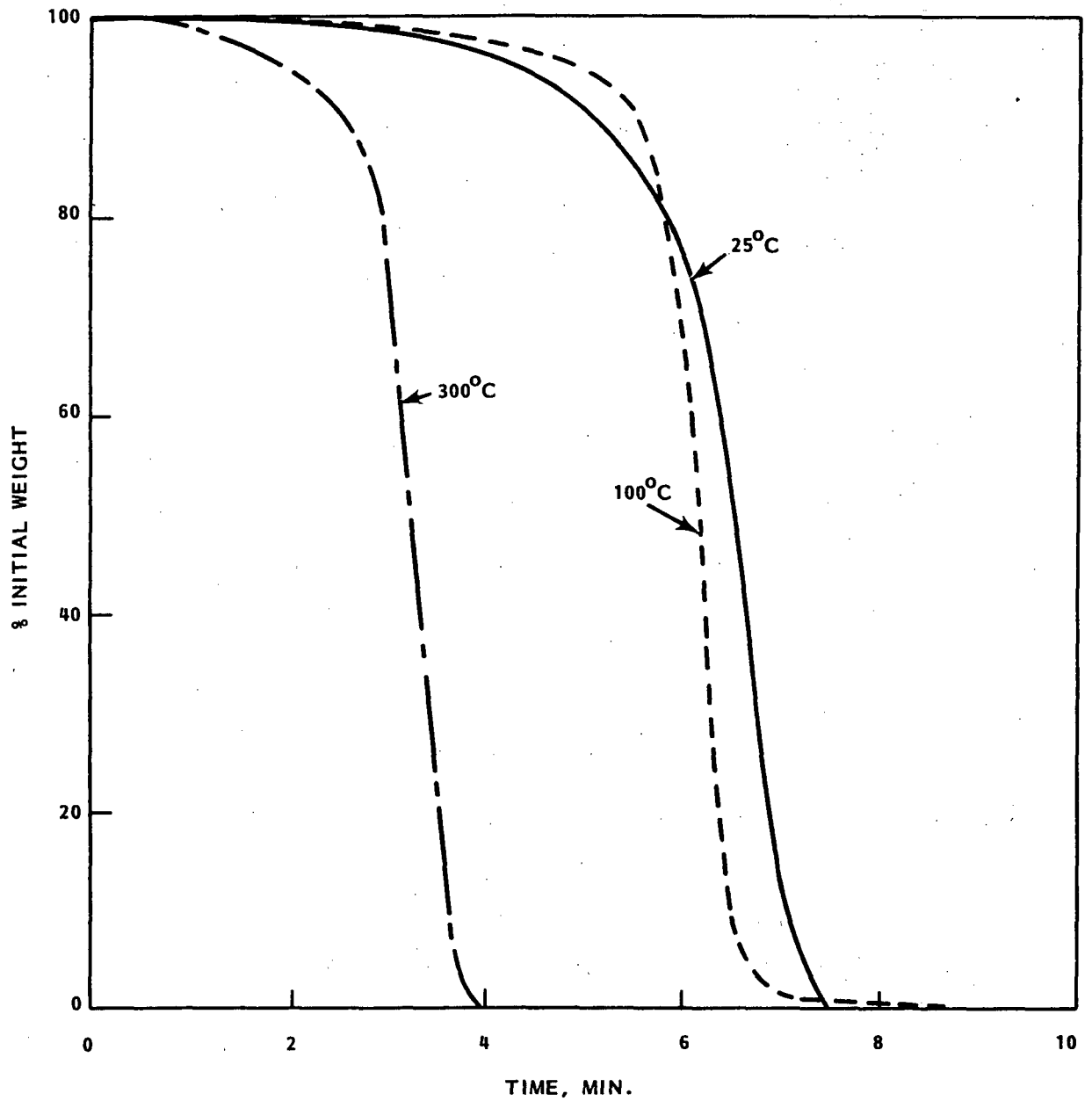
FIGURE A.6.1. Effect of Ventilation Air Temperature on the Sample
Weight Loss for Flaming Combustion of Hydraulic
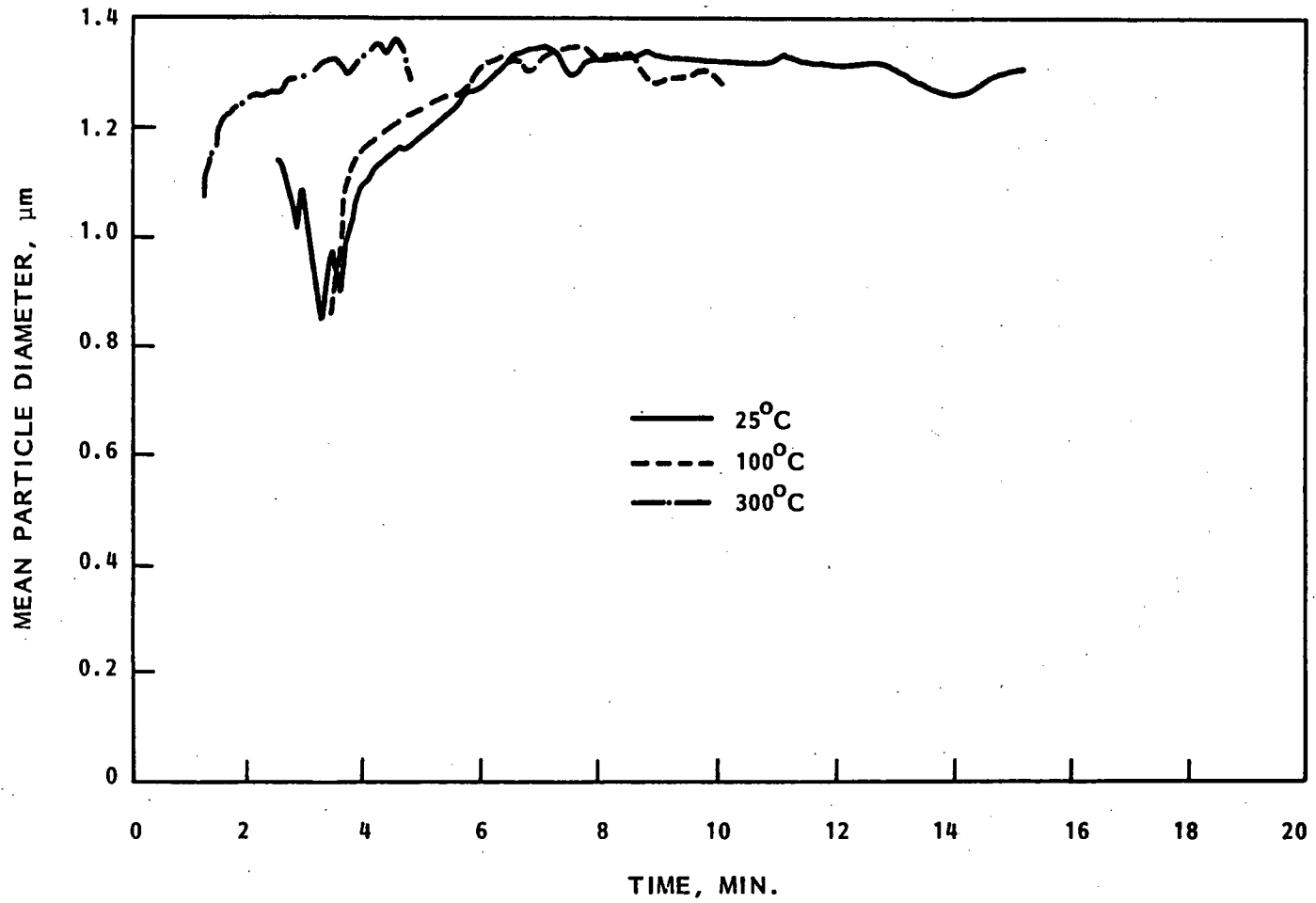Fluid Exposed to a Radiant Flux of 5 W/cm^2

FIGURE A.6.2. Effect of the Ventilation Air Temperature on the Smoke Mean Particle Size for Flaming Combustion of Hydraulic Fluid Exposed to a Radiant Flux of 5 W/cm^2

APPENDIX A.7

LITERATURE SOURCE

Roberts, A. F. and F. R. Brookes. 1981. Hydraulic Fluids: An Approach to
High Pressure Spray Flammability Testing Based on Measurement of Heat
Output. Explosion and Flame Laboratory, Harper Hill, Buxton, Derbyshire,
United Kingdom.

TABLES

A.7.1 Results of Heat Output Tests on Hydraulic Fluids

A.7.2 Comparison of Calorific Values and Heat Output of Hydraulic Fluids

A.7.3 Summary of Table A.7.1 Data for Fluid Temperature of 40°C

TABLE A.7.1. Results of Heat Output Tests on Hydraulic Fluids

Fluid Type	Fluid Temperature, °C	Spraying Rate, $g\ sec^{-1}$	Total Heat Output, $kJ\ g^{-1}$	Radiative Contribution, %	Air Consumption, kg/kg of Fluid
Mineral oil	30	3.6	23.9	34	13.6
	35	3.7	25.2	37	13.4
	40	3.6	25.4	39	13.5
	40	4.0	30.5	44	14.7
	40	4.0	31.5	46	14.2
	50	3.3	26.9	36	14.8
	65	3.5	32.9	44	14.8
Water-in-oil emulsion	30	4.5	18.7	33	7.8
	30	4.6	18.9	32	9.3
	40	4.4	16.3	26	8.5
	60	4.0	17.2	26	6.0
	65	3.7	18.5	25	8.0
	65	3.8	17.8	23	8.8
Phosphate ester	35	5.8	19.8	47	7.8
	40	5.8	19.5	40	6.5
	40	5.8	18.9	42	6.0
	40	5.2	18.7	52	7.6
	50	5.3	18.0	44	7.8
	55	4.3	20.6	49	7.9
	60	4.3	20.0	46	6.6
Water--glycol A	40	4.9	5.3	13	2.7
Water--glycol B[a]					

(a) The heat output for this fluid was too low for accurate measurement.

TABLE A.7.2. Comparison of Calorific Values and Heat Output of Hydraulic Fluids

Fluid Type	Calorific Value (gross), kJ g^{-1}	Total Heat Output from Table A.7.1, kJ g^{-1}	Ratio, B/A
Mineral oil	44.9	27.8	0.62
Water-in-oil emulsion	25.7	17.9	0.70
Phosphate ester	30.8	19.4	0.63
Water-glycol	14.7	5.3	0.36

TABLE A.7.3. Summary of Table A.7.1 Data for Fluid Temperature of 40°C

	Heat Output, kJ g^{-1}	Radiative Contribution, %	Air Consumption, kg/kg of Fluid
Mineral oil[a]	29.1	43	14.1
Water-in-oil emulsion	16.3	26	8.5
Phosphate ester[a]	19.0	45	6.7
Water-glycol	5.3	13	2.7

(a) Averages of three values.

DISTRIBUTION

No. of
Copies

OFFSITE

W. F. Pasedag
Office of Nuclear Reactor
  Regulation
Division of System Integration
Accident Evaluation Branch
Mail Stop P-802
U.S. Nuclear Regulatory Commission
Washington, DC 20555

F. R. Krause
Los Alamos Scientific Laboratory
Los Alamos, NM 87545

James Quintiere
Center for Fire Research
National Bureau of Standards
Washington, DC 20234

No. of
Copies

H. W. Godbee
Oak Ridge National Laboratory
Oak Ridge, TN 37830

ONSITE

Pacific Northwest Laboratory

M. Y. Ballinger
M.K.W. Chan (20)
C. E. Elderkin
J. J. Fuquay
J. A. Glissmeyer
R. L. Hadlock
S. E. King
J. Mishima (5)
P. C. Owczarski
G. N. Slinn
S. L. Sutter
R. K. Woodruff
Publishing Coordination (2)
Technical Information (VG) (5)

4. TITLE AND SUBTITLE *(Add Volume No., if appropriate)*	2. *(Leave blank)*
Characteristics of Combustion Products: A Review of the Literature	3. RECIPIENT'S ACCESSION NO.

7. AUTHOR(S) M. K. W. Chan J. Mishima	5. DATE REPORT COMPLETED
	MONTH: January YEAR: 1983

9. PERFORMING ORGANIZATION NAME AND MAILING ADDRESS *(Include Zip Code)*	DATE REPORT ISSUED
Pacific Northwest Laboratory Richland, Washington 99352	MONTH: July YEAR: 1983
	6. *(Leave blank)*
	8. *(Leave blank)*

12. SPONSORING ORGANIZATION NAME AND MAILING ADDRESS *(Include Zip Code)*	10. PROJECT/TASK/WORK UNIT NO.
Division of Risk Analysis Office of Nuclear Regulatory Research U.S. Nuclear Regulatory Commission Washington, D.C. 20555	11. FIN NO. B2287 and B2407

13. TYPE OF REPORT	PERIOD COVERED *(Inclusive dates)*

15. SUPPLEMENTARY NOTES	14. *(Leave blank)*

16. ABSTRACT (200 words or less)

To determine the effects of fires in nuclear fuel cycle facilities, Pacific Northwest Laboratory (PNL) has surveyed the literature to gather data on the characteristics of combustion products. This report discusses the theories of the origin of combustion with an emphasis on the behavior of the combustible materials commonly found in nuclear fuel cycle facilities. Data that can be used to calculate particulate generation rate, size, distribution, and concentration are included. Examples are given to illustrate the application of this data to quantitatively predict both the mass and heat generated from fires. As the final result of this review, information gaps are identified that should be filled for fire accident analyses in fuel cycle facilities.

17. KEY WORDS AND DOCUMENT ANALYSIS   **17a. DESCRIPTORS**

17b. IDENTIFIERS/OPEN-ENDED TERMS

18. AVAILABILITY STATEMENT	19. SECURITY CLASS *(This report)* Unclassified	21. NO. OF PAGES
Unlimited	20. SECURITY CLASS *(This page)* Unclassified	22. PRICE $

NRC FORM 335 (11-81)